

THE ROLE OF VGLUT3 IN BEHAVIOUR, WITH A FOCUS ON VGLUT3 POSITIVE NEURONS OF THE MEDIAN RAPHE REGION

PhD thesis in Neuroscience

Csilla Lea Fazekas

János Szentágothai Doctoral School of Neurosciences
Semmelweis University, Budapest, Hungary
Laboratory of Behaviour and Stress Studies, Institute of Experimental Medicine,
Budapest, Hungary



Ecole Doctorale Cerveau Cognition Comportement
Sorbonne Université, Paris, France
Laboratory of Neuropharmacology of VGLUTs, NPS -IBPS, INSERM, Sorbonne
Université, CNRS, Paris, France



Supervisors:	Dr. Dóra Zelena, MD, Ph.D., D.Sc Pr Stéphanie Daumas, Ph.D.
Official reviewers:	Márta Jelitai, Ph.D Ingrid Bethus, Ph.D.
Thesis defense committee members:	Dr Klára Gyires, MD, Ph.D., D.Sc Petra Varró, Ph.D. Christelle Rochefort, Ph.D. Ann Lohof, Ph.D.
Head of the Complex Examination Committee:	Gábor Varga, Ph.D, DSc
Members of the Complex Examination Committee:	Krisztina Káldi, Ph.D, DSc Zsuzsanna Helyes, Ph.D, DSc

Budapest
2023

Table of contents

List of Abbreviations.....	6
1. Introduction.....	9
1.1. Vesicular glutamate transporter type 3.....	10
1.1.1. Anatomical distribution.....	10
1.1.2. Glutamate as a secondary neurotransmitter in VGLUT3+ neurons.....	13
1.1.3. Implications of VGLUT3 in physiology.....	17
1.1.4. Role of VGLUTs in shaping the behaviour based on KO mice.....	19
1.2. Median raphe region (MRR).....	22
1.2.1. Anatomy.....	22
1.2.2. Role in locomotion.....	24
1.2.3. Emotional behaviour.....	25
1.2.4. Social behaviour.....	26
1.2.5. Learning and memory formation.....	27
1.3. Technics to investigate specific neuron populations <i>in vivo</i>	30
1.3.1. Cre system and VGLUT3-Cre mice.....	30
1.3.2. Manipulation of neuronal activity.....	32
2. Objectives.....	34
3. Materials and methods.....	35
3.1. Project 1: Behavioural characterisation of the VGLUT3 KO mice.....	35
3.1.1. Project 1/a: Social behaviour.....	35
3.1.1.1. Animals.....	36
3.1.1.2. Behavioural testing.....	36
3.1.1.3. Open field (OF).....	37
3.1.1.4. Sociability test.....	37
3.1.1.5. Social discrimination test (SDT).....	38
3.1.1.6. Social interaction test (SIT).....	39
3.1.1.7. Resident intruder test (RIT).....	39
3.1.1.8. Elevated plus maze (EPM) test.....	39
3.1.1.9. Y-maze test.....	40
3.1.1.10. Statistical analysis.....	41
3.1.2. Project 1/b: Learning and memory formation.....	41

3.1.2.1. Animals.....	41
3.1.2.2. Behavioural testing	41
3.1.2.3. Morris water maze (MWM) task.....	41
3.1.2.4. Statistical analysis.....	42
3.2. Project 2: Anatomical study of VGLUT3 in the mouse and human MRR.....	42
3.2.1. Project 2/a: VGLUT3 mRNA and its co-expression with Tph2 mRNA by sdFISH	42
3.2.2. Project 2/b: VGLUT3 mRNA detection by RT-qPCR in the human MRR- equivalent.....	45
3.3. Project 3: Investigation of the role of MRR-VGLUT3 neurons in behaviour....	46
3.3.1. Project 3/a: Validation of chemogenetics	47
3.3.1.1. Validation 1: Cre-dependent RFP expression in MRR-VGLUT3 cells of VGLUT3-Cre mice.....	47
3.3.1.2. Validation 2: Neurotransmitter concentration measurement in HC by microdialysis after MRR excitation.....	48
3.3.1.3. Validation 3: Validation of chemogenetic-induced neuronal activation by c-Fos immunohistochemistry	51
3.3.2. Project 3/b: Social behaviour.....	51
3.3.2.1. Animals.....	51
3.3.2.2. Surgery.....	52
3.3.2.3. Behavioural testing	53
3.3.2.4. Immunohistochemistry	53
3.3.2.5. Statistical analysis.....	53
3.3.3. Project 3/c: Role of MRR-VGLUT3 neurons in learning and memory formation	54
3.3.3.1. Animals.....	54
3.3.3.2. Surgery.....	54
3.3.3.2.1. <i>Chemogenetics approach</i>	54
3.3.3.2.2. <i>Optogenetics approach</i>	55
3.3.3.3. Behavioural testing	56
3.3.3.4. Open field test.....	56
3.3.3.5. Elevated plus maze test.....	58
3.3.3.6. Morris water maze (MWM) test.....	58

3.3.3.7. Immunohistochemistry and microscopy experiments	59
3.3.3.8. Statistical analysis.....	60
4. Results.....	61
4.1. Project 1: Behavioural characterisation of the VGLUT3 KO mice.....	61
4.1.1. Project 1/a: Social behaviour	61
4.1.1.1. Mobility during exploration based tests	61
4.1.1.2. Anxiety-like behavioural tests	61
4.1.1.3. Social interest	62
4.1.1.4. Social behaviour	64
4.1.1.5. Social discrimination test.....	66
4.1.1.6. Working memory.....	67
4.1.1.7. Summary of Project 1/a	68
4.1.2. Project 1/b: Learning and memory formation	68
4.2. Project 2: Anatomical study of VGLUT3 in the mouse and human MRR.....	69
4.2.1. Project 2/a: VGLUT3 mRNA and its co-expression with Tph2 mRNA by sdFISH.....	69
4.2.2. Project 2/b: VGLUT3 mRNA detection by RT-qPCR in the human MRR- equivalent.....	71
4.2.3. Summary of Project 2	73
4.3. Project 3: Investigation of the role of MRR-VGLUT3 neurons in behaviour....	73
4.3.1. Project 3/a: Validation of chemogenetics	74
4.3.1.1. Validation 1: Cre-dependent RFP expression in MRR-VGLUT3 cells of VGLUT3-Cre mice.....	74
4.3.1.2. Validation 2: Neurotransmitter concentration measurement in HC by microdialysis after MRR excitation.....	74
4.3.1.3. Validation 3: Validation of chemogenetic-induced neuronal activation by c-Fos immunohistochemistry	76
4.3.1.4. Summary of validations of chemogenetics.....	76
4.3.2. Project 3/b: Study of social behaviour.....	76
4.3.2.1. Mobility during exploration based tests	77
4.3.2.2. Anxiety-like behavioural tests	77
4.3.2.3. Social interest	80
4.3.2.4. Social behaviour	82

4.3.2.5. Social discrimination test.....	83
4.3.2.6. Working memory.....	84
4.3.2.7. Summary of Project 3/b.....	84
4.3.3. Project 3/c: Role of MRR-VGLUT3 neurons in learning and memory formation	85
4.3.3.1. Chronic, chemogenetic excitation of MRR-VGLUT3 neurons.....	85
4.3.3.1.1. <i>Mobility during exploration based tests</i>	85
4.3.3.1.2. <i>Anxiety-like behavioural tests</i>	85
4.3.3.1.3. <i>Learning- and memory formation</i>	86
4.3.3.2. Acute, optogenetic excitation of MRR-VGLUT3 neurons	92
4.3.3.2.1. <i>Mobility during exploration based tests</i>	92
4.3.3.2.2. <i>Anxiety-like behavioural tests</i>	92
4.3.3.2.3. <i>Learning and memory formation</i>	94
4.3.3.3. Summary of Project 3/c	97
5. Discussion.....	98
5.1. The behaviour of VGLUT3 KO mice.....	99
5.2. Presence of MRR-VGLUT3 neurons in the brainstem.....	102
5.3. Specific manipulation of MRR-VGLUT3 neurons	103
5.3.1. Validation of chemogenetics	103
5.3.2. MRR-VGLUT3 neurons in behaviour.....	104
6. Conclusions.....	108
7. Summary.....	109
7.1. English	109
7.2. Hungarian.....	110
7.3. French	111
8. References.....	113
9. Bibliography	141
9.1. Publications related to the thesis.....	141
9.2. Other publications.....	141
10. Acknowledgements	143

List of Abbreviations

5-HT:	serotonin	CX:	cortex
AAV:	adenoassociated virus vector	DA:	dopamine
ABC:	avidin-biotin complex	DAPI:	4',6-diamidino-2-phenylindole
ACh:	acetylcholine	DIG:	digoxigenin
AMPA:	α -amino-3-hydroxy-5-methyl-4-isoxazolepropionic acid	DMSO:	dimethyl sulfoxide
Amy:	amygdala	DR:	dorsal raphe
ANOVA:	analysis of variance	DREADDs:	designer receptors exclusively activated by designer drugs
Arch:	archaerhodopsin	EAATs:	excitatory amino acid transporters
BLA:	amygdala	EDTA:	ethylenediamine-tetraacetic acid
BNST:	bed nucleus of stria terminalis	eNpHR:	enhanced halorhodopsin
bp:	basis pair	EPM:	elevated plus maze test
BS:	blocking solution	EPSCs:	excitatory post-synaptic currents
BST:	brainstem	EYFP:	enhanced yellow fluorescent protein
cAMP:	cyclic adenosine monophosphate	FBS:	foetal bovine serum
Cb:	cerebellum	GABA:	γ -aminobutyric acid
CCK:	cholecystokinin	GAD:	glutamate decarboxylase
ChAT:	choline acetyltransferase	Glu:	glutamate
ChR2:	channelrhodopsin 2	GP:	globus pallidus
CNO:	clozapine-N-oxide	GPCR:	G-protein coupled receptor
CNS:	nervous system	H:	hypothalamus
CPu:	caudoputamen	HC:	hippocampus
Cre:	causes recombination		
CRH:	corticotropin-releasing hormone		

HDB:	horizontal limb of the diagonal band of Broca	NAcc:	nucleus accumbens
HPA:	hypothalamic-pituitary-adrenocortical axis	NE:	northeast
HPLC:	high-performance liquid chromatography	NGS:	normal goat serum
iGluR:	ionotropic Glu receptor	Ni-DAB:	nickel-3,3'-diaminobenzidine
ip.:	intraperitoneal	NMDA:	N-methyl-D-aspartate
IP:	interpeduncular nucleus	NW:	northwest
IP3-DAG:	inositol trisphosphate-diacylglycerol	OB:	olfactory bulb
ITI:	intertrial intervallum	OF:	open field
KO:	knockout	PAG:	periaqueductal grey area
lox2222, loxP:	Cre-recognized cleaving sites	PBS:	phosphate-buffered saline
LPB:	lateral parabrachial nucleus	RT-qPCR:	real-time quantitative polymerase chain reaction
LS:	lateral septum	PF:	platform
LSD:	lysergic acid diethylamide	PFA:	paraformaldehyde
MABT:	maleic acid-tween 20	PFC:	prefrontal cortex
MCH:	melanin-concentrating hormone	PLC- β :	phospholipase- β
MDD:	major depressive disorder	Pn:	pontine nuclei
mGluR:	metabotropic Glu receptor	PRF:	pontine reticular formation
MR:	median raphe	PRN:	pontine raphe nucleus
mRNA:	messenger ribonucleic acid	R:	rhombomere
MRR:	median raphe region	RA:	risk assessment
MS:	medial septum	Ra:	raphe nuclei
MWM:	Morris water maze	REM:	rapid eye movement
		RFP:	red fluorescent protein
		RIT:	resident intruder test
		RN:	midbrain raphe nuclei
		RT:	room temperature

RT-qPCR:	reverse transcription quantitative polymerase chain reaction	SSRIs:	selective serotonin reuptake inhibitors
SAP:	stretched attend posture	SW:	southwest
SC:	superior colliculus	T:	thalamus
SD:	social discrimination index	TEA:	triethanolamine
sdFISH:	double-probe fluorescent <i>in situ</i> hybridization	Tph2:	tryptophan hydroxylase 2
SDT:	social discrimination test	Tu:	olfactory tubercle
SE:	southeast	VAcHT:	vesicular acetylcholine transporter
SEM:	standard error of mean	VGAT:	vesicular GABA transporter
SERT:	serotonin transporters	VGLUT:	vesicular glutamate transporter
SI:	social preference index	VGLUT3:	vesicular glutamate transporter type 3
SIT:	social interaction test	VMAT2:	vesicular monoamine transporter 2
SLC17:	solute carrier family 17	VP:	ventral pallidum
SNC:	substantia nigra pars compacta	VTA:	ventral tegmental area
SRM:	spatial reference memory	WT:	wild-type
SSC:	saline-sodium citrate		

1. Introduction

In the central nervous system (CNS) neurons are classified based on the neurotransmitters they express. While Dale's principle originally stated that one neuron utilises one neurotransmitter, we now know that a cell can express multiple different molecules to communicate (Burnstock 1976). However, even today it is still regarded such that neurons have one main "classical" neurotransmitter type (e.g. excitatory glutamate [Glu] or inhibitory γ -aminobutyric acid [GABA]) and express numerous other secondary ones, mainly peptides. These "classical" neurotransmitters are small molecules, they are often intermediates of the metabolism and thus, detectable in all cells. Therefore, neuron classification is based mainly on the transporter proteins that pack the neurotransmitters into vesicles, from which the molecules are later released into the synaptic cleft (Takamori et al., 2000). One of the most abundant types of neurons in the CNS is the glutamatergic cells, which might exert excitation via the release of Glu. Two distinct protein families transport Glu through membranes: the excitatory amino acid transporters (EAATs) and the vesicular glutamate transporters (VGLUTs). EAATs, being responsible for the termination of the synaptic signal, can be found in the plasma membrane of pre- and postsynaptic neurons, as well as in glial cells, and thus, cannot be used to characterise presynaptic glutamatergic neurons (Robinson M. B. 2006).

On the contrary, VGLUTs are expressed on neuronal synaptic vesicles' membrane, and thought to be characteristic to presynaptic neurons only. They belong to the solute carrier family 17 (SLC17), which is a sodium-dependent phosphate transporter family. Their role, as indicated by their name, is to transport Glu into the vesicula to be released at synapses later. According to the current model, during transport VGLUTs utilise electrochemical gradient generated via proton pumps and the co-transport of Cl^- , H^+ or K^+ along with Glu (Fremeau et al., 2002, Preobraschenski et al., 2014, Schafer et al., 2002).

These glutamatergic synaptic vesicles are diverse and can serve as a background mechanism of neuronal heterogeneity (Wichmann and Kuner 2022). According to our present knowledge there are three VGLUT isoforms without significant differences in their Glu uptake when tested in *in vitro* experiments (Preobraschenski et al., 2014) (Weston et al., 2011), but with distinct topological localisation throughout the CNS.

Generally speaking, VGLUT1 mRNA is mainly expressed in the neurons of the cerebral cortex, hippocampus (HC) and cortical areas of the cerebellum (Fremeau et al., 2001, Herzog et al., 2004, Hioki et al., 2003, Vigneault et al., 2015), while VGLUT2 mRNA is more prominent in the neurons of subcortical nuclei such as the thalamus, hypothalamus and different midbrain structures (Bai et al., 2001, Hioki et al., 2003, Szonyi et al., 2019, Vigneault et al., 2015) both in the human and rodent brain. In certain areas, like the amygdala, both can be detected. Even then the two proteins are expressed in separate subnuclei (e.g.: VGLUT1 in the lateral and basolateral amygdala [BLA], VGLUT2 in central and medial amygdala) or cortical layers (e.g.: VGLUT2 is dominant in the cortical layers IV and VI in contrast to other layers) (Fremeau et al., 2001, Herzog et al., 2004, Vigneault et al., 2015). Together, VGLUT1 and 2 specifically mark the vast majority of glutamatergic neurons in the brain.

For many years VGLUT1 and 2 were the only two glutamatergic markers that were used in neuroscience. However, in 2002 a third isoform, the VGLUT3 was identified (Fremeau et al., 2002, Gras et al., 2002, Takamori et al., 2002). Since then, extensive research has been undertaken to elucidate its role in cellular physiology and behaviour, aiming to uncover why it possesses such distinct characteristics when compared to the other two VGLUTs.

1.1. Vesicular glutamate transporter type 3

The DNA sequence of VGLUT3 is over 70% identical to the other isoforms, and it utilises the same molecular mechanism to load vesicles with Glu (Fremeau et al., 2002, Gras et al., 2002, Schafer et al., 2002, Takamori et al., 2002, Weston et al., 2011). Moreover, its sole presence is enough to induce glutamatergic phenotype, as Glu release was detected in GABAergic striatal primary cultures infected with VGLUT3-expressing lentivirus. After 14 days Glu release-induced excitatory post-synaptic currents (EPSCs) were detected in the infected cells, whereas no activation was observed in the control GABAergic cells (Weston et al., 2011).

1.1.1. Anatomical distribution

However, VGLUT3 also shows numerous distinctive characteristics. Firstly, its anatomical distribution is unique: while VGLUT1 and 2 shows complementary localisation, VGLUT3 appears to be co-localised with other transporters, appearing

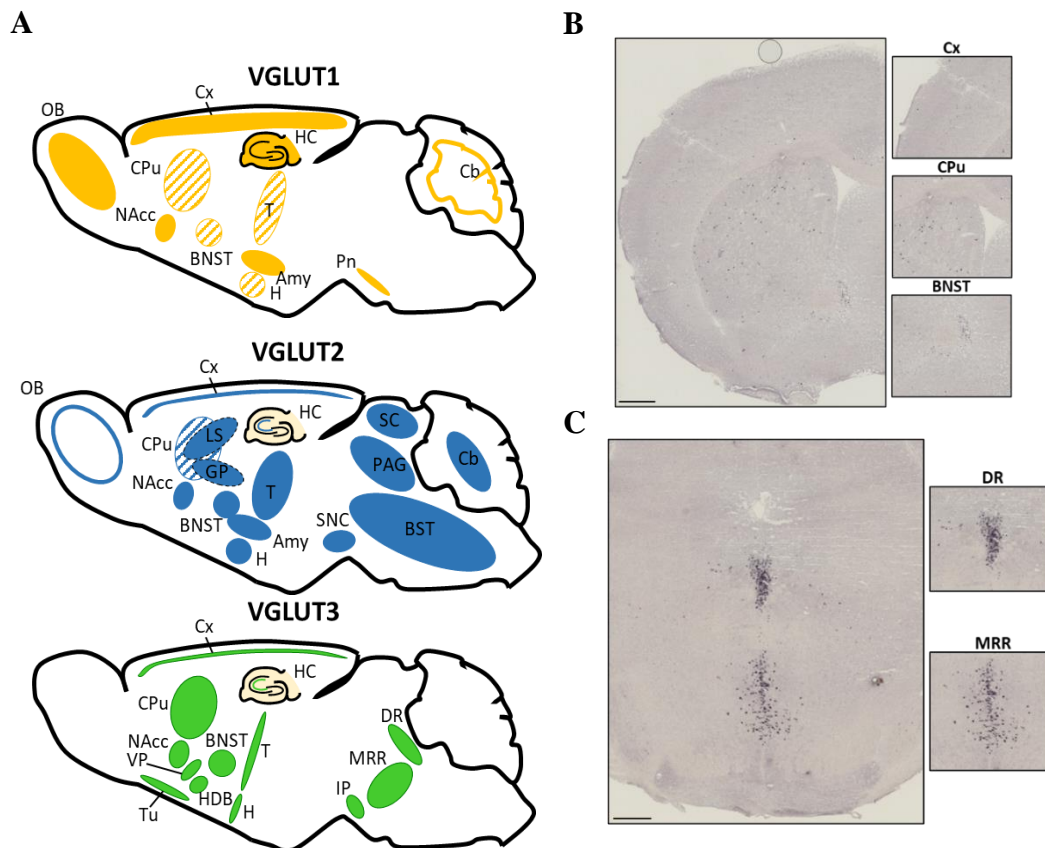


Figure 1. Expression of VGLUTs, with a focus on VGLUT3, in adult rodent brain

(A) Schematic comparison of VGLUT expressing neurons in the mouse brain. VGLUT1 and 2 show a complementary expression in the CNS, while VGLUT3 is present in distinct neuronal populations. Stripped fillings indicate scarce, less abundant expressions. Based on (Fremeau et al., 2002, Herzog et al., 2004, Schafer et al., 2002). (B) Representative pictures of colorimetri *in situ* hybridization against VGLUT3 mRNA in the forebrain areas such as the cortex, CPu and BNST. (C) Representative pictures of colorimetri *in situ* hybridization against VGLUT3 mRNA in midbrain raphe nuclei: DR and MRR. Scale indicates 500 μ m.

Own pictures, *in situ* hybridization conducted in collaboration with Sylvie Dumas (Oramacell).

Amy: amygdala; BNST: bed nucleus of stria terminalis; BST: brainstem; Cb: cerebellum; CPu: caudoputamen; CX: cortex; DR: dorsal raphe; GP: globus pallidus; H: hypothalamus; HC: hippocampus; HDB: horizontal limb of the diagonal band of Broca; IP: interpeduncular nucleus; LS: lateral septum; MRR: median raphe region; NAcc: nucleus accumbens; OB: olfactory bulb; PAG: periaqueductal grey matter; Pn: pontine nuclei; SC: superior colliculus; SNC: substantia nigra pars compacta; T: thalamus; Tu: olfactory tubercule; VGLUT1-3: vesicular glutamate transporter type 1-3; VP: ventral pallidum.

mainly, but not exclusively in subcortical structures (**Figure 1**). On mRNA level, it has been shown in neurons of the cortex (layer II, III and VI), caudoputamen (CPu), amygdala, HC, hypothalamus, nucleus accumbens (NAcc), habenula, bed nucleus of stria terminalis (BNST), ventral tegmental area (VTA), substantia nigra pars compacta and midbrain raphe nuclei (Fremeau et al., 2002, Gras et al., 2002, Harkany et al., 2003, Herzog et al., 2004, Hioki et al., 2004, Hioki et al., 2003, Hioki et al., 2010, Kudo et al., 2012, Schafer et al., 2002, Stornetta et al., 2005), with controversial results in the cerebellum (its presence in the granular layer, molecular layer, Purkinje cells was reported in (Fremeau et al., 2002), but not found by others (Gras et al., 2002, Hioki et al., 2003).

Immunohistochemistry strengthened the mRNA findings on protein level (Hioki et al., 2004). More precisely, inhibitory interneurons and pyramidal cells expressed VGLUT3 proteins in layer II and III of the cortex. Additionally, boutons, representing VGLUT3+ innervation, were found in layer II, III, V and VI (Somogyi et al., 2004). In the HC, pyramidal cell bodies and their dendrites were innervated by VGLUT3+ synapses, while in the stratum radiatum the somas were also VGLUT3 positive (Fremeau et al., 2002, Gras et al., 2002, Hioki et al., 2003, Schafer et al., 2002). Similarly, VGLUT3 proteins were shown in the somas of neurons of the olfactory bulb, CPu, NAcc, striatum, hypothalamus, VTA, substantia nigra pars compacta and raphe nuclei (Fremeau et al., 2002, Gras et al., 2002, Harkany et al., 2004, Herzog et al., 2004, Miot et al., 2012, Rovira-Esteban et al., 2017, Schafer et al., 2002, Tatti et al., 2014). Moreover, VGLUT3 is not exclusively expressed in the nerve terminals or cell bodies, but can also be found in dendrites (Fremeau et al., 2002, Herzog et al., 2004). Interestingly, astrocytes (Fremeau et al., 2002, Ormel et al., 2012) and ependymal cell (Gras et al., 2002, Herzog et al., 2004) were also VGLUT3 positive, however, *in situ* hybridization did not confirm these findings on the mRNA level (Hioki et al., 2010, Li et al., 2013, Schafer et al., 2002).

VGLUT3 is also detectable in the spinal cord. Numerous VGLUT3+ axon terminals can be found in its intermediolateral cell column, where they form both excitatory (asymmetric) and inhibitory (symmetric) synapses, putatively having a role in thermoregulation (Nakamura et al., 2005, Oliveira et al., 2003, Stornetta et al., 2005). The retrotrapezoid nucleus, responsible for chemoreception, is also innervated by VGLUT3+ projections (Rosin et al., 2006). However, VGLUT3 mRNA positive somas were not detected in the spinal cord (Oliveira et al., 2003). Interestingly, in rat, pulpal blood flow

was regulated by VGLUT3+ nerve terminals (Zerari-Mailly et al., 2012), suggesting the possibility of an even more peripheral projection. Moreover, VGLUT3 immunoreactivity was detected in the heart, liver and kidney, but not in intestinal or lung tissue. However, a specific VGLUT3 isoform is characteristic to the CNS (Munguba et al., 2011).

Interestingly, VGLUT3 is present in dendrites and thereby might play a role in retrograde signalling (Fremeau et al., 2002). Crepel et al showed that cerebellar principal cells utilise Glu released from VGLUT3 containing vesicles as retrograde signal and this Glu regulate incoming signals (Crepel et al., 2011). In the cortex, VGLUT3 is also present in the dendrites of layer II principal cells and may negatively control the input from local interneurons (Harkany et al., 2004).

1.1.2. Glutamate as a secondary neurotransmitter in VGLUT3+ neurons

Another interesting characteristic of VGLUT3 is its co-expression with other molecules that are traditionally considered as main neurotransmitters. Controversially, less is known about VGLUT3 co-expression with non-classical, peptide neurotransmitters.

VGLUT3 is often found in symmetric, thus, inhibitory nerve terminals, especially in the HC and the cortex (Fremeau et al., 2002, Gras et al., 2002, Hioki et al., 2004, Kudo et al., 2012, Stensrud et al., 2013). In the HC, glutamate decarboxylase (GAD) positive, GABAergic neurons also express VGLUT3, indicating that inhibitory interneurons may also release Glu (Del Pino et al., 2017, Fremeau et al., 2002, Stensrud et al., 2013, Stensrud et al., 2015). All VGLUT3+ cells were also positive for cholecystokinin (CCK) as well and form basket-like arborisations around other, putatively neurokinin B positive interneurons (Hioki et al., 2004, Somogyi et al., 2004). Similarly, the BNST and amygdala also contain VGLUT3+ GABAergic neurons (Jalabert et al., 2009, Kudo et al., 2012, Omiya et al., 2015, Rovira-Esteban et al., 2017).

In the striatum virtually all cholinergic cells co-express the vesicular acetylcholine transporter (VACHT) and VGLUT3 (Fremeau et al., 2002, Gras et al., 2002, Schafer et al., 2002). Here VGLUT3 plays a crucial role in the vesicular loading of ACh (Gras et al., 2008, Higley et al., 2011) and excite local fast-spiking interneurons via both α -amino-3-hydroxy-5-methyl-4-isoxazolepropionic acid (AMPA) and N-methyl-D-aspartate (NMDA) (both are ionotropic glutamatergic) receptors. In the basal forebrain (horizontal diagonal band of Broca), cholinergic neurons also co-express VGLUT3, however, in a

more restricted way (Case et al., 2017, Harkany et al., 2003, Nickerson Poulin et al., 2006, Stensrud et al., 2013). Some of these cells project to the internal plexiform layer of the main olfactory bulb, although electrophysiological measurements showed that postsynaptic currents are derived from nicotinic and GABAergic activation rather than from Glu release (Case et al., 2017). Other cells from the basal forebrain project to the BLA and express both choline acetyltransferase (ChAT) and VGLUT3 (Nickerson Poulin et al., 2006). It is thought that this co-release of Glu and ACh plays a role in the regulation of locomotor activity (Nelson et al., 2014). Similar results were found in basal forebrain nuclei such as the medial septum (MS), diagonal bands and nucleus basalis (Harkany et al., 2003) (**Figure 2**).

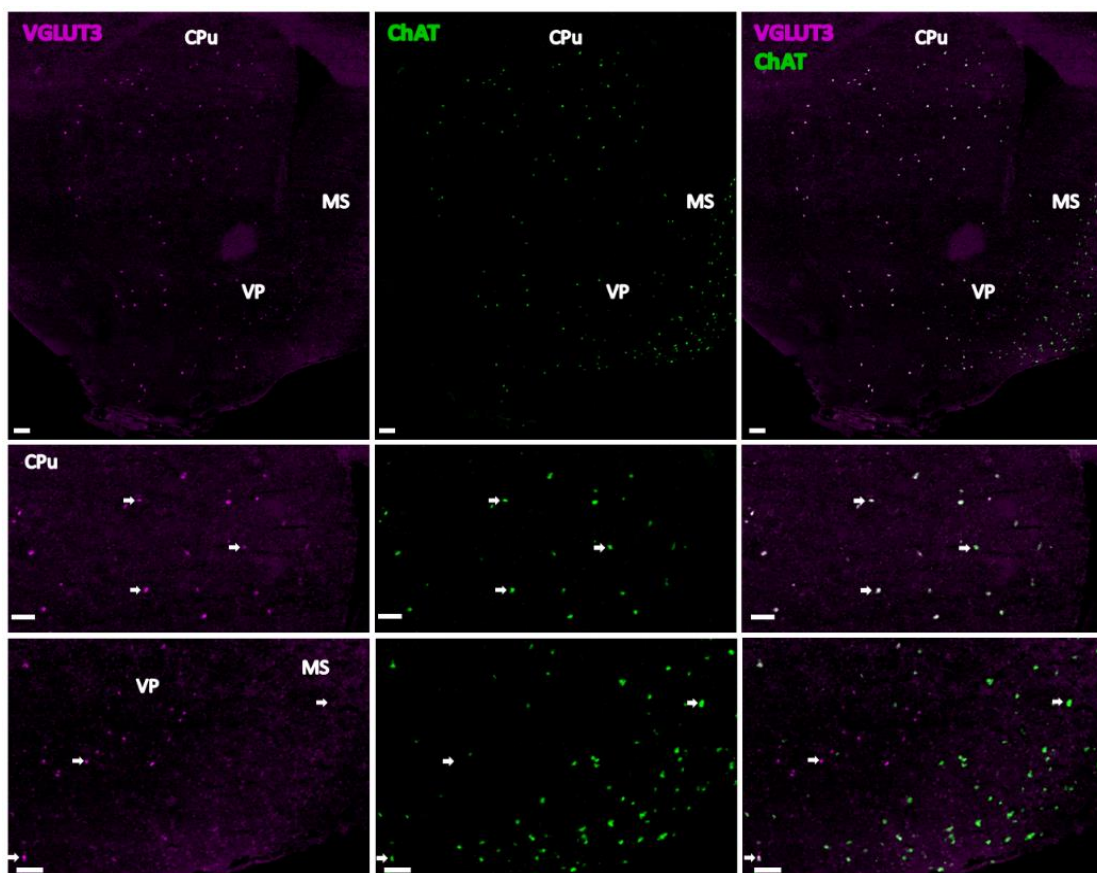


Figure 2. Examples of VGLUT3 and ChAT co-expression in the mouse brain
 Examples of neurons that co-express (white) VGLUT3 (magenta) and the cholinergic marker ChAT (green) mRNAs (CPu), only VGLUT3 (VP) or only ChAT (MS) in the mouse forebrain, indicated by arrows. Scale indicates 100 μ m.

Own pictures, fluorescent *in situ* hybridization conducted in collaboration with Sylvie Dumas (Oramacell).

ChAT: choline acetyltransferase; CPu: caudoputamen; MS: medial septum; VGLUT3: vesicular glutamate transporter type 3; VP: ventral pallidum.

Midbrain raphe nuclei are mostly known for their 5-HT content, marked by serotonin transporters (SERT). Interestingly, in these cell groups SERT+ and VGLUT3+ markers are often, but not exclusively co-expressed (Calizo et al., 2011, Commons 2009, Fremeau et al., 2002, Gagnon and Parent 2014, Gras et al., 2002, Hioki et al., 2004, Hioki et al., 2010, Ren et al., 2018, Shutoh et al., 2008, Voisin et al., 2016) (**Figure 3**). The terminals of these co-expressing neurons project to the cortex, especially to layer II/III (Hioki et al., 2004). The source of these terminals is mainly in the dorsal raphe (DR) (Calizo et al., 2011, Commons 2009, Fu et al., 2010, Gagnon and Parent 2014, Hioki et al., 2010, Liu Z. et al., 2014), which also projects to the striatum (Gagnon and Parent 2014). Interestingly, these axons form varicosities that are morphologically larger than others (Gagnon and Parent 2014). Other projections in the VTA and NAcc play a role in reward signalling (Liu Z. et al., 2014, Wang H. L. et al., 2019, Zou et al., 2020). In VTA, both 5-HT and Glu originating from VGLUT3+ axon terminals are released, contributing to social stress susceptibility: their inhibition facilitated social avoidance after subthreshold social defeat stress (Zou et al., 2020). In another study, it was shown that the VGLUT3+/5-HT+ DR projections to VTA dopaminergic neurons were excitatory and induced DA release in the NAcc, positively driving conditioned place preference (Wang H. L. et al., 2019). Similarly, 5-HT and VGLUT3 co-localisation was detected in the DR-basal amygdala projections, possibly contributing to fear memory (Sengupta and Holmes 2019). In the basal amygdala the axon terminals either released 5-HT or Glu based on the frequency of firing (Sengupta et al., 2017). Other than these areas, DR VGLUT3+ neurons also project to the substantia nigra pars compacta, different thalamic and hypothalamic nuclei, where they do not necessarily co-express 5-HT, and their somas are mainly located in the shell region of the DR (Hioki et al., 2010). Additionally, there is a subset of VGLUT3+ cells in the superior colliculus that also project to substantia nigra pars compacta and form asymmetric, thus, excitatory synapses on local dopaminergic neurons (Martin-Ibanez et al., 2006).

In another known serotonergic nucleus, the median raphe (MR), Glu is packed in vesicles with the help of VGLUT2 and VGLUT3 as well. The latter - similar to other brain areas - is partly co-localised with GABA and 5-HT (Hioki et al., 2010, Somogyi et al., 2004, Sos et al., 2017) (**Figure 3**). However, there seems to be topological

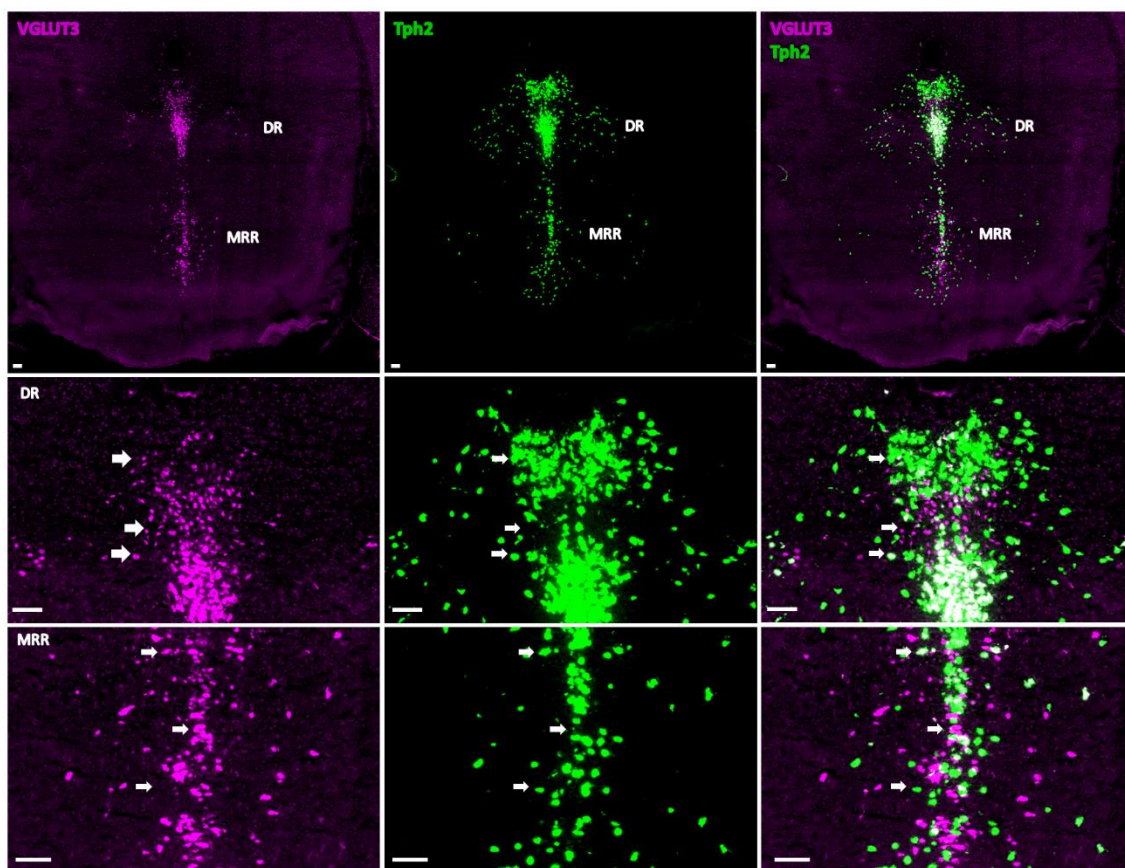


Figure 3. Examples of VGLUT3 and serotonin co-expression in the mouse brain
 Representative pictures of neurons co-expressing VGLUT3 (magenta) and serotonin marker Tph2 (green) mRNA, or only VGLUT3, or only Tph2 in midbrain raphe nuclei DR and MRR. Scale indicates 100 μ m.

Own pictures, fluorescent *in situ* hybridization conducted in collaboration with Sylvie Dumas (Oramacell).

DR: dorsal raphe; MRR: median raphe region; Tph2: Tryptophan hydroxylase 2; VGLUT3: vesicular glutamate transporter type 3.

heterogeneity in the neurochemical characteristics of differently projecting serotonergic and VGLUT3+ axon varicosities. For example, in the cortex, HC, NAcc and striatum most varicosities expressed both SERT and VGLUT3 markers (Belmer et al., 2019, Gagnon and Parent 2014). On the other hand, Voisin et al showed the opposite results: in the MS, striatum and HC these two markers were barely co-expressed in the same varicosities (Voisin et al., 2016). Similarly, in the HC second rhombomere (R2) derived, Pet1+ (transcription factor known to represent serotonergic cells (Gaspar and Lillesaar 2012)) boutons were mostly VGLUT3+, but not 5-HT+. However, serotonergic neurons originating from other rhombomeres co-expressed VGLUT3+ in their terminals (Senft et al., 2021). As of now, it is unknown whether this is a technical (antibody, different animal

strains) or physiologically important observation related to functionality. It is important to note that while this segregation (i.e. 5-HT+, GLUT3+ or co-expressed) in MR-HC projections was confirmed (Amilhon et al., 2010), it was also highlighted that VGLUT3 may be co-expressed in vesicular monoamine transporter 2 positive (VMAT2+) and 5-HT+ terminals even if they were negative for the SERT marker. It is believed that this co-expression facilitates the vesicular filling of the main neurotransmitter (so-called vesicular synergy) (Amilhon et al., 2010, El Mestikawy et al., 2011, Gras et al., 2008). However, in the case of GABAergic co-expression, both pro (Fasano et al., 2017) and contra (Pelkey et al., 2020, Zimmermann et al., 2015) arguments have been published, leaving the question open. A most probable explanation is that the same projection may have different subtypes and different authors found different populations in their samples by chance. The co-expression of "classical" neurotransmitters may be further coloured by an array of peptide co-transmitters (Cropper et al., 2018, Nusbaum et al., 2017).

Similar to the midbrain raphe nuclei, VGLUT3 can be found alone or co-expressed in a subset of putatively GABAergic and/or aminergic cells in the medullary raphe nuclei, such as the raphe pallidus, raphe magnus, raphe obscurus and parapyramidal area. They send projections to the spinal cord (Nakamura et al., 2005, Stornetta et al., 2005). It has also been suggested that VGLUT3 is also co-expressed with VGLUT1 and 2, but this seems to be brain area (Takamori et al., 2002) and species specific (might be different even between rats and mice) (Larsson and Broman 2019, Takamori et al., 2002).

1.1.3. Implications of VGLUT3 in physiology

As a recently discovered protein, the exact role of VGLUT3 is not yet completely understood. Scarce information is available both from the CNS and the periphery. However, transgenic animal models, such as the complete gene knockout (KO) mouse strains, provide an opportunity to explore the role of these transporters *in vivo*.

First of all, VGLUT3 is highly implicated in sensory processes. In the retina, VGLUT3 plays a crucial role in the physiology of a new subtype of putatively excitatory amacrine cells (Fremeau et al., 2002, Gras et al., 2002, Grimes et al., 2011, Munguba et al., 2011).

VGLUT3 is also expressed in the inner hair cells and spiral ganglion cells of the cochlea (Obholzer et al., 2008, Peng et al., 2013, Ruel et al., 2008) as well as in the inhibitory sound-localisation pathway (Noh et al., 2010). They are needed for auditory

coding, as without properly functioning proteins the stereociliary bundle structure and synaptic organisation was lost (Joshi et al., 2021). As a result, VGLUT3 KO mice are deaf (Akil et al., 2012, Ruel et al., 2008, Seal et al., 2008). VGLUT3 mediated glutamatergic neurotransmission is also responsible for noise-induced threshold shifts (Kim et al., 2019).

Lastly, low threshold mechanosensitive cells in the hairy skin that project to the dorsal horn of the spinal cord with C-type fibres also utilise VGLUT3 to signal pleasant touch information (Honsek et al., 2015, Larsson and Broman 2019, Lou et al., 2013). However, unpleasant sensory information of an electric foot-shock was not influenced by the lack of VGLUT3 in KO mice (Balazsfi D., Fodor, et al., 2018).

As numerous brainstem areas involved in respiration and thermogenesis also contain VGLUT3+ neurons (see earlier), we might assume alteration in these systems in VGLUT3 KO mice as well. Indeed, despite preserved structure, the respiratory rhythm generator neurons of their brainstem fired with decreased amplitude and duration in response to hypoxic stress, probably due to an altered 5-HT turnover. Moreover, their thermoregulation was also disrupted (Miot et al., 2012).

The parabrachial nucleus contributes to the sympathetic nervous system activity. After stimulating cardiac sympathetic afferents, c-Fos – a neuronal activity marker – was detected in VGLUT3+ cells, indicating a role of VGLUT3 in cardiovascular responses (Guo et al., 2005).

The participation of VGLUT3 in endocrine regulation was confirmed by several studies. Firstly, Glu may influence the stress response at several points (Horvath et al., 2018), and VGLUT3 might be especially involved in catecholaminergic regulation as around 25% of the chromaffin cells in the adrenal medulla also express VGLUT3 (Olivan et al., 2011). The expression of the hypothalamic regulator of the so-called stress axis (hypothalamic-pituitary adrenocortical axis, HPA), the corticotropin-releasing hormone (CRH) was increased in VGLUT3 KO mice and the stressor-induced corticosterone (end-hormone of the HPA axis) elevation was higher in them compared to their wildtype (WT) littermates (Balazsfi D. et al., 2016, Balazsfi D., Fodor, et al., 2018, Horvath et al., 2018). However, we might assume that VGLUT3 influences the HPA axis indirectly, on remote brain areas influencing the perception/interpretation of the stressor as its presence (both in the somas as well as in afferent fibres) was not confirmed so far on its elements.

Moreover, an array of stressors decreases the number of VGLUT3+ neurons in the DR, where inputs from the central amygdala might play a significant role (Prakash et al., 2020). Additionally, in the periphery VGLUT3 may play an important regulatory role in insulin secretion as its immunopositivity was found in the β -cells of the Langerhans islets of the pancreas (Gammelsaeter et al., 2011).

1.1.4. Role of VGLUTs in shaping the behaviour based on KO mice

Among the three subtypes, VGLUT1 and 2 seem to be utmost important as their lack is fatal: VGLUT1 KO mice die around weaning (unless they get special care), while VGLUT2 KO at birth (Callaerts-Vegh et al., 2013, Moechars et al., 2006, Wallen-Mackenzie et al., 2006, Wallen-Mackenzie et al., 2010).

At birth VGLUT1 KO and WT animals are indistinguishable. However, after birth VGLUT1 expression increases, accounting for 50% of Glu transmission in 3-5-day-old WT mice. Therefore, VGLUT1 KO animals have progressive neurological symptoms, including blindness and incoordination (Freneau et al., 2004). In VGLUT1 KO animals during the first two weeks of life sharp decrease in residual activity was detected, and in mice older than 2 months the excitatory transmission was essentially eliminated, leading to death.

VGLUT2 KO mice die due to a complete loss of stable autonomous respiratory rhythm, generated by the pre-Bötzing complex (Gezelius et al., 2006). Like VGLUT1 KO, the heterozygous VGLUT2 +/- mice are not obviously different from their WT littermates, despite expressing 50% less VGLUT2 protein (Moechars et al., 2006). However, various behavioural tests presented well that partial loss of VGLUT2 significantly affected thalamic function. Among other things, conditioned taste aversion and defensive marble burying behaviours were impaired, while motor function, learning and memory, acute nociception, and inflammatory pain remained intact.

Contrary to the other two isoforms, both heterozygous and homozygous VGLUT3 KO mice are viable and reach adulthood without any need of intervention (Horvath et al., 2018). In the brain of VGLUT3 KO mice, however, no VGLUT1 and 2 alterations (both at mRNA and protein level) were found in their brain (Gras et al., 2008). Moreover, the lack of VGLUT3 expression has no consequences on the co-expressed biochemical markers related to ACh, DA, GABA or neuropeptidergic (substance P, enkephalin).

VGLUT3 KO mice show no major macroscopic anatomical discrepancies in their brain compared to their WT littermates (Miot et al., 2012). Although *in vitro*, raphe primary cell cultures that lack VGLUT3 are less likely to survive (Voisin et al., 2016), *in vivo*, VGLUT3 KO mice do not show reduced serotonergic cell number in their midbrain raphe nuclei. However, in the striatum and dorsal HC of KO mice the number of serotonergic varicosities was decreased while in the ventral HC it was increased (Voisin et al., 2016). On a molecular level, VGLUT3 KO mice show decreased 5-HT (Amilhon et al., 2010, Miot et al., 2012) and ACh turnover (Gras et al., 2008). Moreover, not only ionotropic and metabotropic Glu receptor (iGluR and mGluR, respectively) expression was affected in their cortex, HC and striatum, but there are alterations also in their DA receptor type 1 and muscarinic ACh receptor M1, possibly affecting synaptic plasticity (Ibrahim et al., 2022).

As the main VGLUT isoform expressed in the striatum, an area that has an important role in the regulation of movement, is VGLUT3, locomotor alteration in VGLUT3 KO mice could be supposed. However, their motor-coordination is normal (Horvath et al., 2018). Interestingly, during short observations (e.g. 5-10 min open field) a reduced locomotion was detectable (Balazsfi D., Fodor, et al., 2018, Horvath et al., 2018), while during more prolonged observations (up to 5 hours) even a hyperlocomotion was observed (Gras et al., 2008), especially during the dark, active phase (Divito et al., 2015). The reduced locomotion seems to be due to enhanced anxiety (Amilhon et al., 2010, Balazsfi D., Fodor, et al., 2018), leading to a more cautious behaviour in a new environment, while the hyperlocomotion was connected to their altered DA levels (Divito et al., 2015, Gras et al., 2008), suggesting its possible role in Parkinson disease.

In line with an altered HPA axis reactivity mentioned earlier (Balazsfi D., Fodor, et al., 2018, Horvath et al., 2018), VGLUT3 mice were repeatedly reported to be more anxious (Amilhon et al., 2010, Balazsfi D. et al., 2016, Balazsfi D., Fodor, et al., 2018, Sakae et al., 2019). This anxiety is innate and can be detected already during the early postnatal period (in 8-day-old mice) by enhanced maternal separation-induced ultrasound vocalisation (at 40-90 kHz) (Balazsfi D. et al., 2016). Furthermore, increased anxiety-like behaviour is still detectable in adult mice on numerous behavioural tests such as the elevated plus maze (EPM) (Balazsfi D., Fodor, et al., 2018, Sakae et al., 2019), or in marble burying, and novelty suppressed feeding paradigms (Amilhon et al., 2010).

Sensitivity to pharmacological treatments was also altered in the VGLUT3 KO mice (Divito et al., 2015, Gangarossa et al., 2016, Gras et al., 2008, Sakae et al., 2015, Sakae et al., 2019). Cocaine-induced locomotor activity was exaggerated in them (Gras et al., 2008, Sakae et al., 2019), and their L-DOPA-induced dyskinesia was reduced (Divito et al., 2015, Gangarossa et al., 2016). Additionally, amphetamine-induced locomotion was also decreased after complete deletion of the VGLUT3 gene (Mansouri-Guilani et al., 2019).

In relation to the above-mentioned drug-induced locomotor discrepancies, addictive behaviour was also altered in VGLUT3 KO mice. These animals proved to be more sensitive since they responded to smaller amount of cocaine in a conditioned place preference test than their WT littermates (Fontaine et al., 2022) and were more responsive when it was used as a reward (Sakae et al., 2015). This might have a human relevance, as variations in the VGLUT3 gene in patients also correlated with severe addiction (Sakae et al., 2015).

The previously mentioned contribution of VGLUT3 to hearing was confirmed by the loss of auditory brainstem responses in VGLUT3 KO animals (Akil et al., 2012, Joshi et al., 2021, Ruel et al., 2008). Interestingly, the p.A211V point mutation of VGLUT3 also results in progressive deafness in humans (Ruel et al., 2008). However, in mice, aside from the progressive deafness, no major behavioural phenotype was observed due to the same point mutation, only an *in vitro* decreased VGLUT3 expression was detected (Ramet et al., 2017).

These observed changes are crucial in behavioural neuroscience, as differences between WT and KO mice in the above-mentioned parameters (e.g. locomotion, hearing) might significantly distort other results, such as anxiety-like, depressive-like behaviour, or learning paradigms. Moreover, despite the efforts of the scientific community, the full characterisation of VGLUT3 KO mice is still not complete yet: experiments regarding their social behaviour, for example, are still missing. Although VGLUT3 is a transporter for Glu, a neurotransmitter crucial in learning and memory formation, and being present in key brain areas such as the HC, it is still not known whether, and if so how, VGLUT3 affects learning and memory in general (De Almeida et al., 2023, Fazekas et al., 2019, Horvath et al., 2018). This area was neglected before as an earlier study suggested the

role of VGLUT1 and 2, rather than 3 in learning and memory formation (Cheng et al., 2011).

However, since in KO mouse strains knocking out the genes is constitutive, it might affect the whole body and developmental compensation cannot be ruled out. Thus, brain area specific manipulations are required to investigate the role of VGLUT3 in details.

1.2. Median raphe region (MRR)

Due to the surprisingly high amount of VGLUT3+ neurons and its complex, widespread behavioural effects they have on social behaviour, learning and memory formation, we have chosen the median raphe region (MRR) for further investigation. Moreover, the MRR also densely innervates key brain areas in the forebrain, such as the prefrontal cortex (PFC), MS and HC. Therefore it is plausible to suggest that certain characteristics of the VGLUT3 KO mice can be attributed to this neuron population.

1.2.1. Anatomy

The median raphe region (MRR, in humans: nucleus centralis superior) can be found in the mammalian midbrain. It is one of the raphe nuclei whose major output is believed to be mainly serotonergic.

Traditionally, the previously mentioned cell-rich midline median raphe and the significantly less dense paramedian raphe together is considered as the MRR, and thus includes the B5 and B8 nuclei. However, modern mapping studies suggest substantial differences between developmental origins and the currently conventional anatomy. Relative placement of the primordial cell population to the midbrain-hindbrain boundary defines whether a cell group belongs to the midbrain or the hindbrain. Accordingly, it was found that even the most rostral DR cell groups are actually derived from the isthmus, thus, eventually migrate into the midbrain area. All the other raphe neurons, including those belonging to the MRR, are born and migrate from their respective isthmic and rhombomeric primordia. The presently known MRR (and as defined in our experiments) is actually derived from rhombomere r1-4 (Bang et al., 2012, Jensen et al., 2008, Muzerelle et al., 2016, Okaty et al., 2015). Additionally, serotonergic (Pet1 marker) neurons seem to prefer projection patterns based on their rhombomeric origins: r1-2 derived 5-HT neurons tend to innervate forebrain areas, while r3-5 5-HT neurons more

likely project to brainstem areas (however, in this experiment, the cells were not investigated brain site specifically, e.g. distinguishing DR and MRR neurons) (Bang et al., 2012).

Although even today the MRR is recognised as a major serotonergic nucleus, it has been shown that less than 6% of neurons are actually positive for 5-HT (Sos et al., 2017). Majority of them are GABAergic, characterised by the presence of the vesicular GABA transporter (VGAT) and GAD (Abellan et al., 2000, Sos et al., 2017), but there are some VGLUT2 (Szonyi et al., 2019) positive populations as well. Although numerous other neurons show the conventionally serotonergic marker ePet/Pet1 expression, they are negative for the rate limiting enzyme tryptophan hydroxylase 2 (Tph2) that is required for 5-HT synthesis (Okaty et al., 2019, Okaty et al., 2015, Ren et al., 2019). Instead, they express VGLUT3, and thus, are putatively glutamatergic (Sos et al., 2017). From r2 progenitor cells derived VGLUT3+/Pet1+, but Tph2- neurons have specific projection patterns (Okaty et al., 2015, Senft et al., 2021). For example, they preferentially innervate the cortex and HC, often forming pericellular baskets around inhibitory interneurons. In accordance, when retrograde tracers were used in HC, over 80% of the labelled MRR neurons were VGLUT3+, while only few were 5-HT+. On the other hand, 5-HT+/VGLUT3- neurons targeted the olfactory bulb or the thalamus. However, the MS proved to be an exception as both co-labelled and single-labelled VGLUT3+ boutons were found there. Interestingly, there is still a minor r2 derived neuron population that showed both transcripts equally (Senft et al., 2021). Unfortunately, such detailed description for other rhombomeres is missing as of now. However, different neuron types can be electrophysiologically distinguished *in vivo* in rats: VGLUT3+/5-HT- neurons have higher frequency, but narrower action potentials compared to VGLUT3-/5-HT+ neurons, while co-expressing cells show an intermittent phenotype (Domonkos et al., 2016). Interestingly, on an anatomical level, VGLUT3 and Tph2 mRNAs are highly co-expressed within the MRR (~80% according to (Hioki et al., 2010)), yet on a protein level this is only around ~30% (Sos et al., 2017). This could be due to species differences, e.g.: mRNAs were measured in rats, while the proteins in mice, but nevertheless presents a stark difference.

MRR neurons send axons to key brain areas such as the PFC, MS, basal forebrain, HC, thalamus, hypothalamus, habenula, amygdala, supramammillary nucleus, mammillary nucleus, locus coeruleus, periaqueductal grey area (PAG), substantia nigra, VTA, reticular formation, DR and other raphe nuclei throughout the pons and medulla (Leranth and Vertes 1999, Vertes et al., 1999). Interestingly, opposite to DR, MRR preferentially innervates midline structures and rarely deviates laterally (Vertes et al., 1999). Similarly, medial brain regions, for example the anterior cingulate, MS, diagonal band of Broca, hypothalamus, supramammillary nucleus and the habenular areas innervate the MRR (Ogawa et al., 2014, Pollak Dorocic et al., 2014). Moreover, when fluorescent retrograde tracers were injected into the MS, different subregions of the HC (Mckenna and Vertes 2001), or into the PFC (Szonyi et al., 2016), around 8-12% of MRR cells were double-positive, indicating that these neurons can innervate different brain areas (i.e. PFC-HC or PFC-MS) simultaneously (**Figure 4**).

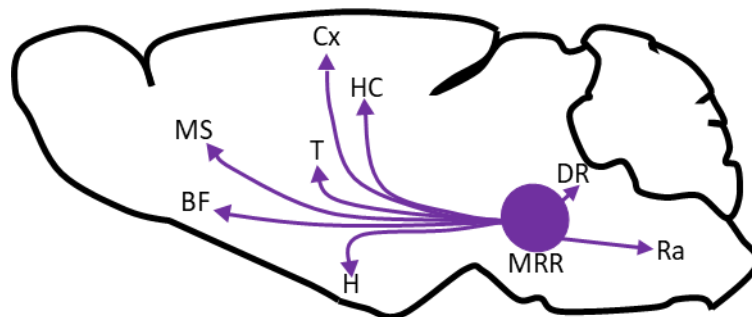


Figure 4. Main projection areas of the MRR

Schematic representation of the projection targets of the MRR. The MRR densely innervates key areas regulating behaviour, such as PFC, MS, T or DR, or the centrum of learning and memory formation, the HC. Moreover, the same neurons send parallel axons to the PFC and MS, PFC and HC or MS and HC. Based on (Gras et al., 2002, Harkany et al., 2003, Herzog et al., 2001, Herzog et al., 2004, Hioki et al., 2004, Hioki et al., 2003, Hioki et al., 2010, Kaneko et al., 2002, Kudo et al., 2012, Leranth and Vertes 1999, Liguz-Lecznar and Skangiel-Kramska 2007, Stornetta et al., 2005, Vertes et al., 1999).

BF: basal forebrain; Cx: cortex; DR: dorsal raphe; H: hypothalamus; HC: hippocampus; MRR: median raphe region; MS: medial septum; PFC: prefrontal cortex; T: thalamus; Ra: raphe nuclei.

1.2.2. Role in locomotion

Due to its widespread projections, it is not surprising that MRR plays a crucial role in numerous behaviours. It affects basic skills like locomotion and activity.

Electrolytic lesions of the MRR resulted in hyperactivity (Geyer et al., 1976, Kusljic and Van Den Buuse 2012, Maru et al., 1979). This was due to the denervation of its caudal, but not anterior parts (Wirtshafter et al., 1986). Pharmacologically, infusion of opioid and GABA receptor agonists, and Glu receptor antagonists into the MRR also increased locomotion. However, D2 receptor blockade only antagonized the effect of the opioid agonist, suggesting that MRR could potentially influence locomotion via both dopamine-dependent and independent ways (Shim et al., 2014). In line with these observations, injection of kainic acid, a glutamate receptor agonist, into the MRR suppressed locomotor activity in rats (Wirtshafter and McWilliams 1987). Interestingly, although mid-center MRR electric excitation decreased mobility (Bland et al., 2016, Wirtshafter and McWilliams 1987), but optogenetic excitation increased it. It is worth to note that even during the latter experiment the animals spent less time with exploration (Balazsfi D. G. et al., 2017).

Moreover, the MRR regulates several complex behaviours as well. For example, MRR excitation via 5-HT receptor type 7 improved stress adaptation (Lazarini-Lopes et al., 2020), but also has the potential to affect emotional, social behaviour, learning and memory formation due to its anatomical connections.

1.2.3. Emotional behaviour

For the longest time the MRR was known as a serotonergic nucleus, thus, most of the studies concentrated on the effects of its 5-HT or 5-HT receptors in behaviour. Via its projections to the interpeduncular nucleus and dorsal HC, MRR Tph2+ neurons both reacted to and promoted aversive behaviour, while their inhibition was rewarding (Kawai et al., 2022). Interestingly, another glutamatergic neuronal population characterised by VGLUT2 in the MRR also plays a role in aversive behaviour, however, via their habenular, VTA, MS and HC projections (Szonyi et al., 2019). Similarly, inhibition via 5-HT1A autoreceptors in the MRR facilitated place preference (Fletcher et al., 1993), or inhibition by GABAA receptor agonist (muscimol) provoked alcohol seeking and impulsive behaviour (Le et al., 2008).

Selective serotonin reuptake inhibitors (SSRIs) have been one of the most often prescribed antidepressants since the late 1980s (Perez-Caballero et al., 2014). As the raphe nuclei are the major source of 5-HT, they were actively studied in relation to emotions. Although MRR was not the major focus, a lot of scattered information is

available. For example, in patients suffering from major depressive disorder (MDD), lower SERT binding of MRR on positron emission tomography recordings predicted a better SSRI response (Lanzenberger et al., 2012). In rats, inhibition of the 5-HT_{1A} autoreceptor expressing neurons via 8-OH-DPAT injection into the MRR elicited antidepressant effect in the forced swim test (FST) (Almeida et al., 2013). Similar antidepressant effect was detected by melanin-concentrating hormone (MCH) administration and confirmed that dense MCH innervation is coming from the hypothalamus (Lopez Hill et al., 2013). However, DR was even more implicated in depression (Bruschetta et al., 2020, Juneja et al., 2020, Michelsen et al., 2007, Vincent and Jacobson 2014). According to newer studies, the relative activity of the DR and MRR defines the appearance of anxiety- and depressive-like behaviour (Teissier et al., 2015, Turcotte-Cardin et al., 2019). In a developmental model, postnatal fluoxetine (SSRI) treatment resulted in a decreased DR, but increased MRR serotonergic activity leading to depression-like behaviour (Teissier et al., 2015). Similarly, when we specifically excited the MRR neurons of mice via chemogenetics, we found increased depressive-like behaviour in FST (Fazekas et al., 2021).

The MRR has a profound effect on anxiety too: in female mice, the excitation of MRR ePet⁺ cells resulted in an increased anxiety-like behaviour, for which dorsal HC projections were responsible (Abela et al., 2020). Knocking down the mRNA of MRR-SERT by interference increased short-term cocaine intake and anxiety-like behaviour in rats (Verheij et al., 2018). On the other hand, general electric excitation or GABA_A receptor blockade of MRR via bicuculline was anxiolytic (Hsiao et al., 2013).

1.2.4. Social behaviour

The regulation of social behaviour cannot be accounted to a single brain region. However, key brain areas – most of them belonging to the limbic system - have already been identified: for example, the amygdala is responsible for the emotional value of social stimuli (Adolphs 2010), but also HC for social recognition (Banker et al., 2021, Montagrin et al., 2018). Specifically, HC-CA2 neuronal activity (Lopez-Rojas et al., 2022), (Oliva et al., 2020), (Hitti and Siegelbaum 2014), and reactivation during sleep is needed for the formation of social memory (Oliva et al., 2020). On the other hand, cortical regions like the PFC – and its rodent homologue, the medial PFC – are also highly implicated. It is hypothesised that excitatory-inhibitory balance in the PFC is necessary

to maintain healthy social behaviour (Bicks et al., 2015, Ko 2017, Yizhar 2012), in which NMDA receptors play a crucial role (Finlay et al., 2015). However, less is known about the brainstem regulation of these higher-order brain areas and how they affect social behaviour. In a previous experiment of our group optogenetic excitation of the whole MRR increased not only 5-HT but also Glu levels in the PFC (Balazsfi D., Zelena, et al., 2018), suggesting its possible contribution.

Indeed, lesions of both DR and MRR decreased social interactions (File and Deakin 1980). In BALB/c mice, characterised by a loss of function mutation of the Tph2 enzyme, social behaviour was reduced (Russo et al., 2019), supporting the major role of 5-HT in shaping social contacts. Social isolation increased 5-HT turnover not only in the MRR, but also in the HC compared to grouped housing conditions along with enhanced anxiety-like behaviour, and interestingly only imipramine, a tricyclic antidepressant could reverse both changes (Dos Santos et al., 2010). If solely the MRR is manipulated, then the inhibition of serotonergic neurotransmission via 8-OH-DPAT injection promoted social interaction in rats (Andrews et al., 1994). In line with this, optogenetic excitation of MRR resulted in a decrease of aggressive behaviour (Balazsfi D., Zelena, et al., 2018) and chemogenetic activation led to increased friendly social behaviour (Fazekas et al., 2021). Interestingly, when the GABAergic (marked by VGAT) neurons were selectively excited chemogenetically, similar enhanced social interest was detected (Chaves et al., 2022).

As for social memory, optogenetic manipulation of MRR 5-HT terminals in the MS influenced social memory stability (Wu X. et al., 2021).

1.2.5. Learning and memory formation

While Glu is considered as one of the main neurotransmitters playing a role in learning and memory formation, HC is regarded as the key brain area, among many others, that enables mammals to continuously adapt to their environment. Moreover, HC also encodes spatial information via its place cells (Burgess et al., 2002, Morris R. G. et al., 1982, Moser et al., 2017, Robinson N. T. M. et al., 2020, Wilson and McNaughton 1993), with major contribution of its local interneurons (Hangya et al., 2010, Jeong and Singer 2022). From the HC, two major oscillations can be detected: theta (Korotkova et al., 2018, Seager et al., 2002) and ripple activity (Colgin 2016, Csicsvari and Dupret 2014, Ego-Stengel and Wilson 2010, Girardeau and Zugaro 2011, Tang and Jadhav 2019). Both

are prominent during the different stages of sleep (Buzsaki 1986, Buzsaki et al., 1983, Louie and Wilson 2001) and believed to play a role in learning and memory consolidation (Buzsaki 2015, Colgin 2016, Kudrimoti et al., 1999), especially in spatial learning tasks (Aleman-Zapata et al., 2022, Ego-Stengel and Wilson 2010). The innervation and regulation of these processes are intricate and is still being discovered. What is even less known is how brainstem areas, such as the MRR, regulate hippocampal activity.

It has been long known that the MRR projects to the HC (Aznar et al., 2004, Crunelli and Segal 1985, Freund 1992, Kohler and Steinbusch 1982, Mckenna and Vertes 2001, Papp et al., 1999, Szonyi et al., 2016), but the role of this projection is still not completely understood. Indeed, a fresh study showed that in a mouse model of Alzheimer's disease, MRR 5-HT signalling is decreased, and thus, contributes to the excitotoxicity affecting HC pyramidal neurons, resulting in memory deficits (Wang J. et al., 2023).

It has been shown that electrolytic lesions (Maru et al., 1979) and inhibition (Bland et al., 2016, Crooks et al., 2012, Varga et al., 2002, Vinogradova et al., 1999) of the whole MRR increased HC neuronal activity and theta oscillations. Accordingly, excitation resulted in suppressed HC activity (Hsiao et al., 2013, Peck and Vanderwolf 1991). These experiments indicated that the MRR has a role in hippocampal desynchronization (Crooks et al., 2012, Maru et al., 1979), via the excitation of local inhibitory interneurons (Freund et al., 1990, Varga et al., 2009, Vertes et al., 2004). Increasing electrophysiological data support the participation of non-serotonergic neurons, as they show theta coupled activity (Kocsis and Vertes 1996). In fact, two coupling neuronal subpopulations were identified within the MRR: theta-on cells that fired when theta oscillations were present, and theta-off cells, that were silent during this time (Viana Di Prisco et al., 2002). Later it was found that these non-serotonergic MRR-HC projections innervate local inhibitory calbindin positive neurons (Aznar et al., 2004, Szonyi et al., 2016, Varga et al., 2009). Interestingly, MRR-VGLUT3+ cells were remarkably silent during rapid eye movement (REM) sleep, but were active in the absence of theta, while (VGAT+) GABAergic cells showed the opposite behaviour (Huang et al., 2022). Moreover, similar findings were shown in relation to HC ripple oscillation, which is a major contributor to memory consolidation: serotonergic neuronal activity showed little correlation, while the majority of non-serotonergic neurons – putatively

glutamatergic - either remarkably decreased (Type I) or increased (Type II) their firing rate (Wang D. V. et al., 2015).

Additionally, MRR may influence HC indirectly through the interneurons (both parvalbumin and calbindin positive) of the MS (Aznar et al., 2004, Crunelli and Segal 1985, Leranath and Vertes 1999, Szonyi et al., 2016, Vertes et al., 1999, Wu X. et al., 2021), which are known regulator of HC activity and memory formation (Dragoi et al., 1999, Gonzalez et al., 2022, Griguoli and Pimpinella 2022, Jin et al., 2020, Papp et al., 1999, Staib et al., 2018, Tsanov 2018, Wu D. et al., 2021, Wu X. et al., 2021). This can be either direct projections or collaterals, both serotonergic and non-serotonergic (Acsady et al., 1996, Aznar et al., 2004, Crooks et al., 2012, Leranath and Vertes 1999, Mckenna and Vertes 2001). Indeed, the MRR-innervated GABAergic, parvalbumin+ interneurons of the MS regulate local cholinergic neurons that act as a pacemaker and control hippocampal theta rhythm and desynchronization (Alreja 1996, Leranath and Vertes 1999, Liu W. and Alreja 1997). Subsequent studies found that vast majority of these innervations is VGLUT3+ (Aznar et al., 2004, Jackson et al., 2009, Szonyi et al., 2016). On the other hand, the MRR-VGLUT3 cells projecting to the hippocampus also send collaterals to the medial prefrontal cortex (Szonyi et al., 2016), which may ensure prefrontal-hippocampal interaction in the process of spatial decision-making (Tavares and Tort 2022).

However, behavioural consequences of this anatomically and electrophysiologically described connection is not fully understood. The best-studied phenomenon is the conditioned fear paradigm, when freezing in a previously trauma-associated compartment is measured. The excitation of the whole MRR immediately after conditioning impaired fear memory consolidation (Wang D. V. et al., 2015). Chemical lesion of the MRR impaired only long-term fear memory (Melik et al., 2000). Similarly, electrolytic lesion of the MRR decreased freezing, but only if it was done 1 day after the conditioning, as opposed to 7 days lesioning, and it was proved to be 5-HT dependent (Silva et al., 2004). Optogenetic manipulation of the whole nucleus had a long-term effect: excitation without any aversive condition elicited freezing behaviour seven days later in mice, while inhibition during shock ameliorated fear response only one week later, but not the next day (Balazsfi D. G. et al., 2017). However, despite the intensive innervation of the HC, not much is known about how the MRR influences spatial learning,

for which numerous behavioural paradigms already exists. Such is the Morris water maze (MWM) paradigm, which is an HC dependent learning and memory task for rodents, even used in progressive disease models characterised by cognitive decline such as Alzheimer's disease (Lissner et al., 2021, Morris R. G. et al., 1982, Vorhees and Williams 2014).

As described above, the MRR is rather complex regarding both its neuronal populations and its role in behaviour. For a long time it was not possible to separate its neurons and investigate how each population contributes to the regulation of behaviour. Thus, most of its effects are tied to its serotonergic neurons, while other populations, such as the VGLUT3+ cells were less implicated. However, advancements in technology enabled us to specifically target these neuronal subpopulations *in vivo* to investigate their effect on a behavioural level.

1.3. Technics to investigate specific neuron populations *in vivo*

1.3.1. Cre system and VGLUT3-Cre mice

One way to achieve cell specific manipulations *in vivo* is achievable by using transgenic animals. These mice contain a P1 bacteriophage derived enzyme, the so-called 'causes recombination' Cre protein, which recognises specific DNA sequences (locus of crossing over/ \times /P1, loxP sites) and performs recombination (McLellan et al., 2017, Sternberg and Hamilton 1981). When Cre is placed under the expression of a specific promoter, neuronal types can be selectively targeted: for example, in the VGLUT3-Cre mouse line, Cre recombinase is expressed under the promoter of VGLUT3, thus, all cells that utilise VGLUT3 also produce Cre. With the help of adenoassociated virus vectors (AAVs), it is possible to encode gene sequences in opposite reading order between loxP sites, and by stereotaxic surgery, these AAVs can be delivered to selected brain areas (Zelena et al., 2017). If the injection is into a Cre transgene animal, Cre-mediated inversion of the sequence is only possible in the selected neuronal population at the target nucleus (**Figure 5**).

VGLUT3-Cre mice strains are commercially available from Jackson laboratory (e.g.: <https://www.jax.org/strain/018147>), however, thorough validation and careful breeding is necessary (Karray et al., 2004, Vooijs et al., 2001, Wunderlich et al., 2001). For example, a major problem is the possibility of ectopic Cre expression (Fazekas et al.,

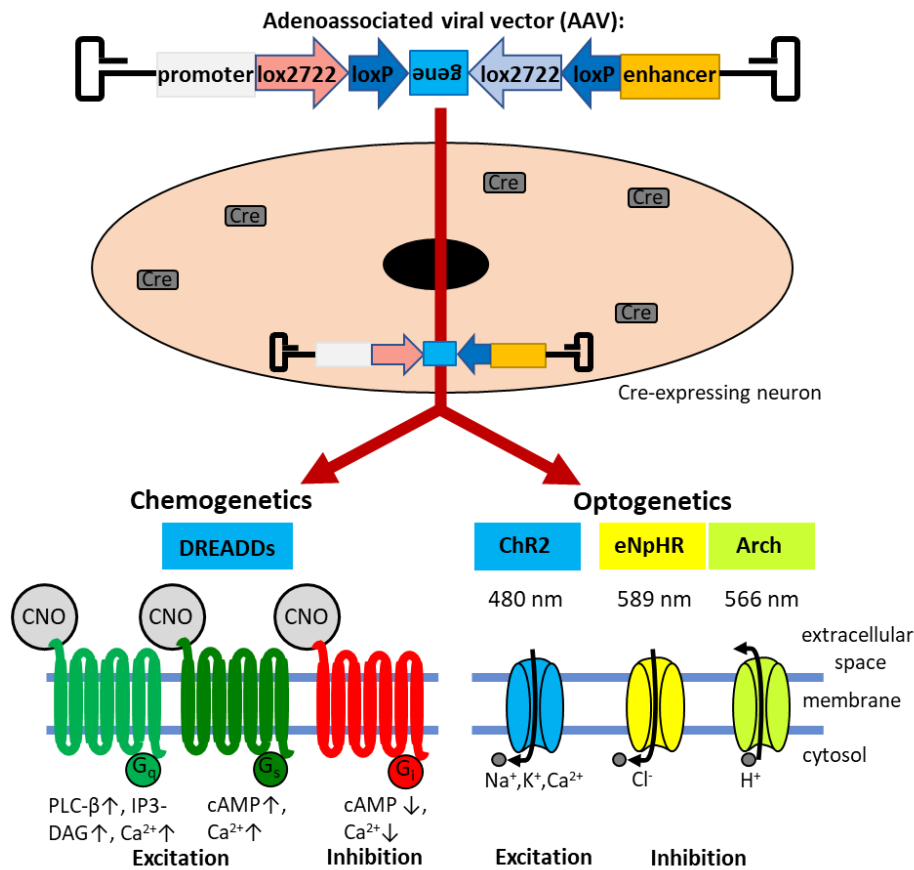


Figure 5. Schematic representation of Cre-mediated AAV expression, chemogenetics and optogenetics

In the AAV, the double-floxed genes can be transcribed only by cells expressing the Cre enzyme. Based on the encoded gene, manipulation of neuronal activity can be achieved by multiple ways. With chemogenetics, the introduced gene encode a DREADD, and after the binding of the artificial ligand, CNO, different signalling pathways are induced: for excitation, G_q (IP3-DAG pathway) and G_s (cAMP production- not that prevalent), while for inhibition G_i (cAMP production inhibition). On the other hand, with optogenetics light sensitive ion channels are introduced: the cation channel ChR2 (activated by blue, 480 nm light) excites the cells, while eNpHR (yellow, 589 nm) inhibits activity by Cl⁻ influx, and Arch (yellow-green, 566 nm) has inhibitory effect through H⁺ efflux.

Arch: Archaerhodopsin; cAMP: cyclic adenosine monophosphate; ChR2: Channelrhodopsin 2; CNO: clozapine-N-oxide; Cre: causes recombination; DREADDs: designer receptors activated exclusively by designer drugs; eNpHR: enhanced halorhodopsin; IP3-DAG: inositol trisphosphate- diacylglycerol; lox2222, loxP: Cre-recognized cleaving sites; PLC-β: phospholipase-β.

2022, Papathanou et al., 2019), which could be due to developmental expression, normally disappearing in adulthood. This led numerous laboratories to breed their own VGLUT3-Cre strain (e.g.: (Fortin-Houde et al., 2023)]. Replicability in science is a hot

debate even nowadays, and the source of differences in results might not only derive from different technics and protocols across the laboratories in different countries, but also due to different animal strains. However, the robustness of a study can be improved in case the experiment is repeated in two independent laboratories and yields the same results despite these differences. In this spirit, part of my experiments was done both in Hungary and France on separate VGLUT3-Cre mouse lines with the same protocol.

1.3.2. Manipulation of neuronal activity

To manipulate neuronal activity during behaviour, two major technics can be used nowadays: chemogenetics and optogenetics. With chemogenetics, AAVs encode designer receptors exclusively activated by designer drugs (DREADDs), which are artificial receptors mutated from the human muscarinic acetylcholine receptor from the G-protein coupled receptor (GPCR) family and can excite (mostly through the G_q pathway) or inhibit (G_i pathway) the host cells. They are activated by clozapine-N-oxide (CNO) (Armbruster et al., 2007, Campbell and Marchant 2018) (**Figure 5**), although many other artificial ligands (e.g. compound 21, perlapine) have already been synthesized (Chen et al., 2015, Thompson et al., 2018). Recent studies showed that although CNO is an inert, physiologically inactive molecule, it also barely penetrates the brain-blood barrier. Moreover, it back metabolizes to clozapine (Dobrzanski and Kossut 2017, Manvich et al., 2018, Roth 2016), which have a better penetration and several off-targets (e.g.: 5-HTR_{2A}, 5-HTR_{2C}, histamine receptor 1) in the brain, inducing sedative effects in high concentrations (10 mg/kg). However, it has also been proved that the CNO concentrations needed for DREADD activation (0.1-3 mg/kg) have no behavioural effects per se (Roth 2016, Thompson et al., 2018). However, careful planning of the control group (e.g.: they also receive CNO injection, but express no DREADD), usage of proper concentrations (1 mg/kg) and monitoring of animals before experiment ensures valuable results. However, due to the nature of DREADDs, chemogenetic manipulations are induced within 15 minutes of CNO administration and can last for at least 1 hour (Roth 2016), or more, thus, it has bad temporal resolution.

Another similar technic is optogenetics, which utilises light-sensitive ion channels to excite (e.g.: cation channel Channelrhodopsin) or inhibit (Archeorhodopsin, Halorhodopsin) cells (Jiang et al., 2017, Nagel et al., 2003). The gene sequence of these can be encoded into AAVs and expressed Cre dependently, just like chemogenetics, but

their activation has to be done via invasive implantation of optic fibres, which delivers the light intracranially. However, laser activity can be controlled by the experimenter, thus, giving greater freedom in the time and/or intensity of the manipulation. Excitation pattern still needs to be chosen carefully, as both overexcitation and tissue heating can be detrimental to the animals (Zelena et al., 2017).

Technology in neuroscience has developed enough to realise experimental designs that investigate specific neuron populations not only *in vitro*, but also *in vivo*, in freely behaving animals. Thus, with the help of VGLUT3-Cre mice, chemogenetics and optogenetics, the more generic conclusions of experiments regarding VGLUT3 KO mice can be detailed by examining brain area specific subpopulations – in this case, the MRR-VGLUT3 neurons.

2. Objectives

The objective of my PhD work was to complement the existing literature on VGLUT3 involvement in social behaviour, learning and memory, specifically focusing on the subpopulation of VGLUT3+ neurons of the MRR. Additionally, experiments were conducted to validate our technics and confirm the literature in mice, and to assess relevance for humans as well.

To achieve these goals, three projects and a validation process were realised:

Project 1: Behavioural characterisation of the VGLUT3 KO mice, with a focus on:

- a) Social behaviour (*paper under review 1*);
- b) Learning and memory (Fazekas et al., 2019).

Project 2: Anatomical study of VGLUT3 in the mouse and human MRR:

- a) In mice by fluorescent *in situ* hybridization (sdFISH), with 5-HT co-expression on mRNA level;
- b) In humans by real time quantitative polymerase chain reaction (RT-qPCR) (*paper under review 1*).

Project 3: Investigation of the role of MRR-VGLUT3 neurons:

- a) Validation of chemogenetics:
 1. Confirmation of AAV-transmitted RFP expression in MRR-VGLUT3 cells of VGLUT3-Cre mice (*paper under review 1*);
 2. Chemogenetic-induced neurotransmitter release in HC by microdialysis (Fazekas et al., 2021);
 3. Confirmation of CNO-induced neuronal activation by c-Fos immunohistochemistry (*paper under review 1*);
- b) Social behaviour by chemogenetic interventions (*paper under review 1*);
- c) Learning and memory formation after chemo- and optogenetic interventions (*paper under review 2*).

With this design we wished to assess whether any of the behavioural phenotypes exhibited by the VGLUT3 KO strain can be directly replicated via MRR-VGLUT3 excitation/inhibition. Extensive behavioural test batteries were performed to answer our questions, complemented by anatomical and molecular biological approaches to further characterise the VGLUT3+ neuronal population. Investigations on molecular levels ensured the validity of our manipulations in mice and the relevance in humans.

3. Materials and methods

Adult male mice (14-15-week-old, C57BL/6J background) were obtained from the local colonies of the Institute of Experimental Medicine, Budapest, Hungary (if not stated otherwise). They were housed in Macrolon cages (40 cm x 25 cm x 26 cm) under constant environmental conditions ($21\pm 1^{\circ}\text{C}$, 50-60% humidity), with food (standard mice chow, Charles River, Hungary) and tap-water available *ad libitum*.

All tests were approved by the local committees of animal health and care (France: Ministère de l'Agriculture et de la Forêt, Service Vétérinaire de la Santé et de la Protection Animale, authorization #01482.01 from ethics committee Darwin #5; Hungary: Animal Welfare Committee of the Institute of Experimental Medicine, Budapest, Hungary and Government Office for Pest County, PEI/001/33-4/2013, PE/EA/254-7/2019) and performed according to the European Communities Council Directive recommendations for the care and use of laboratory animals (2010/63/EU).

For the statistical analysis StatSoft 13.4 (Tulsa, USA) software was used throughout. Data were expressed as mean \pm standard error of mean (SEM) and $p < 0.05$ was considered statistically significant, while $0.1 < p < 0.05$ was accepted as a marginal difference. All marks on figures represent the results of post hoc comparison, while main ANOVA effects are described as texts, where appropriate. All other details of statistics are given at each project.

3.1. Project 1: Behavioural characterisation of the VGLUT3 KO mice

Despite the presence of VGLUT3 in brain areas related to social behaviour (see **1.1.1. chapter**), only the aggressive behaviour of VGLUT3 KO mice has been assessed before. Moreover, VGLUT3 is abundant in the HC, which is a known centrum of spatial learning. Although electrophysiological recordings in VGLUT3 KO mice suggest changes in plasticity in the HC (Fasano et al., 2017), its effects on behavioural level is unknown. Thus, behavioural experiments complementary to the current literature were conducted to answer these questions.

3.1.1. Project 1/a: Social behaviour

3.1.1.1. Animals

Male VGLUT3 WT (N=10) and KO (N=11) mice were bred in heterozygous mating pairs. Their genotype was determined by polymerase chain reaction (PCR) from a small tail sample collected from 2-3-day-old animals. The animals were separated at the first day of the behavioural test battery to increase social interest during subsequent testing.

3.1.1.2. Behavioural testing

Experiments were conducted similarly as in (Chaves et al., 2022), between 9 a.m. and 1 p.m., during the subjective dark period of the mice (lights on at 7 p.m.). Half an hour before the start of the first experiment the animals were socially isolated and remained so until they were sacrificed. This was necessary for investigating social behaviour. The following aspects of behaviour were measured (**Figure 6** illustrates the timeline of the test battery):

1. Mobility in the open field (OF) and elevated plus maze test (EPM) and Y-maze test to rule out any motor problems that would confound other data;
2. Social behaviours with sociability, social interaction test (SIT) and resident intruder test (RIT);
3. Anxiety-like behaviour in the OF and EPM tests, which can also negatively affect social behaviour;
4. Memory processes in the Y-maze and the 24-hour social discrimination (SDT) tests, as problems with short-term memory may affect the amount of social interactions (e.g. not remember seeing the conspecific earlier).

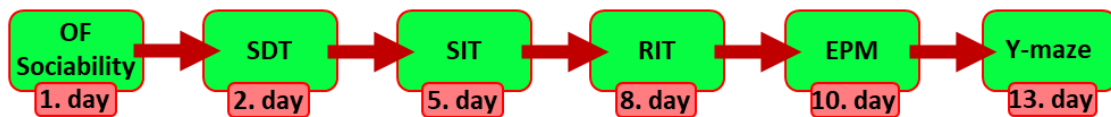


Figure 6. Timeline of the experimental protocol for VGLUT3 WT and KO mice

Detailed investigation of social behaviour (sociability, SIT, RIT) was conducted to complement the existing literature. Confounding factors such as locomotion (OF), anxiety-like behaviour (EPM), and short-term memory impairments (SDT, Y-maze) were also examined.

EPM: elevated plus maze test; KO: knockout; OF: open field; RIT: resident intruder test; SDT: social discrimination test; SIT: social interaction test; VGLUT3: vesicular glutamate transporter type 3; WT: wild-type.

The experimental room was only lit by infrared light during the experiments (except for SIT and EPM, with 100 lux). The experiments were recorded by ceiling-mounted camera (Samsung SNB 7000; OF, sociability, SDT, EPM and Y-maze) or hand-cameras (SIT, RIT) and analysed later by computer-based event recorders (H77, Budapest, Hungary; Solomon Coder [<https://solomoncoder.com>]; Noldus EthoVision, Wageningen, the Netherlands). The test apparatuses were cleaned with 20% ethanol between animals except for SIT and RIT (bedding was used in these cases). There were 48-72-hour intervals between behaviour tests (except for SDT, where only 24 hours passed).

3.1.1.3. *Open field (OF)*

OF was first used to measure the locomotor activity and anxiety-like behaviour of mice. Animals were put into an empty white plastic box (40 cm × 36 cm × 15 cm) without bedding for 5 minutes (**Figure 7A**). Distance moved, frequency and time spent in periphery and centrum (75% of the arena) were analysed by the Noldus Ethovision XT 13 automatic system.

3.1.1.4. *Sociability test*

Sociability test measures the inclination of the animals to behave socially. Right after the OF, 2 identical wired cages (with identical weights on them) were placed into the empty plastic boxes for 5 minutes of habituation. Based on their location they were either labelled as ‘left’ or ‘right’ (object habituation phase). After that an unknown, smaller, juvenile male conspecific was placed under one of the cages for 5 minutes (sociability phase) (**Figure 7A**). At the end of this phase the animals were put back into their home-cages.

During habituation, the frequency and time spent with the two cages were measured to analyse place preference. During sociability the frequency and time spent with its conspecific were measured to reflect social interest. Social preference index (SI) was calculated based on the following equation:

$$SI = \frac{t_{mouse}}{t_{mouse} + t_{cage}} \times 100,$$

where t_{mouse} stands for the time spent sniffing the cage containing the stimulus mouse during sociability; t_{cage} stands for the time spent sniffing the empty cage during sociability. Any other type of behaviour was labelled as ‘other’.

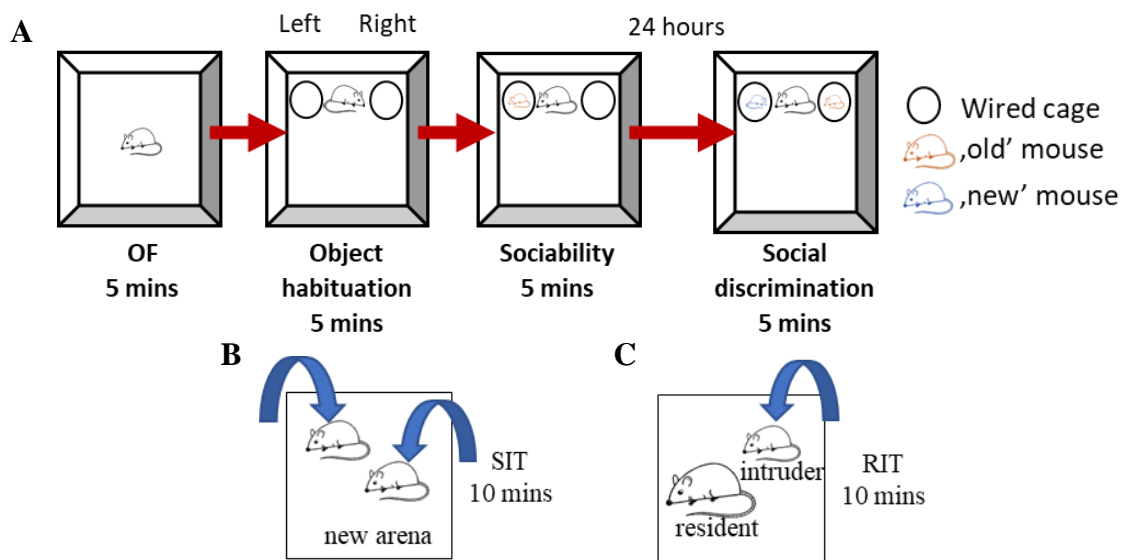


Figure 7. Schematic illustration of the protocols of social behaviour tests

(A) OF-sociability-SDT tests: on the first day of the protocol, 5 minutes of OF, object habituation and sociability phases were conducted consecutively. Then, 24-hour later an SDT took place, during which the stimulus mouse from sociability phase ('old') was placed under a new wired cage and an unfamiliar, 'new' mouse was also introduced. (B) During SIT, two experimental animals from the same treatment group were placed into a neutral territory (plastic aquarium with bedding) under normal lighting conditions, to which they were habituated on the previous day for 2x15 mins. The animals could freely behave for 10 mins. (C) RIT was conducted in the home cage of the experimental animal. For 10 mins, an unfamiliar, physically smaller intruder conspecific was introduced.

KO: knockout; OF: open field; RIT: resident intruder test; SDT: social discrimination test; SIT: social interaction test; WT: wild-type.

3.1.1.5. Social discrimination test (SDT)

SDT is based on the innate preference for novelty of mice. This means that during the test the experimental animal is expected to spend more time with an unknown conspecific than with a familiar one. Twenty-four hours later, the sociability test SDT was conducted. The experimental setting was identical to that of sociability. Under each wired cage one conspecific was placed. One was the same as the one used in sociability (subsequently called 'old' mouse), while the other one was another unknown (subsequently called 'new') mouse. The position of the 'old' mouse was interchanged compared to the previous day to avoid place preference. The test animal could freely behave for 5 minutes (Figure 7A).

The frequency and time spent with sniffing each conspecific were measured. Any other type of behaviour was labelled as ‘other’. Social discrimination index (SD) was calculated based on this equation:

$$SD = \frac{t_{old} - t_{new}}{t_{old} + t_{new}} \times 100,$$

where t_{old} stands for the time spent sniffing the cage containing the familiar stimulus mouse during SDT; t_{new} stands for the time spent sniffing the cage containing the unfamiliar stimulus mouse during SDT.

3.1.1.6. *Social interaction test (SIT)*

SIT is used to investigate the social behaviour of mice influenced by anxiety. The test was conducted in a transparent Plexiglass aquarium (35 cm × 20 cm × 25 cm) with bedding on the bottom. The day before the test animals were put into the respective aquarium one at a time for 2×15 minutes, 4 hours between them, for habituation. During the experiment two animals from the same group (e.g.: KO vs KO), weighting approximately the same were placed into the aquarium. The mice could freely behave for 10 minutes. The test was conducted in normal light (100 lux) (**Figure 7B**).

Social (e.g.: sniffing), aggressive (e.g.: biting, aggressive dominance) and defensive behaviours were analysed (frequencies and time spent) for both test animals. Any other type of behaviour was labelled as ‘other’.

3.1.1.7. *Resident intruder test (RIT)*

RIT measures the aggressive, territorial behaviour of the rodents. An unfamiliar, physically smaller, but adult conspecific was put into the home cage of the test animals. For 10 minutes the animals could freely behave (**Figure 7C**). Only the behaviour of the test animal was analysed (for details see SIT).

3.1.1.8. *Elevated plus maze (EPM) test*

EPM can be used to assess the anxiety-like behaviour of rodents. The animals were placed onto the middle, central zone of the EPM apparatus (height: 25 cm; width: 7 cm; length: 30 cm; 67 cm above the floor) with two open and two closed arms. The mice could freely explore the apparatus for 5 minutes. The test was conducted in bright light (120 lux) (**Figure 8A**).

The number of open and closed arm entries and time spent in each compartment were measured. Open arm entries reflecting mobility independent anxiety were calculated based on this equation:

$$\frac{\textit{open}}{\textit{total}} (\%) = \frac{\textit{number of open arm entries}}{\textit{sum of open + closed arm entries}}$$

The frequency of risk assessment (RA) behaviour (such as head dipping, stretched attend posture [SAP] and rearing) and grooming were also evaluated.

3.1.1.9. Y-maze test

The Y-maze is a test used to study short-term (working) in rodents, as reflected by spontaneous alternation. The apparatus consists of three arms (A, B and C; 25 cm × 5 cm × 21 cm) at 120°, connected by a central zone. The consecutive arm entries reflect the short-term memory of the animals. Mice were placed at the end of arm A and were allowed to freely explore the maze for 5 min (**Figure 8B**).

Spontaneous alternation was calculated based on this equation:

$$\textit{Spontaneous alternation} = \frac{\textit{'correct' alternation}}{\textit{sum of all arm entries} - 2} \times 100.$$

‘Correct’ alternation means entry into all three arms on consecutive choices (i.e. ABC, BCA, or CAB, but not CAC, BAB, or ABA) (Chaves et al., 2022, Fazekas et al., 2019).

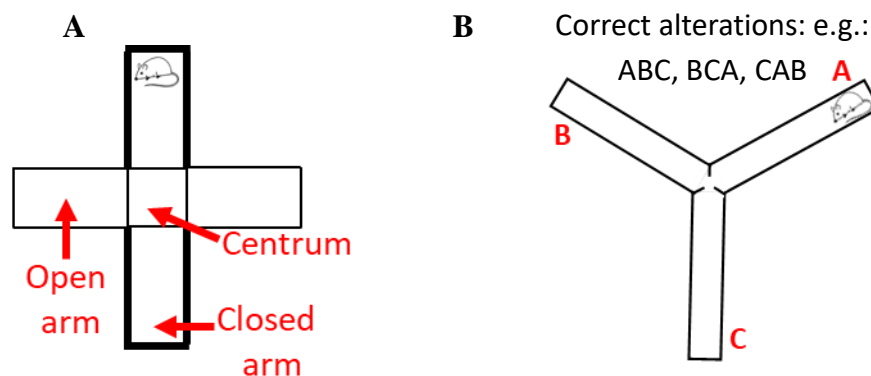


Figure 8. Schematic illustration of the protocols for EPM and OF

(A) At the start of the elevated plus maze test the experimental animals were placed at the centrum of the apparatus and could freely explore it for 5 minutes. (B) Mice spent 5 minutes in the Y-maze test, where their consecutive arm entries were counted. Correct short-term (working) memory is reflected by more than 50% spontaneous alternation value, which is above the chance level of the ‘correct’ arm.

3.1.1.10. Statistical analysis

Outliers were defined as data points which were not in the interval of group mean $\pm 2 \times \text{SD}$ for the given parameter, and thus, were excluded from the statistical analysis. This outlier analysis revealed uncharacteristically inactive behaviour resulted in the following number of animals: 1 WT mouse in the OF test; 3 WT mice in the Y-maze test; 1 WT and 1 KO mice in sociability and social discrimination tests.

To compare WT-KO animals, t-test (effect of genotype) was used when conditions were met (normality and homoscedasticity). SI and spontaneous alteration were tested with single-sample t-test against 50%, while SD values were tested against 0%. The comparison of sides (left vs. right), social preferences in sociability (mouse vs. cage) and social discrimination (old vs. new) tests were conducted by mixed-design analysis of variance (ANOVA; effect of genotype and effect of choice as repeated factor). For aggressive behaviour of WT-KO animals in SIT contingency table was made and Pearson Chi-square test was conducted (see in **4.1.1.4. chapter**). Fisher LSD was used as a post hoc analysis.

3.1.2. Project 1/b: Learning and memory formation

3.1.2.1. Animals

Another batch of adult (13-25-week-old) male VGLUT3 WT (N=8) and KO (N=8) mice were housed individually under a standard 12 h light–dark cycle (lights on at 6 a.m.).

3.1.2.2. Behavioural testing

Tests were carried out between 9 a.m. and 1 p.m. in a separate room under similar lighting conditions as in the animal facility (~150 lux) and recorded by ceiling-mounted camera (Samsung SNB 7000) and analysed using Noldus EthoVision XT 13.

3.1.2.3. Morris water maze (MWM) task

MWM is a HC based, spatial learning and memory task motivated by the aversive behaviour of mice towards water. A circular pool made of bright grey plastic (90 cm in diameter and 40 cm in height) was filled with tap water (24 ± 2 °C), made opaque by white wall paint, and the level of the water was 1 cm higher than the platform (6 cm in diameter) except for learning day 1, when the platform was above the water. The

apparatus was divided into 4 quadrants (northeast [NE], northwest [NW], southeast [SE] and southwest [SW]) and the platform was installed in the middle of one quadrant.

Mice were released into the water from different points across trials and were allowed to swim freely for 1 min to find the platform. If they did not find the platform in time, they were helped to find it and allowed to stay there for 10 sec. The learning phase (day 1-6) consisted of 4 trials with a 30 min intertrial interval (ITI), during which the animals were returned to their home cages. On day 7 (probe 1) the platform was removed from the water and the mice had 1 min to search for the missing platform. From day 8 the platform was put to another quadrant and the animals were tested using the same protocol (cognitive flexibility, day 8-10). On the last day (day 11, probe 2) the platform was once again removed (Morris R. 1984). Latency to reach the platform, distance moved, and time spent in as well as frequency to enter the different zones were calculated.

3.1.2.4. Statistical analysis

Data were analysed by single sample t-test (quadrant preference vs chance level 25%), ANCOVA with locomotor activity as covariate, repeated measure ANOVA or General linear module (repeated measures on time) followed by Newman Keuls post hoc comparison.

3.2. Project 2: Anatomical study of VGLUT3 in the mouse and human MRR

As it was mentioned in the introduction previously, there is a significant VGLUT3 neuron population in the MRR (around 11% of all MRR neurons), which either co-express 5-HT markers, or are exclusively glutamatergic regarding their classical neurotransmitter type. We wished to confirm the literature at mRNA level by conducting double probe fluorescent *in situ* hybridization (sdFISH) in the MRR against the VGLUT3 and Tph2, the rate-limiting enzyme of 5-HT production, and quantify what percentage of VGLUT3+ neurons co-expressing 5-HT. Moreover, we also checked whether human homologue brain sites in the brainstem also contain VGLUT3 mRNA by RT-qPCR in healthy *port-mortem* samples.

3.2.1. Project 2/a: VGLUT3 mRNA and its co-expression with Tph2 mRNA by sdFISH

C57BL/6NRj mice (4 males and 4 females, 7-week-old all) were acquired from Janvier Laboratories (France) were sacrificed and their brains were fresh-frozen in -30°C

isopentane. The samples were sectioned to 16 μm thick slices in cryostat on -20°C , adhered to SuperFrost® Plus slides, and kept on -80°C until further processing. Samples were serially sectioned into 10 series, meaning that in one series adjacent slices were 160 μm apart. Half of the animals, equally from each sex, were cut in rostral-caudal direction, while the rest were cut from caudal-rostral orientation.

After air drying, the samples were fixed in 4% paraformaldehyde (PFA, Merk Millipore, #1040051000, 10 mins, room temperature [RT]) and equilibrated in triethanolamine (TEA, Sigma-Aldrich, #T58300, pH 8) before being acetylated in 0.25% acetic-anhydride (Sigma-Aldrich, #A6404, solved in TEA, RT) (Dumas and Wallen-Mackenzie 2019). After phosphate- buffered saline (PBS, diluted from original stock: x10, EUROBIO, #GAUPBS0007) wash (3x10 mins) samples were hybridized (16-18 hours, 65°C) in formamide-buffer containing 1 $\mu\text{g}/\text{ml}$ digoxigenin (DIG) and fluorescein antisense riboprobe (specificity verified by NCBI blast). **Table 1** contains the details of these probes.

Table 1. Specifications of riboprobes used for the sdFISH experiments

All probes were synthesized by a transcriptional reaction.

AS: antisense; DIG: digoxigenin; S: sense; sdFISH: double-probe Fluorescent in situ hybridization; Tph2: tryptophan hydroxylase 2; VGLUT3: vesicular glutamate transporter type 3.

Probe	Bases	Sequence		Label	Reference
Tph2 NM_173391.3	1899- 2320	Tph2_ S_T3	AATTAACCCTCACT AAAGGGACAAAGA GCCCCGCAAAGGC G	DIG	Sigma- Aldrich - 11277073910
		Tph2_ AS_T7	TAATACGACTCACT ATAGGGCTGCTCCA TACGCCCGCAGT		
VGLUT3 NM_182959.3	270- 1262	VGLUT3- S-T3	AATTAACCCTCACT AAAGGGAGAAAA CAGGACTGGGCTG ACCC	Fluorescein	Sigma- Aldrich - 11685619910
		VGLUT3- AS-T7	TAATACGACTCACT ATAGGGAGAGAGA CCAAGGTCCATATT CCC		

Next day, the slides were washed with saline-sodium citrate (SSC) buffer of descending concentrations (x5-x0.2; diluted from original stock: x20, Invitrogen,

#AM9763) on 65°C. Final wash was on RT, which was followed by maleic acid-tween 20 (MABT, Sigma-Aldrich, #M0375 and 0.1% Tween 20, Sigma-Aldrich, #P1379) wash (3x10 mins, RT). Slides were blocked with 20% foetal bovine serum (FBS, Invitrogen, #10106-169) and 1% blocking solution (BS, Roche, #11096176001) for 20 mins (RT). First revelation was done by anti-fluorescein-peroxidase (1:5000, Roche, #11426346910) solved in FBS+BS for 1.5 hour. After MABT (3x10 mins) and PBS-0.1% Tween (3x10 mins) washes, revelation was done by placing fluorescein (Cy2)-tyramide (1:250) in 0.001% H₂O₂ (Sigma Aldrich, # 216763) – PBST solution for 1 hour, then washed with PBST (3x10 mins). For peroxidase inhibition a 20-minute-long glycine buffer (0.1 M, pH=2.1, Sigma-Aldrich, #G7125, diluted in PBS) and a 20-minute 3% H₂O₂ wash was used. The slides were left in PBST overnight on 4°C. MABT (3x10 mins) washes and a 20-minute-long FBS-BS blocking was followed by a 1.5-hour incubation in anti-DIG-peroxidase (1:1000, Roche, #11207733910) -FBS-BS solution. Revelation followed MABT (3x10 mins) and PBST (3x10 mins) washing: Cy3-tyramide (1:100) was diluted in 0.001% H₂O₂-PBS solution and incubated for 1-hour on RT. After PBST (5x10 mins), nuclear 4',6-diamidino-2-phenylindole (DAPI; 20 mins, Sigma-Aldrich, #D9542) staining and a final PBST wash (3x5 mins) were applied. Fluoromount (Southern Biotech, #0100-01) was used for mounting. Cy2-tyramide and Cy3-tyramide were synthesized as previously described (Hopman et al., 1998). Slides were scanned by NanoZoomer 2.0-HT (20x resolution, Hamamatsu Photonics). Laser intensity and time of acquisition were set separately for each riboprobe. Images were created by using NDP.view2 software (Hamamatsu Photonics) and ImageJ (Rasband, W.S., ImageJ, U. S. National Institutes of Health, Bethesda, Maryland, USA, <https://imagej.nih.gov/ij/>, 1997-2018).

Cell counting was done using the QuPath software for Windows (Bankhead et al., 2017). The MRR was identified based on “The mouse brain in stereotaxic coordinates” (Paxinos 2001). VGLUT3+ cells which had a clear DAPI stained nuclei, and VGLUT3-Tph2 co-positive cells were manually counted from Bregma -4.04 mm to -5.02 mm. For every animal, the number of cells were averaged to the number of slides (7.875 slide/animal on average). The percentage of co-expressing cells were counted as the following: average number of VGLUT3+/Tph2+ co-positive cells divided by all VGLUT3+ cells, multiplied by 100.

3.2.2. Project 2/b: VGLUT3 mRNA detection by RT-qPCR in the human MRR-equivalent

The study was approved by the Hungarian Medical Research Council – Scientific and Research Ethical Committee (Egészségügyi Tudományos Tanács – Tudományos és Kutatásetikai Bizottság, #40197-2/2019/EKU), in accordance with the Ethical Rules for Using Human Tissues for Medical Research in Hungary (HM 34/1999) and the Code of Ethics of the World Medical Association (Declaration of Helsinki). *Post-mortem* brain samples were obtained from the Human Brain Tissue Bank, Semmelweis University (Budapest, Hungary). The brain of eleven individuals who died of natural causes were used in the measurement. Average \pm SEM age was 56.454 \pm 4.332 years, while the *post-mortem* delay was 5.727 \pm 0.705 hours. For detailed information, see **Table 2**.

Table 2. Subject information for the RT-qPCR measurements in the brainstem of humans

Brain No.	Biological sex	Age	<i>Post mortem</i> delay	Cause of death
#165	female	88	2.5 h	cardiac and respiratory insufficiency
#186	female	56	5 h	myocardial infarction
#211	female	56	6 h	cardiorespiratory insufficiency
#216	male	53	5 h	pulmonary embolism
#227	male	55	6 h	acute myocardial infarction
#228	male	27	8 h	pneumonia
#231	female	55	5 h	bronchopneumonia, cardiorespiratory insufficiency
#242	male	50	5.5 h	stroke, brain haemorrhage
#244	male	53	2 h	acute myocardial infarction
#256	male	67	10 h	pancreas cancer
#266	male	61	8 h	stroke
#267	female	91	8 h	stroke
#272	female	75	10 h	stroke
#273	male	64	10 h	stroke
#282	female	94	4 h	stroke, hypertension

Total RNA was isolated by using the RNeasy® Mini Kit (Biomarker Kft., Gödöllő, Hungary) according to the manufacturer's instructions. RNA was diluted with RNase-free water. The quality and quantity of extracted RNA was determined using NanoDrop ND-1000 Spectrophotometer (Thermo Fisher Scientific, Waltham, MA,

USA), and only those with A260/A280 ratio between 1.8 and 2.1 were used in subsequent experiments. The isolated RNA concentration was calculated and normalized with RNase-free water and reverse transcribed into cDNA using SuperScript II reverse transcriptase kit (Invitrogen, Carlsbad, CA, USA). After 10-fold dilution, 2.5 μ L of the resulting cDNA was used as template in PCR reactions using SYBR Green dye (Sigma, St Louis, MO, USA). The PCR reactions were performed on CFX-96 C1000 Touch Real-Time System (Bio-Rad Laboratories, Hercules, CA, USA) with iTaq DNA polymerase (Bio-Rad Laboratories) in total volumes of 12.5 μ L under the following conditions: 95°C for 3 min, followed by 35 cycles of 95°C for 0.5 min, 60°C for 0.5 min, and 72°C for 1 min. A melting curve was performed at the end of amplification cycles to verify the specificity of the PCR products. All the determinations were conducted in duplicate. The primers used for RT-qPCR were synthesized by Integrated DNA Technologies, Inc., (IDT, Coralville, IA USA) and used at 300 nM final concentration. Sequences of intron spanning primers were designed based on the common parts of the two splice variants (NM_001145288.2 and NM_139319.3, 122nt-3834nt). The forward primer was GTC TGT CCC CTC ATT GTC GG (20 bases), while the reversed primer was CAC AAT TCT GGG AGG TGG CT, with an expected product size of 280 bp. Final cDNA products were sequenced by BIOMI Kft (Gödöllő, Hungary) and showed matching to the originally used primers (available upon request). One third of the amplified PCR product was loaded in an agarose gel (1.2%) containing Eco Safe nucleic acid staining solution (1:20.000, Pacific Image Electronics, New Taipei City, Taiwan) and the electrophoresis was conducted in 1x TAE (40 mM Tris-Acetate, 1 mM EDTA, pH 8.0) buffer. The applied separation voltage was 100 V. After the electrophoresis the DNA bands were visualized by ultraviolet transillumination.

3.3. Project 3: Investigation of the role of MRR-VGLUT3 neurons in behaviour

As mentioned in the introduction, we wondered whether VGLUT3 was highly expressed in the MRR, and whether the behavioural changes observed in VGLUT3 KO mice could be attributed to this MRR-VGLUT3 neuronal population. Moreover, it is known from the literature that these neurons not only project to brain areas relevant to social behaviour, such as the mPFC (Szonyi et al., 2016), but also to the HC, which plays a crucial role in learning and memory formation. Previously we showed that MRR

excitation not only results in the release of 5-HT, but also of Glu and GABA in the mPFC (Balazsfi D., Zelena, et al., 2018). Additionally, we measured neurotransmitter (5-HT, Glu, GABA) release in the HC in **3.3.1.2. chapter**.

For this reason, we used the previously validated VGLUT3-Cre mice in behavioural paradigms. We conducted the same experiments as described in **Project 1**. However, as the MWM protocol described in **3.1.2.3. chapter** did not prove to be sensitive enough, we therefore adapted a modified protocol from (Daumas et al., 2017). Moreover, since **Project 3/c** was conducted in the form of a joint, international PhD program, aiming not only to widen the available techniques, but also to reinforce the reproducibility of our experiments, it was imperative to use identical protocols between labs.

3.3.1. Project 3/a: Validation of chemogenetics

Since chemogenetics was newly introduced to the laboratory at the start of this project, we wished to validate the technic by measuring neurotransmitter release in the HC after AAV-delivered, excitatory DREADD activation of the MRR. Then, AAV coded RFP expression was checked in the VGLUT3+ cells of the MRR with fluorescent double-immunohistochemistry. Additionally, we also conducted c-Fos staining after CNO administration to prove that functional DREADDs were present in MRR-VGLUT3 cells.

3.3.1.1. Validation 1: Cre-dependent RFP expression in MRR-VGLUT3 cells of VGLUT3-Cre mice

To validate that after AAV injection the RFP indeed appears in VGLUT3+ neuron in VGLUT3-Cre strain we used adult male animals (8-week-old, original breeding pair from Jackson Laboratories, strain #018147, kept in homozygous Cre breeding pairs). Mice were anaesthetized by an intraperitoneal (ip.) cocktail (0.1 ml/10 g mixture of 0.5 ml ketamine [Produlab Pharma B.V., Raamsdonksveer, The Netherlands], 0.1 ml xylazine [Produlab Pharma B.V.] and 2.4 ml saline [KabiPac, Bad Homburg, Germany]) and fixed in a stereotaxic frame (David Kopf Instruments, Tujunga, CA, USA). Recombinant AAV (serotype 8) were obtained from Addgene (Watertown, MA, USA) containing Cre-dependent red fluorescent protein (RFP) sequences (20 nl; #50459) into the MRR (AP: -4.1 mm; L: 0 mm; DV: 4.6 mm from Bregma).

Specificity of the virus expression was validated by double fluorescent immunohistochemistry against VGLUT3 and the AAV-coded RFP. Animals were

anaesthetized with the previously described ketamine-xylazine solution and their brains were perfused with PBS and 4% PFA, then kept in PFA for 4 hours. The solution was replaced by PBS containing azide (1g/L). Before sectioning, the solution was changed to 10% sucrose-PBS for cryoprotection for some days, then the MRR region was cut by a sliding microtome (30 μ m) and the slides were kept at -20°C in cryoprotective solution till further processing. The slices were washed with PBS for 3 \times 10 minutes. Blocking was done with 5% normal goat serum (NGS, Jackson) and 0.2% TXT (Sigma Aldrich) diluted in PBS for 30 minutes. For 2 nights they were incubated in anti-RFP (1:1000, rat, Chromotek, #5f8-100, Planegg-Martinsried, Germany), anti-VGLUT3 (1:600, rabbit, Synaptic Systems, #135203, Goettingen, Germany), 5% NGS and 0.2% TXT primer solutions diluted in PBS on 4°C. After 3 \times 10 minutes of PBS washing they were incubated in a solution containing anti-rabbit antibody conjugated with Alexa-488 (1:500, goat, Jackson, #111-545-003,) and anti-rat antibody conjugated with Alexa-594 (1:1000, goat, Invitrogen, #A11029, Waltham, MA, USA) diluted in PBS. After 3 \times 10 minutes of PBS washing the slices were mounted with gelatine and covered with Mowiol (Sigma-Aldrich). The double immunofluorescent staining was evaluated by C2 confocal laser-scanning microscope (Nikon Europe; 20 \times objective).

3.3.1.2. Validation 2: Neurotransmitter concentration measurement in HC by microdialysis after MRR excitation

C57BL/6J mice were prepared for surgery as described in **3.3.1.1. chapter**. Recombinant AAV (serotype 8) encoding excitatory DREADDs (hM3Dq, Addgene, #114472, N=4) or only RFP (control; Addgene, #50474, N=3) gene sequences. The AAVs were injected (20 nL) into the MRR (AP: -4.1 mm; L:0.0 mm; DV:4.6 mm from Bregma; **Figure 9**) (Balazsfi D., Zelena, et al., 2018, Balazsfi D. G. et al., 2017, Chaves et al., 2022, Fazekas et al., 2021).

Microdialysis samples were collected four weeks after surgery from head-fixed, anaesthetized animals (Balazsfi D., Zelena, et al., 2018, Goloncser et al., 2017). A microdialysis probe (EICOM CX-I Brain Probe [membrane: artificial cellulose, molecular weight cut off: 50,000 Da, OD: 0.22 mm, length: 2 mm]) was placed into the dorsal HC (AP: -2.4 mm; L: -2.2 mm; DV: 2.5 mm from Bregma). Sample collection started after 2-hour equilibrium. Samples were collected every 30 minutes for 3 hours. After 1 hour all animals received ip. CNO injection (1 mg/10 mL/kg solved in saline,

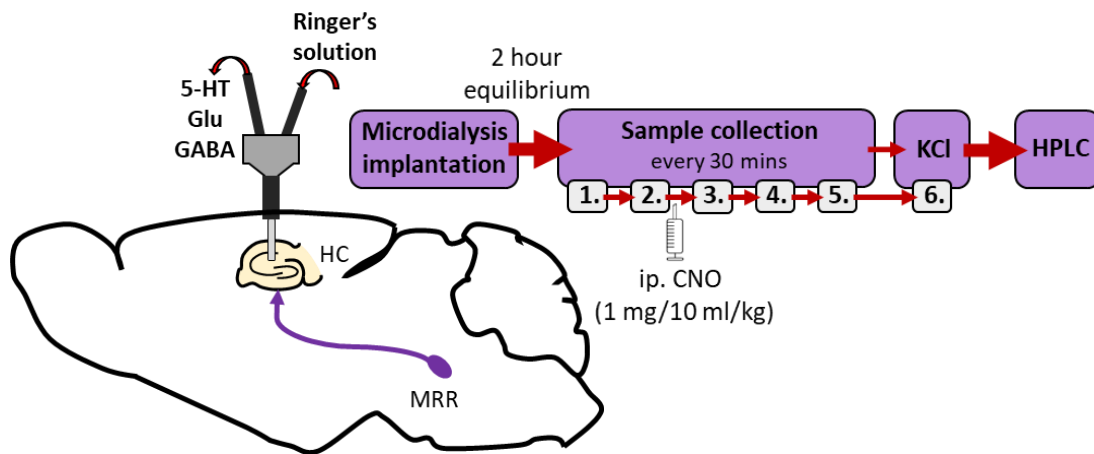


Figure 9. Schematic illustration of MRR neurotransmitter release in the HC

WT C57BL/6J mice were injected with AAVs containing either control (RFP) or excitatory (G_q +RFP) sequences in the MRR. Four weeks later the animals were anaesthetised and microdialysis probes were implanted into dorsal HC. After 2 hours of equilibrium, samples were collected every 30 minutes. After the second sample was collected (1 hour), ip. CNO injection (1 mg/10 ml/kg) was given to all animals. Survival of neurons were validated by KCl injection. Neurotransmitter concentrations were measured by HPLC.

CNO: clozapine-N-oxide; HC: hippocampus; HPLC: high performance liquid chromatography; ip.: intraperitoneal; MRR: median raphe region; AAV: recombinant adenoassociated viral vector; RFP: red fluorescent protein; WT: wildtype.

Tocris) and for another 1.5-hour samples were collected every 30 minutes. Before the start of the last 30 minutes, Ringer's solution was exchanged to KCl (100 mM in Ringer's solution) for 5 minutes in order to validate the viability/reactivity of the cells around the microdialysis probe. The placement of the probe was verified on coronal sections of the dorsal HC by using C2 confocal laser-scanning microscope (Nikon Europe; 4x objective).

The high-performance liquid chromatography (HPLC) system was the following: Shimadzu LC-20 AD Analytical & Measuring Instruments System, Agilent 1100 Series Variable Wavelength Detector set at 253 nm and an electrochemical amperometric detector BAS 400, Bioanalytical System set at 730 mV potential. HPLC separation was performed by Shimadzu LC 20 AD Analytical System, using UV (Agilent 1100 VW set at 253 nm), Fluorescence (Gilson model 121 fluorimeter, at 340 nm excitation and 450 nm emission wavelengths) and amperometric detection (by BAS CC-4 thin layer electrochemical cell at an oxidation potential of 0.73V). ACE Ultra Core Super columns were used for analysis; Phenyl-Hexyl packed column (75×2.1 mm) was used for sample

enrichment and purification and the separation was completed by connecting the analytical C-18 (150×2.1 mm) column.

5-HT content was determined by online column switching separation using Discovery HS C18 50×2mm and 150×2mm columns. The flow rate of the mobile phases (A:10 mM potassium phosphate, 0.25 mM ethylenediaminetetraacetic acid [EDTA]; B: with 0.45 mM octane sulphonyl acid sodium salt, 8% acetonitrile, 2% methanol; pH 5.2) was 350 or 450 $\mu\text{L}/\text{minute}$, respectively, in a step gradient application. The enrichment and stripping flow rate of the buffer (10 mM potassium phosphate, pH 5.2) was 4 minutes. The total runtime was 55 minutes.

The remaining sample (60 μL) was diluted with water and the pH was adjusted to 10.5 (with 2.7 M Na_2CO_3 solution containing 100 μM nor-Valine, as an internal standard). Samples were reacted with 20 mM dansyl chloride at 70°C for 15 minutes and the dansylated Glu and GABA separation was performed on the above-described HPLC system. The flow rate of mobile phases (A: 10 mM ammonium formate, 16.8% acetonitrile, methanol 4.8%; B: 10 mM ammonium formate, 70% acetonitrile, methanol 20%, pH 3) was 400 $\mu\text{L}/\text{minute}$ in a linear gradient mode. The enrichment and stripping flow rate of the buffer (10 mM ammonium formate, 1.9% acetonitrile, 1.1% methanol) was 300 $\mu\text{L}/\text{minute}$ during 4 minutes, with a total runtime of 55 minutes.

The recovery of the microdialysis probes was evaluated at the end. The *in vitro* extraction efficiency for 5-HT, glutamate and GABA were estimated to be $21.1\pm 4.8\%$, $17.1\pm 2.8\%$, and $21.9\pm 3.4\%$, respectively. The concentrations were given in pmol/mL for 5-HT, while for Glu and GABA in nmol/mL.

The change in neurotransmitter concentration is expressed in percentage compared to the average of the first 2-hour concentrations: $\text{change (\%)} = \{c_k / [(c_1 + c_2) / 2] \times 100\}$, where c_k stands for the concentration of given neurotransmitter at given time; c_1 and c_2 stands for the concentration of given neurotransmitter in the first and second sample collection time points, respectively.

For every neurotransmitter, data were compared with repeated measures ANOVA (effect of time, effect of excitation, excitation×time interaction).

3.3.1.3. Validation 3: Validation of chemogenetic-induced neuronal activation by c-Fos immunohistochemistry

Another group of mice were injected with an AAV containing the G_q signalling DREADD and RFP, called excitatory group (Addgene, #44361). Two weeks later VGLUT3-Cre mice (control: N=6; excitatory: N=3) were injected ip. with CNO (1 mg/10 mL/kg) and perfused 30 (time for CNO to take effect) +90 minutes (c-Fos expression peak) later. c-Fos cell counting in MRR was done by nickel-3,3'-diaminobenzidine (Ni-DAB) staining. Brains were prepared as described in **3.3.1.1. chapter**. After 10 minutes of PBS washing the slices were incubated in 0.5% TXT and 0.3% H₂O₂ for 30 minutes. Then they were washed in PBS for 3×10 minutes. Blocking was done with 2% BSA diluted in PBS for an hour, then they were incubated in the anti-c-Fos primer solution (1:1000, rabbit, #sc-52, Santa Cruz, CA, USA; 2% BSA and 0.5% TXT diluted in PBS) for 2 nights on 4°C. The secondary solution consisted of biotinylated (biotin-SP) anti-rabbit secondary solution (1:1000 donkey, #711-065-152, Jackson, Cambridgeshire, UK; 2% BSA diluted in PBS). The signal was strengthened with avidin-biotin complex (1:1000, ABC; Vector Laboratories, Newark, CA, USA), then developed in the presence of DAB ($10 \frac{mg}{ml}$) and 1% NiNH₄SO₄ (Sigma-Aldrich) and H₂O₂ (Sigma-Aldrich). The mounting was done in gelatine (G9391, Sigma-Aldrich), then the slides were dehydrated in xylol and covered with DPX (Sigma-Aldrich).

The stained slices were scanned by Panoramic MIDI II Slidescanner (3DHISTECH, Budapest, Hungary) and cell bodies were counted with ImageJ automatically. For every animal 3 slices were counted and averaged per brain area. To compare c-Fos positive cell numbers t-test (effect of manipulation) was used.

3.3.2. Project 3/b: Social behaviour

3.3.2.1. Animals

All male VGLUT3-Cre mice were obtained from the same source as described in **3.3.1.1. chapter** and kept in a 'reversed' 12-hour light–dark cycle (lights on at 7 p.m.). The animals were separated at the first day of the behavioural test battery to increase social interest during subsequent testing.

3.3.2.2. Surgery

Animals went under the same surgery as described in **3.3.1.1. chapter**. The AAVs used in this project contained the same control (RFP, N=8) and excitatory (G_q +RFP, N=13) sequences as described in **3.3.1.3. chapter**, and additionally an inhibitory group (G_i +RFP, Addgene, #44362, N=15) was also included (**Figure 10A**). Animals had 28 days to recover, during which they were accustomed to the reversed light-dark cycle (lasted 14 days).

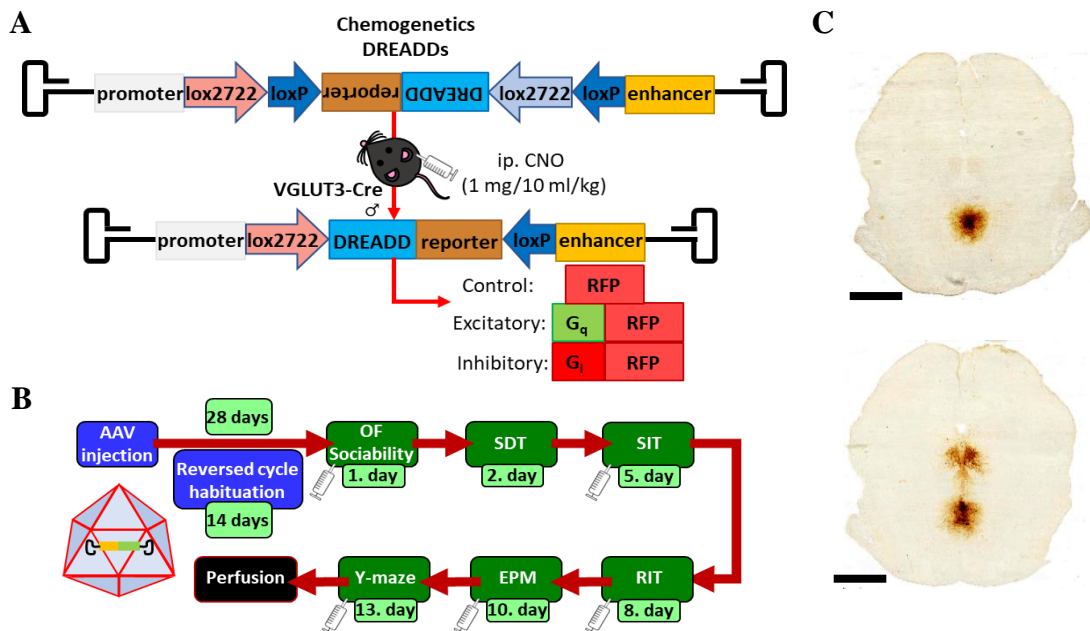


Figure 10. Preparation of VGLUT3-Cre mice for Project 3/b

(A) Schematic representation of the Cre-dependent AAVs used in VGLUT3-Cre mice. The vectors contained floxed sequences (lox2722, loxP) of DREADDs (G_q excitatory and G_i inhibitory) and the reporter protein (RFP, control), which can be properly expressed by only Cre-expressing VGLUT3+ neurons. Activation of the DREADDs was done via their artificial ligand, the CNO (1 mg/10 ml/kg), which was ip. injected 30 minutes before the start of the experiments. (B) Timeline of the experiments. The same protocols as described in **3.1.1.2. chapter**. Pictograms of syringes indicate CNO injections. (C) Example of a proper (upper) and excluded (lower) RFP expression in VGLUT3-Cre mice. Scale indicates 1000 μ m.

CNO: clozapine-N-oxide; DREADD: designer receptor activated by designer drugs; EPM: elevated plus maze test; ip.: intraperitoneal; OF: open field; AAV: recombinant adenoassociated viral vector; RFP: red fluorescent protein; RIT: resident intruder test; SDT: social discrimination test; SIT: social interaction test; VGLUT3: vesicular glutamate transporter type 3.

3.3.2.3. *Behavioural testing*

Exactly the same protocols as described in **3.1.1. chapter** were repeated. All groups received ip. CNO injection (1 mg/10 ml/kg solved in saline, CAS No.:34233-69-7, Tocris Bioscience, Ellisville, Missouri, USA) 30 minutes before the start of the experiments, except for SDT, when they were not injected in order to investigate the effect on memory consolidation. **Figure 10B** illustrates the timeline of the experiments.

3.3.2.4. *Immunohistochemistry*

At the end of the test battery the animals were euthanized as described previously, and their viral expression was validated with the same protocol as described in **3.3.1.3. chapter** checking for the presence of RFP (anti-RFP: 1:4000, rabbit, #600-401-379, Rockland Inc., Swedesboro, NJ, USA) (Biro et al., 2017, Chaves et al., 2022, Fazekas et al., 2021). The Ni-DAB-stained slices were evaluated by Olympus DP70 light microscope (4× objective). The virus expression was examined from -4.04 mm to -4.96 mm from Bregma. If there was no staining, or it was unilateral, or other brain regions (e.g.: DR) were also stained, then the test animal and the data belonging to it were excluded (17 from a total of 53 animals) from the statistical analysis (see example **Figure 10C**).

3.3.2.5. *Statistical analysis*

Outliers were defined as data points which were not in the interval of group mean $\pm 2 \times \text{SD}$ for the given parameter, and thus, were excluded from the statistical analysis. This outlier analysis revealed uncharacteristically inactive behaviour resulted in the following number of animals: 1 mouse in the inhibitory group in the Y-maze test; 2 mice in the excitatory group during sociability test – object habituation phase, out of which 1 had to be also excluded from the rest of the experiment (sociability phase, social discrimination test) as well. In the SIT and the EPM test, 1-1 mouse from the excitatory group was excluded, respectively. Finally, 2 mice (1 control and 1 inhibitory) had to be removed from RIT analysis.

To compare the groups one-way ANOVA (effect of manipulation) was used. SI and spontaneous alteration were tested with single-sample t-test against 50%, while SD values were tested against 0%. The comparison of sides (left vs. right), social preferences in sociability (mouse vs. cage) and social discrimination (old vs. new) tests were done with repeated-measures ANOVA (effect of manipulation, effect of choice). Fisher LSD was used as a post hoc analysis.

3.3.3. Project 3/c: Role of MRR-VGLUT3 neurons in learning and memory formation

3.3.3.1. Animals

The experiments were conducted at two locations. The chemogenetics experiment was performed at Sorbonne Université, Paris, France, while the optogenetics one was done at the Institute of Experimental Medicine, Budapest, Hungary. The protocols, handling procedures and environments (lights on at 7 a.m.) were kept identical in the two countries. Any discrepancies between the labs are indicated. All VGLUT3-Cre (heterozygous) male and female mice were obtained from their respective local colonies (C57BL/6J background, France: locally bred from heterozygous breeding pairs, genotyped by PCR; Hungary: as described in **3.3.1.1. chapter**). All animals were accustomed to handling 3-4 days before the start of the behavioural experiments.

3.3.3.2. Surgery

VGLUT3-Cre mice went under stereotaxic surgery as described previously in **3.3.1.1. chapter**. For details see the corresponding individual experimental descriptions and **Figure 11A**.

3.3.3.2.1. Chemogenetics approach

In order to manipulate MRR-VGLUT3 neurons and assess their involvement in learning and memory processes, we used the chemogenetics approach in France. Briefly, the same AAVs were used as described in **3.3.1.3. chapter**: control (N=6♀7♂) and excitatory groups (N=6♀6♂) were established (Balazsfi D., Zelena, et al., 2018, Balazsfi D. G. et al., 2017, Chaves et al., 2022, Fazekas et al., 2021). Half an hour before the start of the behavioural experiments the animals received an ip. CNO (Tocris Bioscience, CAT No.: 4936/10) injection (1 mg/10 ml/kg solved first in dimethyl sulfoxide [DMSO; 0.25% of the final solution], then in saline). After task completion, animals were euthanized with ip. Euthasol (10 mg/20 g; Ceva Santé Animale, France). Their brains were fixed by transcardial perfusion with PBS, then 4% PFA and stored in PFA for 1 day. Then the solution was changed to PBS. Thirty µm thick slices were cut by vibrotome (Leica VT 1000S) and stored in azide-PBS (0.2 g/L) until further processing.

Additionally, in order to prove the reproducibility of our experiments, the same chemogenetic experiments were repeated in Hungary as well, with control (N=7♀7♂)

and excitatory (N=8♀5♂) groups in VGLUT3-Cre animals as described in 3.3.1.1. chapter.

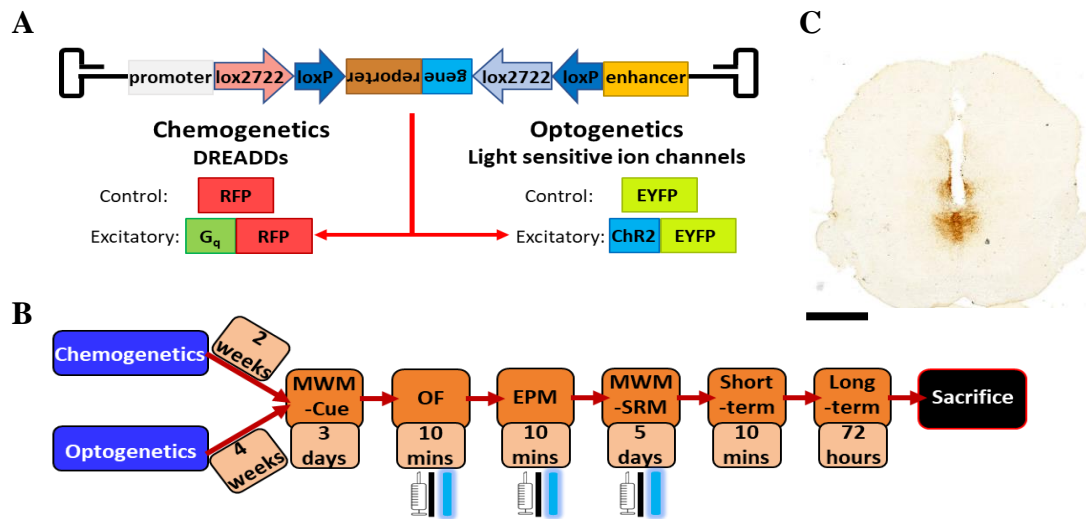


Figure 11. Preparation of VGLUT3-Cre mice for Project 3/c

(A) Schematic illustration of the AAVs used in the experiments. In France (left), chemogenetics with DREADDs were utilised that encoded either solely RFP (control), or excitatory DREADD (G_q) and RFP. In Hungary (right), optogenetics with light sensitive ChR2 (excitation) was expressed in the VGLUT3+ neurons with EYFP reporter protein (control). (B) Timeline of the behavioural experiments. After preparation of the animals for either chemogenetics or optogenetics, all animals went through the same protocols in both countries. Modified version of MWM was divided into 3 phases: Cue task (3 days), SRM (5 days) and memory probes (10 minutes and 72 hours). Manipulation during experiments is indicated by pictograms of a syringe (chemogenetics) and blue laser (optogenetics). (C) An example of an accepted virus expression and optic fibre placement for the optogenetic experiments. Scale indicates 1000 μm.

ChR2: Channelrhodopsins; DREADDs: designer receptors exclusively activated by designer drugs; EPM: elevated plus maze; EYFP: enhanced yellow fluorescent protein; MRR: median raphe region; MWM: Morris watermaze; OF: open field; RFP: red fluorescent protein; SRM: spatial reference memory task; VGLUT3: vesicular glutamate transporter type 3.

3.3.3.2.2. Optogenetics approach

In Hungary, AAVs (serotype 5, #26973, 40 nl) encoded the sequences of Channelrhodopsins (ChR2) and enhanced yellow fluorescent protein (EYFP) as a reporter protein were injected into the MRR of the excitatory group (N=6♀7♂) (Balazsfi D. G. et al., 2017). Control animals (#27056, N=5♀6♂) received an AAV containing only the reporter protein. Two weeks post-surgery custom made optic fibres (multimode optical

fibres, flat tip, 0.22 NA, low-OH Ø105 µm core, FG105LCA, Thorlabs Corp.; flanged zirconia ferrule [LC MM C35 Chamfer Ferrule 127 µm with Flange, Senko]) were implanted over the MRR (AP: -4.8 mm; L:0 mm; DV:-4.1 mm; 10° inclination to posterior) and fixed to the skull by screws and acrylic resin (Duracryl Plus; SpofaDental) (Balazsfi D., Zelena, et al., 2018, Balazsfi D. G. et al., 2017). The animals were then single-housed and had another 2 weeks to recuperate. On the last five days they were daily handled and trained to the application and weight of the patch cords for 10 minutes. Before the animals were placed into the arenas, fibre-optic patch cords (custom made, multimode optical fibre, 0.22 NA, low-OH Ø105 µm Core, FG105LCA, FT900KY tubing, End A: LC/PC, End B: LC/PC, and multimode optical fibre, 0.22 NA, low-OH Ø105 µm Core, FG105LCA, FT030 tubing, End 1:FC/APC, End:2 LC/PC, Thorlabs Corp.) were applied, which collimated and guided the laser beams from the laser source (473 nm, low noise diode-pumped solid-state laser, Ikecool Corp.). Net energy output was measured by laser power meter (Coherent, Laser Check) and laser intensity was adjusted to 20±0.5mW net energy at continuous light emission. The laser was automatically controlled by Noldus Ethovision XT 15, exciting the cells at 20 Hz (5 msec square pulse + 45 msec break, **Figure 12A**).

At the end of the behavioural tests, animals were decapitated and their brains were fixed by immersion in 4% PFA for one day, then stored at 4°C in azide-PBS (1 g/L) until further processing. Before starting cutting, the solution was changed to 10% glucose azide-PBS for at least 24 hours, and then 30 µm thick slices were cut with a sliding microtome. The slices were stored in a cryoprotectant at -20°C.

3.3.3.3. *Behavioural testing*

Modified protocol of MWM experiments (Daumas et al., 2017) were conducted between 12 p.m. and 17 p.m., while OF and EPM tests took place between 9 a.m. and 2 p.m. The animals were randomized before the start of the experiments. The experiments were recorded and automatically analysed by ANY-maze (France) or Noldus Ethovision XT 15 (in Hungary). See the schematic timeline of the experiments on **Figure 11B**.

3.3.3.4. *Open field test*

Animals were put into an empty white plastic box (France: 50 cm × 50 cm × 40 cm, Hungary: 40 cm × 36 cm × 15 cm) without bedding for 10 minutes with ~25 lux

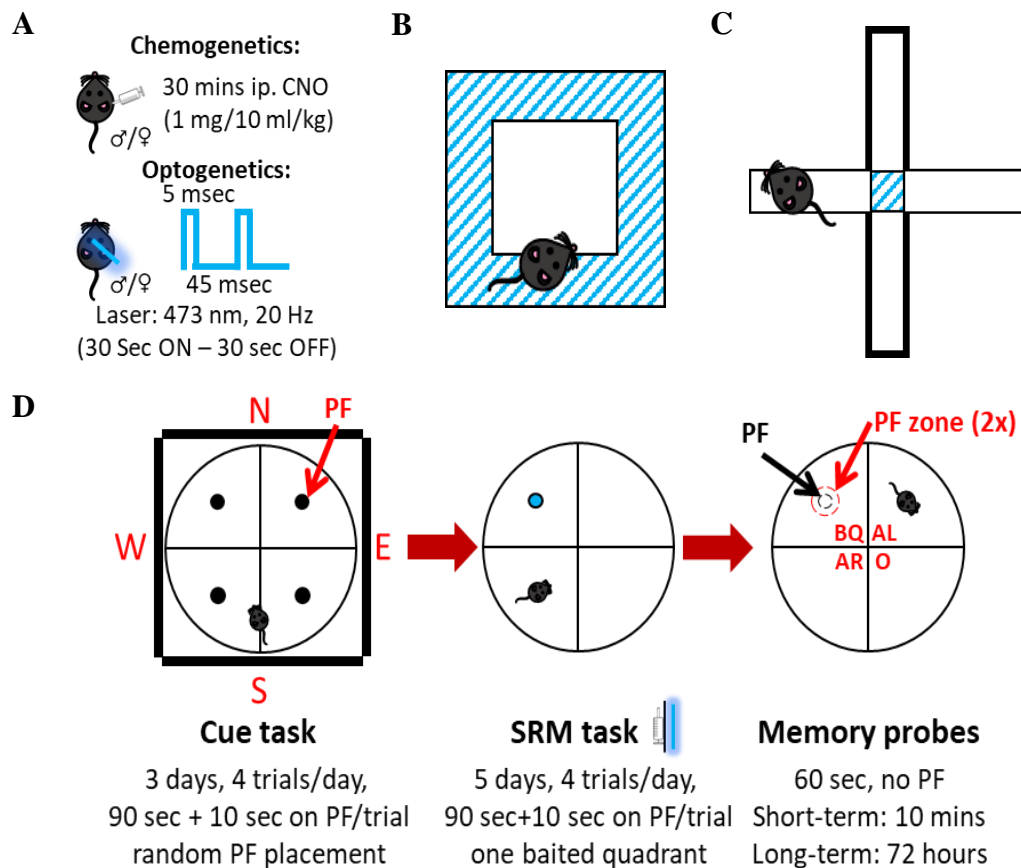


Figure 12. Schematic illustrations of protocols and excitation used in Project 3/c
(A) Ways of excitation achieved during the experiments. For chemogenetics, ip. CNO injection was given 30 minutes before the start of the experiments. In case of optogenetics, 473 nm, 20 Hz (5 msec light + 45 msec break) laser excitation was delivered via optic fibres implanted over the MRR. In case of longer experiments (OF, EPM), laser activity was divided into 30 sec ON and 30 sec OFF. **(B)** In the OF laser was activated (indicated by blue lines) when the animals entered the periphery. **(C)** On EPM, laser was activated when mice entered and stayed in the central part. **(D)** Different phases of the water maze experiment. During the first 3 days, the arena is surrounded by dark curtains to block external spatial cues. All quadrants are baited at least once, in a random order. Starting points are in random order (N, E, S, W). SRM lasts for 5 days and only one quadrant is baited, while all spatial cues are available for the mice. Excitation was delivered 30 minutes before the start of the experiment (chemogenetics), or while sitting on the PF for 10 sec (optogenetics). Short-term memory probe was 10 minutes after the last learning trial, while long-term memory probe was 72 hours later. latency to extended (x2) PF zone and time spent in different quadrants (BQ, AL, AR, O) were also measured.

AL: adjacent left; AR: adjacent right; BQ: baited quadrant; CNO: clozapine-N-oxide; E: east; EPM: elevated plus maze; ip.: intraperitoneal; MRR: median raphe region; MWM: Morris water maze; N: north; O: opposite; OF: open field; PF: platform; S: south; SRM: spatial reference memory task; VGLUT3: vesicular glutamate transporter type 3; W: west.

illumination in the centrum (75% of the floor). Distance moved, frequency and time spent in the periphery and centrum were analysed automatically.

As the complete knockout of VGLUT3 results in a highly anxious behaviour in mice, we hypothesised that excitation of MRR-VGLUT3 neurons would be anxiolytic. Therefore, with optogenetics, the animals received excitation whenever they entered and stayed at the periphery (target compartment) (**Figure 12B**). However, due to the length of the test and the limitations of constant optogenetic manipulation (tissue overheating, neuronal inhibition induced by overstimulations, etc.), we applied the 20 Hz laser excitation in 30 sec ON, followed by 30 sec OFF periods whenever the animals were in the target compartment (**Figure 12A**).

3.3.3.5. *Elevated plus maze test*

Animals were placed onto the middle, central zone of the EPM apparatus (both countries: 67 cm × 7 cm × 30 cm) with two open and two closed arms. The mice could freely explore the apparatus for 5 minutes. The test was conducted at ~25 lux illumination in the open arms.

The number of open and closed arm entries and time spent in each compartment were measured. Open arm entries independent from mobility were calculated based on this equation:

$$\frac{\text{open}}{\text{total}}(\%) = \frac{\text{number of open arm entries}}{\text{sum of all arm entries}}.$$

For the optogenetic experiments, the lasers switched on whenever the animals entered the central part of the apparatus, just before making a decision between open and closed arm entry (**Figure 12C**).

3.3.3.6. *Morris water maze (MWM) test*

MWM consisted of three phases: cue task, spatial reference memory (SRM) task and probes (Daumas et al., 2017). The tanks (France: 1.6 m, Hungary: 1.8 m in diameter) were filled up with 21±1°C water and made opaque with liquid latex or white tempera (respectively in the two countries). The animals were randomly divided into two equal batches, each of them having their separate random order of baited quadrant and starting points, then were socially isolated 30 mins before the start of the experiment (for chemogenetics, as for optogenetic experiments, they were separated at the time of the optic fibre implantation). During learning, there were four trials per day. One trial lasted

until the animal found the platform (France: 9 cm, Hungary: 10 cm in diameter), or after 90 sec had elapsed. If the animals could not find the platform within the time limit, they were gently guided there. On the platform, the animals could rest for 10 sec before removal and being placed under an infrared heating lamp, or over a heating pad. Cue task lasted for 3 days, with ITI of 20 mins. The tank was surrounded by curtains (~80 lux inside), blocking spatial cues from the room. The platform was submerged ~ 1 cm below the water surface and cued with a colourful 20 mL falcon tube. In every trial the platform was placed in the middle of a different quadrant (NE, NW, SE and SW) and the animals were released from a different starting point (north, south, west or east), facing the wall. The task was considered learnt when the animals could reach the cued platform within 15 sec. During this phase the animals did not get any treatment (CNO or light), the goal was to learn the task. For the SRM task, the curtains were removed and all spatial cues in the room were visible (~80 lux in the middle of the tank) throughout the remaining of the experiment. For each batch, one quadrant (NW or SE) was baited with a submerged (~1 cm below the water surface level) platform. This phase lasted for 5 days, with an ITI of 10 mins. A 60-second-long short-term memory probe was performed 10 mins after the last trial of SRM (on day 5) without the platform in the tank. After that, an additional trial was conducted with the platform placed inside once again to avoid memory extinction (but it was not evaluated). Because the MRR is known to have a long-term effect on behaviour (Balazsfi D. G. et al., 2017), a long-term probe test was also conducted 72 hours later (**Figure 12D**).

For the chemogenetic approach, the animals received their single ip. CNO injection at the beginning of the isolation during all SRM days, but not during the cue task or the long-term memory probe. As previous studies imply that MRR affects consolidation (Sarihi et al., 1999, Wang D. V. et al., 2015), optogenetic excitation was conducted during the 10 sec while the mice were sitting on the platform, whether they found it by themselves or were guided there.

3.3.3.7. *Immunohistochemistry and microscopy experiments*

Appropriate virus infection and expression were validated by immunohistochemistry with the same protocol in both countries as described in **3.3.1.1.** and **3.3.2.4. chapters**. The mounting was done in gelatine or TRIS, then the slides were dehydrated in xylol or series of alcohol solutions in ascending concentrations. The slices

were covered with DPX or Eukitt (Sigma-Aldrich). The Ni-DAB-stained slices were evaluated by light microscopes (France: Axioskop 2 plus, Zeiss; Hungary: Panoramic Midi II, 3DHitech) and evaluated according to the criteriums described in **3.3.2.4. chapter** (see example for optic probe placement **Figure 11C**). For chemogenetics, 27 out of 39 mice were included in Hungary and 25 out of 47 in France. For optogenetics, 25 animals out of 46 were included in the statistical analysis.

3.3.3.8. *Statistical analysis*

For the statistical analysis GraphPad Prism version 8.0.0 for Windows, GraphPad Software (San Diego, California USA, www.graphpad.com) and StatSoft10 (StatSoft,Inc., Tulsa, OK) softwares were used. Outliers were defined as data points which were not in the interval of group mean $\pm 2 \times \text{SD}$ for the given parameter, but no animals had to be excluded.

Differences between the groups (effect of excitation) and sexes (effect of sex) was measured by two-way ANOVA (for distance moved, frequency of arm entries and open/total% parameters). Time spent in different compartments (effect of choice: periphery vs centrum, closed arm vs open arm vs centrum, quadrants), latency to (extended) platforms (effect of time) and quadrant preference (**Figure 12D**) were tested with three-way repeated measures ANOVA. Additionally, time spent in baited quadrants were tested against random chance 25% with single-sample t-test. In case of OF and EPM, laser activity was place dependent rather than fixed time, and to avoid tissue heating, ON and OFF periods were defined. This resulted in different amounts of time of excitation not just between groups, but also between animals within the same treatment group (e.g.: EPM – control: 73.110 ± 8.521 sec, with a standard deviation of 29.517 sec vs excitatory: 97.151 ± 20.698 sec, with a standard deviation of 74.628 sec). Thus, for all animals that took part in optogenetics OF and EPM experiments, active laser time (sec) was collected from Ethovision, which controlled laser activity based on animal detection, and was used as a covariate for correction in ANCOVA analysis. Normal distribution of the data was checked with Shapiro-Wilks test. Homogeneity of variances was tested by Spearman's test for heteroscedasticity and Geisser-Greenhouse correction was applied during repeated measures ANOVA. Sidak correction was used for post hoc tests.

4. Results

4.1. Project 1: Behavioural characterisation of the VGLUT3 KO mice

4.1.1. Project 1/a: Social behaviour

4.1.1.1. Mobility during exploration based tests

We observed no difference between the WT and KO animals in the total distance moved in OF, frequency of closed arm entries on EPM or arm entries in Y-maze (**Table 3**). Thus, VGLUT3 KO mice show comparable mobility to WT littermates during their active period.

Table 3. Parameters of locomotion in different behavioural experiments for VGLUT3 WT-KO mice

There were no differences between the VGLUT3 WT and KO animals regarding their locomotion during their active period. Data are expressed as mean±SEM.

EPM: elevated plus maze test; KO: knockout; OF: open field; VGLUT3: vesicular glutamate transporter type 3; WT: wild-type.

Genotype		WT	KO
OF	Distance moved (cm)	2244.798±100.006	2251.459±225.590
EPM	Closed arm (frequency)	13.500±1.827	13.818±1.872
Y-maze	Locomotion (frequency of arm entries)	18.200±3.269	19.818±3.173

4.1.1.2. Anxiety-like behavioural tests

In the OF, no difference was observed in the frequencies of entry into different compartments between the genotypes (data not shown). However, there was a significant effect of genotype ($t_{(18)}=2.963$, $p<0.01$) for the percentage of time spent in the centrum: the KO animals spent less time there compared to WT ($p<0.01$) (**Figure 13A**).

This increased anxiety-like behaviour was confirmed in the EPM: open/total parameter showed a significant effect of genotype ($t_{(19)}=2.019$, $p=0.058$): KO animals entered the open arm less than the WT mice (**Figure 13B**). Additionally, the frequency of rearing (risk assessment) was lower for the KO animals ($t_{(19)}=2.645$, $p<0.05$). Overall, the KO group exhibited less risk assessment behaviours (RA: sum of head dipping, SAP and rearing; $RA_{WT}=67.500\pm 5.584$; $RA_{KO}=49.091\pm 6.511$; $t_{(19)}=2.125$, $p<0.05$) (**Figure 13C**). Based on the previously mentioned lack of differences in mobility, these results indicate enhanced anxiety-like behaviour in VGLUT3 KO mice.

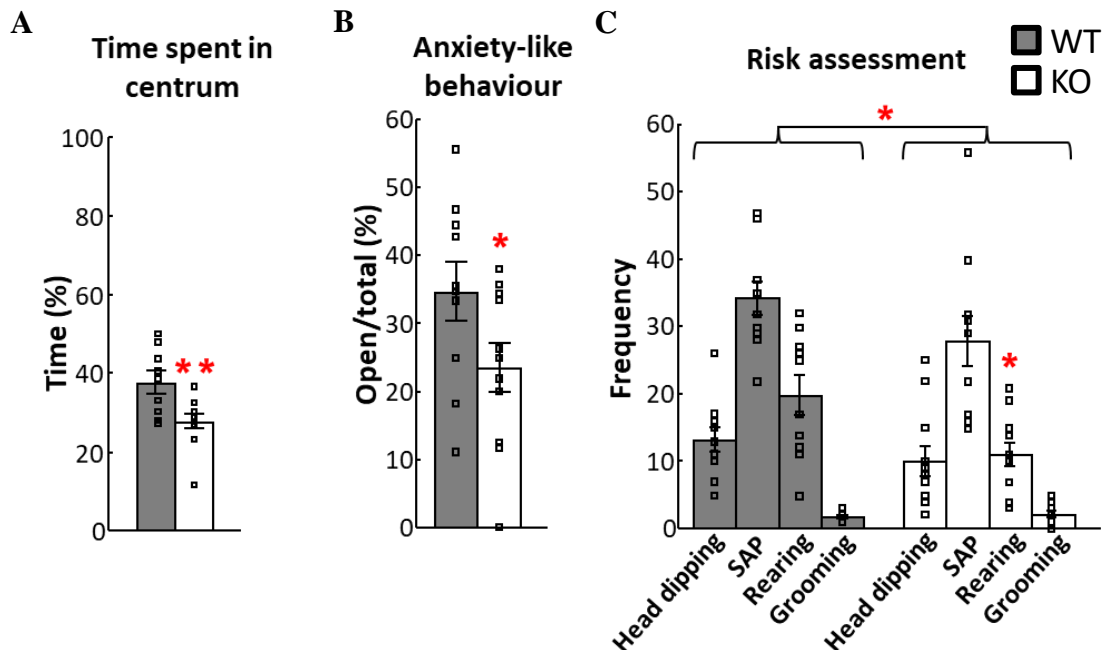


Figure 13. Anxiety-like behaviour in VGLUT3 WT and KO mice in OF and EPM tests

(A) KO mice spent less time in the aversive centrum of the OF arena compared to their WT littermates. (B) KO mice exhibited increased anxiety-like behaviour, which is reflected by the decrease in their time spent in the open arms (open/total%). (C) Overall risk assessment behaviour was also decreased in KO mice, as well as the frequency of rearing. Data are expressed as mean±SEM.

EPM: elevated plus maze; KO: knockout; VGLUT3: vesicular glutamate transporter type 3; WT: wild-type.

* $p<0.05$, ** $p<0.01$ vs WT.

4.1.1.3. Social interest

During object habituation of the sociability test there were no differences in the sniffing frequencies, but there was a significant effect of genotype in the time spent with

objects ($F_{(1,17)}= 4.378$, $p=0.05$) without side differences. WT and KO animals spent equal time with the two objects separately, however, KO spent more cumulative time with the two objects than the WT. This is also reflected by the reduced percentage of time spent doing ‘other’ behaviours in KO mice ($t_{(17)}=2.09$, $p=0.05$) (**Table 4**).

Table 4. Results of VGLUT3 WT-KO sociability test, with object habituation and sociability phases

Animals showed no side preferences during the object habituation phase. Both groups preferred the social stimulus, but the VGLUT3 KO mice spent more time with the conspecific compared to their WT littermates, which is also reflected by the higher SI value. Data are expressed as mean±SEM.

KO: knockout; SI: sociability index; VGLUT3: vesicular glutamate transporter type 3; WT: wild-type.

$p<0.01$ vs cage; * $p<0.05$, ** $p<0.01$ vs WT; \$ $p<0.05$, \$\$ $p<0.01$ vs random 50.

		Genotype	WT	KO
Object habituation phase	Frequency	Left cage	18.889±1.767	18.400±2.023
		Right cage	17.333±2.211	17.800±1.769
		Other	37.111±3.276	37.100±3.291
	Time (%)	Left cage	7.652±1.036	9.685±0.761
		Right cage	6.954±1.184	9.945±0.945
		Other	85.394±2.026	80.370±1.370*
Sociability test	Frequency	Mouse	18.111±1.859	22.818±1.853
		Cage	15.000±2.034	14.636±1.870
		Other	32.556±3.105	36.091±2.859
	Time (%)	Mouse	24.341±5.785 ##	40.336±3.514 ## **
		Cage	8.463±1.311	8.661±1.180
		Other	67.196±6.043	51.003±3.333
	SI	69.263±5.246 \$\$	81.236±2.938\$\$ *	

During the sociability phase a significant difference was detected in sniffing frequencies for the effect of choice ($F_{(1,18)}=16.503$, $p<0.01$) and a tendency for genotype×choice interaction ($F_{(1,18)}=3.327$, $p=0.08$) (**Table 4**). Post hoc analysis of effect

of choice showed a preference for the cage containing the conspecific ($p < 0.01$), however, only KO animals sniffed the conspecific more often than the object ($p < 0.01$). For the percentage of time interacting there was a significant effect of genotype ($F_{(1,18)} = 6.066$, $p < 0.05$), choice ($F_{(1,18)} = 47.541$, $p < 0.01$) and genotype \times choice interaction ($F_{(1,18)} = 5.246$, $p < 0.05$). Post hoc analysis of the interaction revealed that both groups spent more time with the conspecific ($p < 0.01$), with KO mice spending significantly more time with the conspecific than WT animals ($p < 0.01$). Both groups showed higher than 50% sociability index (SI: WT: $t_{(8)} = 3.672$, $p < 0.01$; KO: $t_{(10)} = 10.630$, $p < 0.01$), with a higher average SI for the KO animals than WT mice ($t_{(18)} = -2.087$, $p = 0.05$). Additionally, the KO group spent less time with ‘other’ behaviours compared to WT group ($t_{(18)} = 2.463$, $p < 0.05$). In summary, the complete knockout of VGLUT3 gene does not impair sociability: on the contrary, it facilitates social interest.

4.1.1.4. Social behaviour

During SIT, a marginal effect of genotype was observed for the frequency of defensive and ‘other’ behaviours ($t_{(19)} = -1.808$, $p = 0.08$ and $t_{(19)} = -1.936$, $p = 0.07$, respectively) with significant differences in aggressive behaviour. We observed an increase in the percentage of time spent with aggressive behaviour ($t_{(19)} = -2.15$, $p < 0.05$)

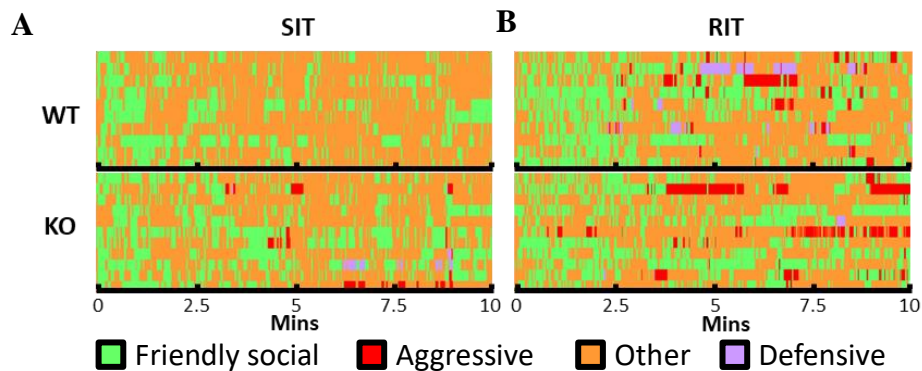


Figure 14. Gantt-diagrams showing the social behaviour of VGLUT3 WT and KO mice during SIT and RIT

(A) In the anxiogenic context of the SIT aggressive behaviour appeared more frequently in KO than WT animals. (B) During RIT, KO mice did not differ significantly from their WT littermates. Each row represents one animal in the Gantt-diagrams.

KO: knockout; RIT: resident intruder test; SIT: social interaction test; VGLUT3: vesicular glutamate transporter type 3; WT: wild-type.

and also in the frequency of aggressive behaviour ($t_{(19)}=-2.76$, $p<0.05$) in the KO mice compared to WT littermates (**Figure 14A** and **Table 5**). Despite these differences, the total time spent with aggressive behaviour was relatively low (~2%) compared to the full length of the test (10 minutes). Thus, our continuous data were transformed into discrete variables: those animals who showed any kind of aggressive behaviour were marked with ‘yes’, while those who did not, were marked with ‘no’. The number of ‘yes’ and ‘no’ marks were counted, and a contingency table was created. Pearson Chi-square test showed a significant difference ($\chi^2=7.636$, $p<0.01$): 6 KO animals out of 11 exhibited aggressive behaviour, while the WT group showed none at all (**Table 6**). In the RIT, there was no observed difference between WT and KO animals in this test, only a marginal effect of genotype was found in the frequency of defensive behaviour ($t_{(19)}=1.878$, $p=0.08$) (**Figure 14B** and **Table 5**).

Table 5. Results of VGLUT3 WT-KO SIT and RIT experiments

Detailed analysis of social behaviour in VGLUT3 WT and KO mice. There were no major differences between the groups, only the appearance of inadequate aggressive behaviour during SIT. Data are expressed as mean±SEM.

KO: knockout; RIT: resident intruder test; SIT: social interaction test; VGLUT3: vesicular glutamate transporter type 3; WT: wild-type.

* $p<0.05$ vs WT.

	Genotype		WT	KO
	Social interaction test	Frequency	Social	42.500±2.062
Aggressive			0.000±0.000	2.818±0.971*
Defensive			0.000±0.000	1.545±0.813
Other			43.400±2.077	52.545±4.082
Time (%)		Social	28.994±2.971	34.364±2.923
		Aggressive	0.000±0.000	2.673±1.181*
		Defensive	0.000±0.000	0.880±0.682
		Other	67.706±4.760	62.082±3.039
Resident intruder test	Frequency	Social	55.700±3.839	56.273±3.300
		Aggressive	6.100±1.215	7.636±3.566
		Defensive	2.900±1.394	0.364±0.244
		Other	55.000±3.095	57.636±2.688
	Time (%)	Social	35.226±4.156	35.925±4.000
		Aggressive	4.384±1.577	6.566±3.354
		Defensive	3.084±2.007	0.261±0.208
		Other	57.308±3.980	57.248±3.829

The results of SIT and RIT together indicate that VGLUT3 KO mice might exhibit inappropriate aggressive behaviour in non-aggressive social contexts, while their territorial aggression is not affected.

Table 6. Contingency table of VGLUT3 WT-KO mice during SIT

VGLUT3 WT-KO contingency table showing the numbers of animals who exhibited aggressive behaviour in social interaction test, followed by a Pearson Chi-square test.

df: degree of freedom; KO: knockout; SIT: social interaction test; VGLUT3: vesicular glutamate transporter type 3; WT: wild-type.

Social interaction test	Aggressive behaviour		Total
	Yes	No	
Genotype			
WT	0	10	10
KO	6	5	11
Total	6	15	21
Pearson Chi-square: 7.636; df=1; p=0.006			

4.1.1.5. Social discrimination test

There was no difference between the WT and KO animals in the frequencies of sniffing the conspecific containing cages (**Table 7**). However, there was a marginal effect of genotype in the percentage of time spent with stimulus animals ($F_{(1,18)}=3.142$, $p=0.09$) and a significant genotype \times choice interaction ($F_{(1,18)}=4.281$, $p=0.05$). Post hoc analysis showed that KO mice spent more time with the ‘old’ mouse compared to the WT group ($p<0.05$), and also compared to the ‘new’ mouse ($p<0.05$) (**Figure 15A**).

This was also reflected by the SD: WT animals did not differ significantly from 0, but the KO group did ($t_{(10)}=-2.352$, $p<0.05$). Nevertheless, their average SD was -19.329 ± 8.217 , which reflected a preference for the ‘old’ mouse. Additionally, the SD difference between the WT and KO animals was significant ($t_{(17)}=2.503$, $p<0.05$) (**Table 7**). These results show that VGLUT3 KO mice not only show impaired social memory, but also prefer an already familiar conspecific over a new one.

Table 7. Results of social discrimination test of VGLUT3 WT-KO mice
VGLUT3 KO mice not only preferred the 'old' animal, but also spent more time with social stimuli. Data are expressed as mean±SEM.
KO: knockout; SD: social discrimination index; VGLUT3: vesicular glutamate transporter type 3; WT: wild-type.
* p<0.05 vs WT; \$ p<0.05 vs random 0.

Genotype		WT	KO
Frequency	'Old' mouse	16.333±2.333	18.727±2.632
	'New' mouse	15.778±1.535	17.091±2.302
	Other	32.111±3.510	34.636±4.012
SD		10.945±7.069	-19.329±8.217\$*

4.1.1.6. Working memory

In the y-maze test both groups had intact spontaneous alteration (WT: $t_{(6)}=15.154$, $p<0.01$; KO: $t_{(10)}=3.61$, $p<0.01$) without differences between the genotypes (**Figure 15B**).

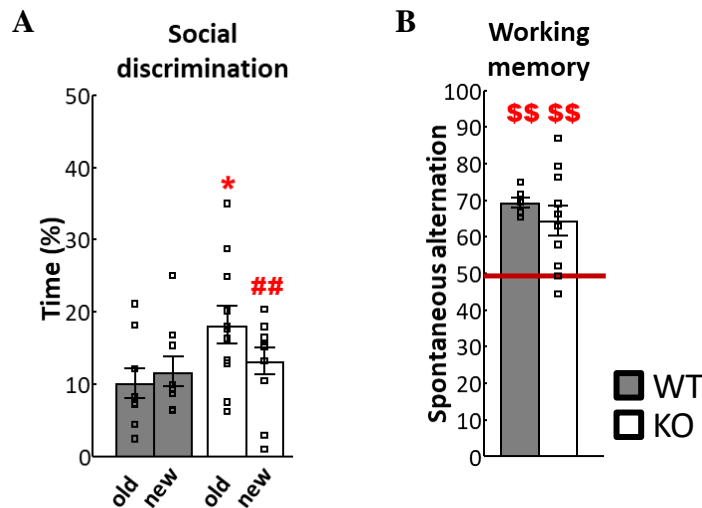


Figure 15. Short-term memory in VGLUT3 WT and KO mice

(A) Although WT mice did not differentiate between the conspecifics, KO animals not only preferred the old one, indicating memory impairments, but also spent more time with that conspecific compared to WT in SDT. (B) Short-term working memory was not impaired in the KO animals in Y-maze. Data are expressed as mean±SEM. KO: knockout; SDT: social discrimination test; VGLUT3: vesicular glutamate transporter type 3; WT: wild-type.

* p<0.05 vs WT; ## p<0.01 vs old; && p<0.01 vs random 50.

4.1.1.7. Summary of Project 1/a

With a detailed behavioural test battery, we showed that the constitutive VGLUT3 gene knockout has a circadian dependent effect on mobility but increases anxiety-like behaviour and social interest. Additionally, rigorous analysis of social behaviour revealed that although aggressive behaviour is not changed in VGLUT3 KO mice in the RIT, more of them show aggression inappropriately during SIT.

4.1.2. Project 1/b: Learning and memory formation

In the MWM task, WT and KO mice showed spatial learning as the latencies to reach the platform significantly decreased during the learning phase (day 1-6) in both genotypes (effect of time: $F_{(5,65)}=8.715$, $p<0.001$) (**Figure 16A**). Both groups spent significantly more than 25% (chance level) in the baited quadrant (WT: $t_{(7)}=2.254$, $p=0.058$; KO: $t_{(7)}=2.849$, $p<0.05$), however, there was no genotype effect during probe 1 on day 7 (**Figure 16C**). A closer look on the latency to reach the supposed platform location on probe 1 (day 7) vs. on the latest day of the learning phase revealed a significant interaction between time \times genotype (day 6 vs 7: $F_{(1,14)}=6.417$, $p<0.05$), with a decrease in the latency in the WT and an increase in the KO mice (**Figure 16A**).

During the cognitive flexibility phase (days 8-10), the latencies to find the platform showed a significant decrease across the days (effect of time: $F_{(2,28)}=16.579$, $p<0.001$) (**Figure 16B**). On day 11 (probe 2), there was no difference in latencies between the genotypes, but only the WT animals had proper quadrant preference (WT: $t_{(7)}=3.253$, $p<0.05$; KO: $t_{(7)}=0.916$, $p>0.1$) (**Figure 16C**). The distance moved during the test days also did not differ between the groups (**Figure 16D**). However, because in other experiments we found significant differences between the mobility of VGLUT3 WT and KO mice, an analysis by ANCOVA with locomotor behaviour as a covariate was also conducted to rule out any possible confounding factors, but it did not show any significant influence of the locomotion, either.

In sum, VGLUT3 KO mice did not show major spatial learning and memory impairment in the MWM task, only a slight disturbance in memory during cognitive flexibility phase.

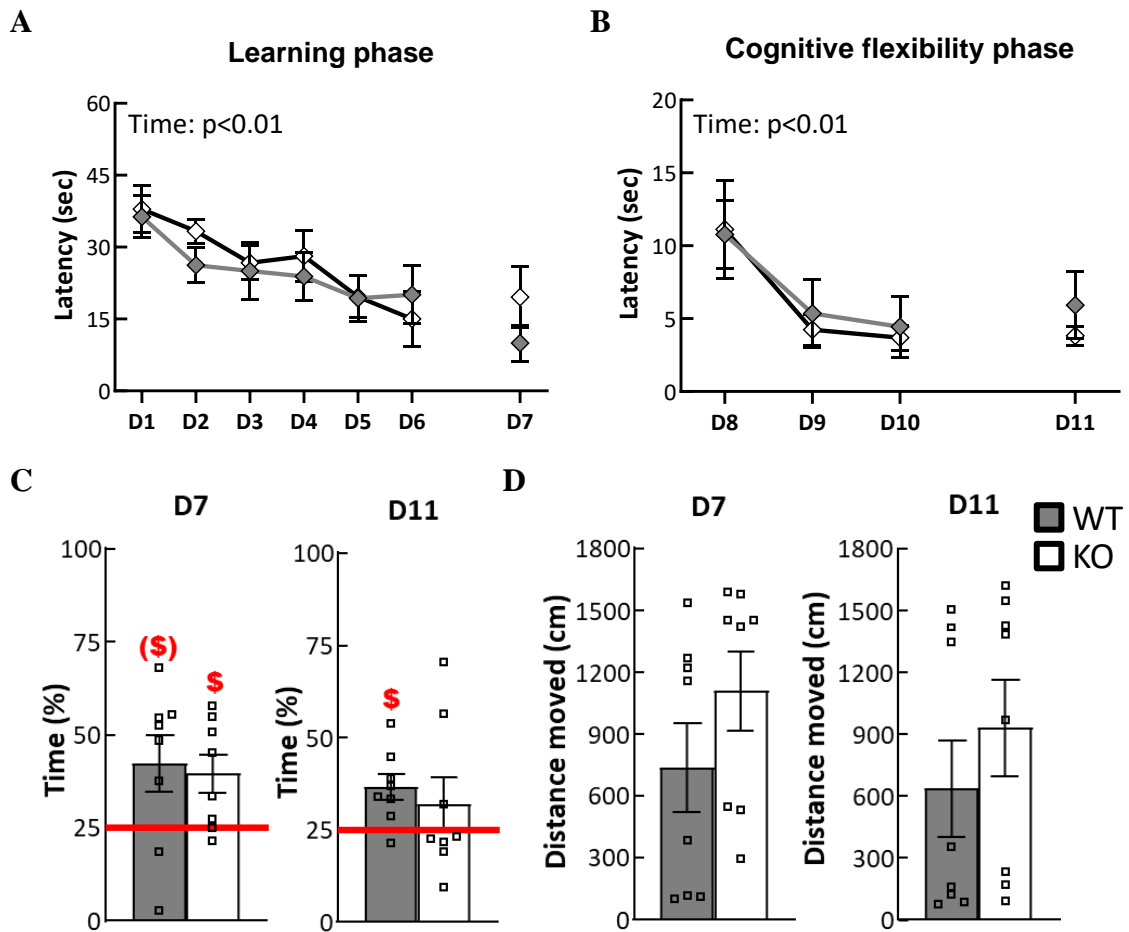


Figure 16. Results of VGLUT3 WT and KO mice in MWM

(A) Latencies to platform decreased across the days (day 1-6), without differences between the groups. While the performance on test day (day 7) did not differ, there was a time×genotype interaction between day 6-7. (B) During cognitive flexibility phase (day 8-10) and its test (day 11), there was no difference between the groups. (C) Baited quadrant preference on test day 7 was higher than chance level 25% (red line) for both groups, but on test day 11, after cognitive flexibility test, only the WT group had proper preference. (D) Distance moved on either of the test days did not differ between the groups.

KO: knockout; MWM: Morris water maze; WT: wildtype.

(\$) $p=0.06$, § $p<0.05$ vs random 25%.

4.2. Project 2: Anatomical study of VGLUT3 in the mouse and human MRR

4.2.1. Project 2/a: VGLUT3 mRNA and its co-expression with Tph2 mRNA by sdFISH

As suggested by the literature (Hioki et al., 2010, Sos et al., 2017), VGLUT3 and Tph2 are often co-expressed in the MRR, both on mRNA and protein levels. Our sdFISH

experiment proved the same (**Figure 17A**). On average 496.875 ± 28.934 VGLUT3+ neurons were found in the MRR per animal, with 95 ± 857 of it also co-expressing Tph2 mRNA. By quantifying these expression ratios, we found that in the MRR approximately $19.329\% \pm 1.641\%$ of VGLUT3+ cells also co-express Tph2 mRNA (**Figure 17B**). Detailed results are shown in **Table 8**.

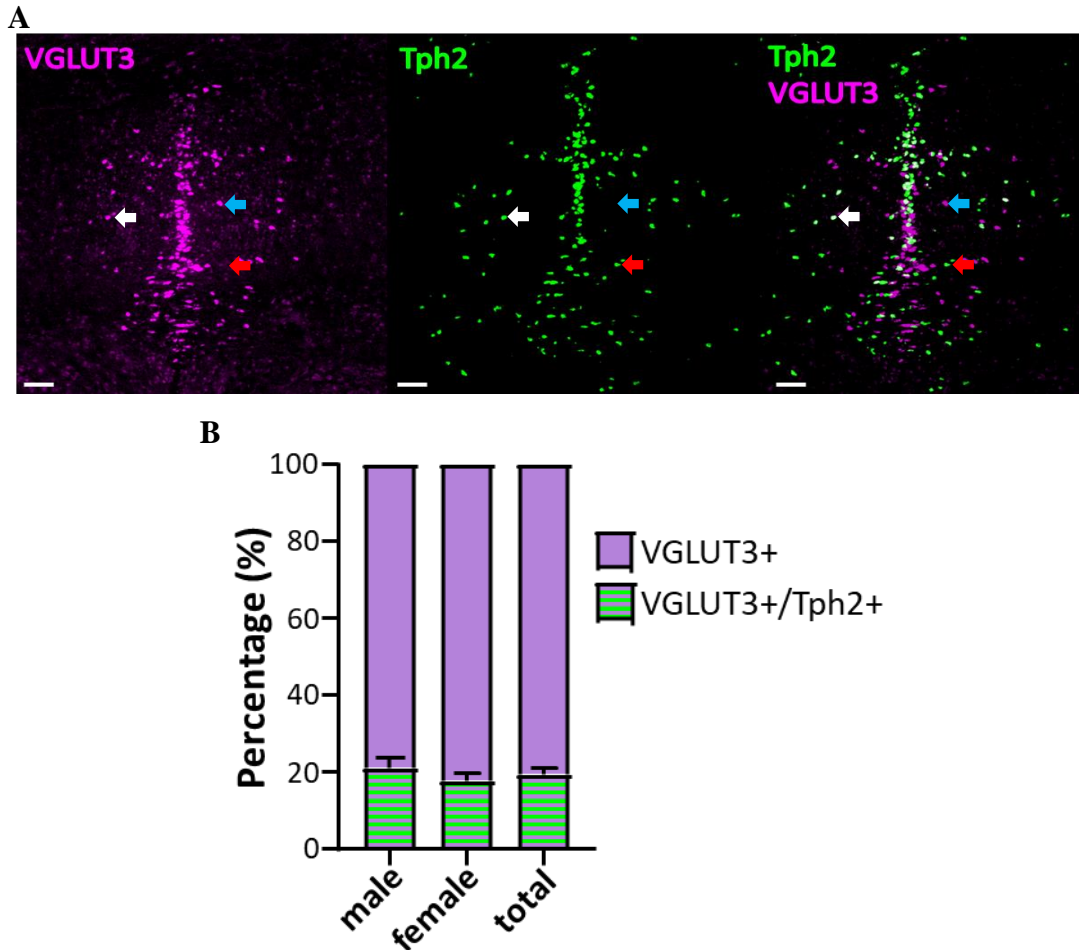


Figure 17. Representative picture of a sdFISH staining in the MRR

(**A**) Examples of purely VGLUT3+ (magenta) glutamatergic, Tph2+ (green) serotonergic, and double positive in the MRR on mRNA level. Arrows indicate examples of a purely VGLUT3+ (red arrow), a purely Tph2+ (blue arrow), and co-expressing neurons (white arrow), respectively. Scale is 100 μ m. (**B**) Approximately, 20% of all VGLUT3+ neurons also co-express Tph2+ in both male and female mice. MRR: median raphe region; sdFISH: double-probe fluorescent *in situ* hybridization; Tph2: tryptophan hydroxylase 2; VGLUT3: vesicular glutamate transporter type 3.

Table 8. Detailed results of sdFISH experiment

All VGLUT3+ cells which included a DAPI stained nucleus and VGLUT3+ and Tph2+ co-expressing cells were manually counted on all MRR containing slices. These raw cell numbers were averaged to their corresponding number of slices, and percentages of co-expressing VGLUT3+ cells were calculated. Numbers represent average±SEM.

DAPI: 4',6-diamidino-2-phenylindole; MRR: median raphe region; sdFISH: double probe fluorescent in situ hybridization; Tph2: tryptophan hydroxylase 2; VGLUT3: vesicular glutamate transporter type 3.

ID	Sex	Number of slices	Number of VGLUT3+/slice	Number of VGLUT3+/Tph2+/slice
1	male	9	51.111	12.444
2	male	9	67.556	8.889
3	male	7	74.571	17.714
4	male	8	59.375	13.500
5	female	6	56.667	11.500
6	female	9	54.556	6.667
7	female	8	72.875	15.000
8	female	7	70.857	12.429
males		8.250±0.479	63.153±5.075	13.137±1.817
females		7.500±0.645	63.739±4.730	11.399±1.742
total		7.875±0.398	63.446±3.213	12.268±1.211

4.2.2. Project 2/b: VGLUT3 mRNA detection by RT-qPCR in the human MRR-equivalent

VGLUT3 mRNA levels were investigated in four human brainstem areas: lateral parabrachial nucleus, pontine reticular formation, pontine raphe nucleus and midbrain raphe nuclei (**Figure 18A**). As negative control, temporal and frontopolar cortex samples were used (**Figure 18B**). All brain areas – except negative controls - expressed VGLUT3 mRNA (**Table 9**).

Table 9. RT-qPCR results of human raphe samples

Four major brainstem nuclei were investigated, and all showed VGluT3 expression on mRNA level. The results show averaged and normalized CT values.

CT: cycle threshold; LPB: lateral parabrachial nucleus; PRF: pontine reticular formation; PRN: pontine raphe nucleus; RN: midbrain raphe nuclei; VGluT3: vesicular glutamate transporter type 3.

Brain area	Donor	housekeeping genes	VGluT3	Relative expression
LPB	#227	15.706	29.53	6.90E-05
	#256	15.563	28.6	1.19E-04
	#266	17.972	0	0.00E+00
PRF	#165	15.935	28.54	1.60E-04
	#186	16.815	29.92	1.14E-04
	#211	15.266	28.05	1.42E-04
	#216	15.576	29.04	8.85E-05
	#227	14.385	27.49	1.13E-04
	#228	15.533	30.18	3.90E-05
	#231	18.547	33.63	2.88E-05
	#242	18.836	31.97	1.11E-04
	#244	19.397	31.79	1.86E-04
PRN	#256	15.115	28.51	9.28E-05
	#211	14.808	23.49	4.66E-03
	#216	14.339	26.98	1.31E-04
	#227	14.495	27.06	2.58E-04
	#231	18.203	32.83	5.40E-06
	#244	14.326	25.81	4.85E-04
RN	#256	15.715	28.43	8.17E-05
	#186	17.547	30.84	1.54E-05
	#244	15.515	26.66	5.04E-04
	#266	14.773	28.93	9.47E-05

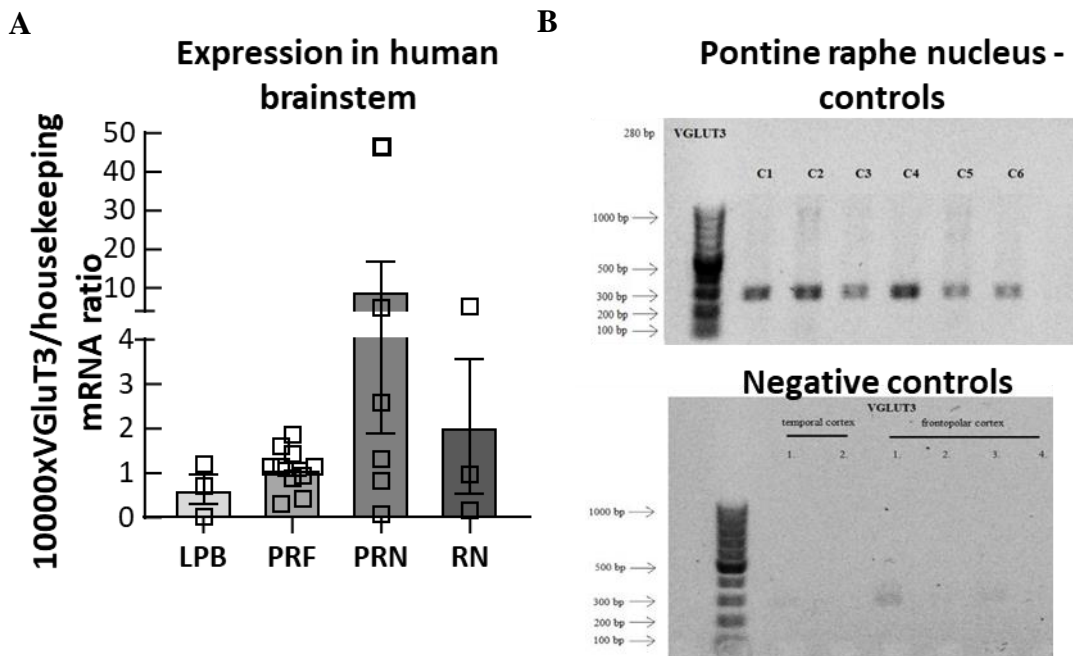


Figure 18. VGLUT3 mRNA levels in healthy human brainstem samples
(A) Relative expression of VGLUT3 mRNA to the measured housekeeping gene (GAPDH) in the investigated brainstem areas (LPB: N=3; PRF: N=10; PRN: N= 6; RN: N=3). **(B)** After RT-qPCR, samples containing VGLUT3 cDNA were run with gel electrophoresis and sequenced (BIOMI Kft.) to validate the specificity of primers. Brain samples from pontine raphe nuclei, which contain the human equivalent of mouse MRR, all expressed VGLUT3 (N=6), while different cortical areas of healthy human samples were used as negative controls (N=6). Data are expressed as average±SEM. Empty squares represent individual values.
 bp: basis pair; LPB: lateral parabrachial nucleus; PRF: pontine reticular formation; PRN: pontine raphe nucleus; RN: midbrain raphe nuclei; RT-qPCR: reverse transcription quantitative polymerase chain reaction; VGLUT3: vesicular glutamate transporter type 3.

4.2.3. Summary of Project 2

We successfully confirmed the presence of VGLUT3 mRNA in mouse MRR and also quantified the approximate ratios of VGLUT3+ and VGLUT3+/Tph2+ double positive cells – that is, the ratios of purely VGLUT3+ glutamatergic and VGLUT3-serotonin co-expressing neurons. Additionally, in healthy human brainstem samples, we also showed the presence of VGLUT3 mRNA, indicating human relevance for our studies.

4.3. Project 3: Investigation of the role of MRR-VGLUT3 neurons in behaviour

4.3.1. Project 3/a: Validation of chemogenetics

4.3.1.1. Validation 1: Cre-dependent RFP expression in MRR-VGLUT3 cells of VGLUT3-Cre mice

Double immunofluorescent staining in the MRR against VGLUT3 protein and the reporter protein of the AAV, the RFP showed perfect co-expression, indicating a properly working Cre system in our viral injected VGLUT3-Cre mice (**Figure 19**).

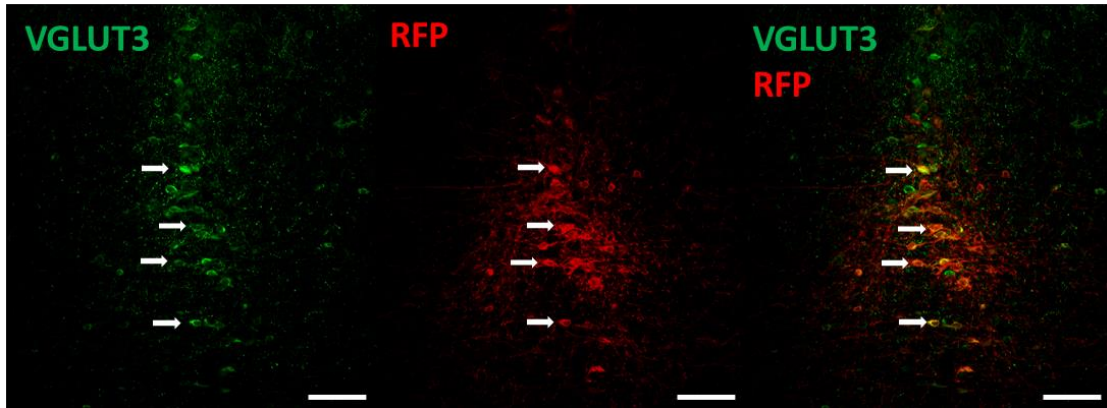


Figure 19. Representative fluorescent picture of the MRR in a AAV injected VGLUT3-Cre mouse

In the MRR of our VGLUT3-Cre mouse line, VGLUT3 (Alexa-488, green) protein and the AAV coded, floxed RFP (Alexa-594, red) was co-expressed, indicating a properly working Cre system. White arrows show examples of such co-expressing (yellow) neurons. Scale is 100 μm .

MRR: median raphe region; AAV: adenoassociated viral vector; RFP: red fluorescent protein; VGLUT3: vesicular glutamate transporter type 3.

4.3.1.2. Validation 2: Neurotransmitter concentration measurement in HC by microdialysis after MRR excitation

It was proved that MRR-VGLUT3 neurons project to dorsal HC (Szonyi et al., 2016), where they establish potentially functional NMDA containing synapses. Indeed, we measured MRR excitation-induced neurotransmitter release there (Fazekas et al., 2021).

The extracellular concentrations of measured substances varied with time, being the highest in the 3rd sample, just after the ip CNO injection both for 5-HT ($F_{(4,20)}=4.909$; $p<0.01$) (**Figure 20A**) and Glu ($F_{(4,20)}=3.303$; $p<0.05$) (**Figure 20B**). However, Glu levels were increased only in the group containing stimulatory DREADD construct in their MRR, but not in animals treated with control virus (excitation \times time interaction: $F_{(4,20)}=2.976$; $p<0.05$) in contrast to the 5-HT levels showing an increase in both cases. In

all cases local KCl administration in sample 6. induced significant elevation of the measured neurotransmitter (in all cases $p < 0.01$ vs sample 1.), confirming the viability of the neurons even at the last timepoint of the experiment. GABA levels were increased only in sample 6., due to local KCl administration (**Figure 20C**).

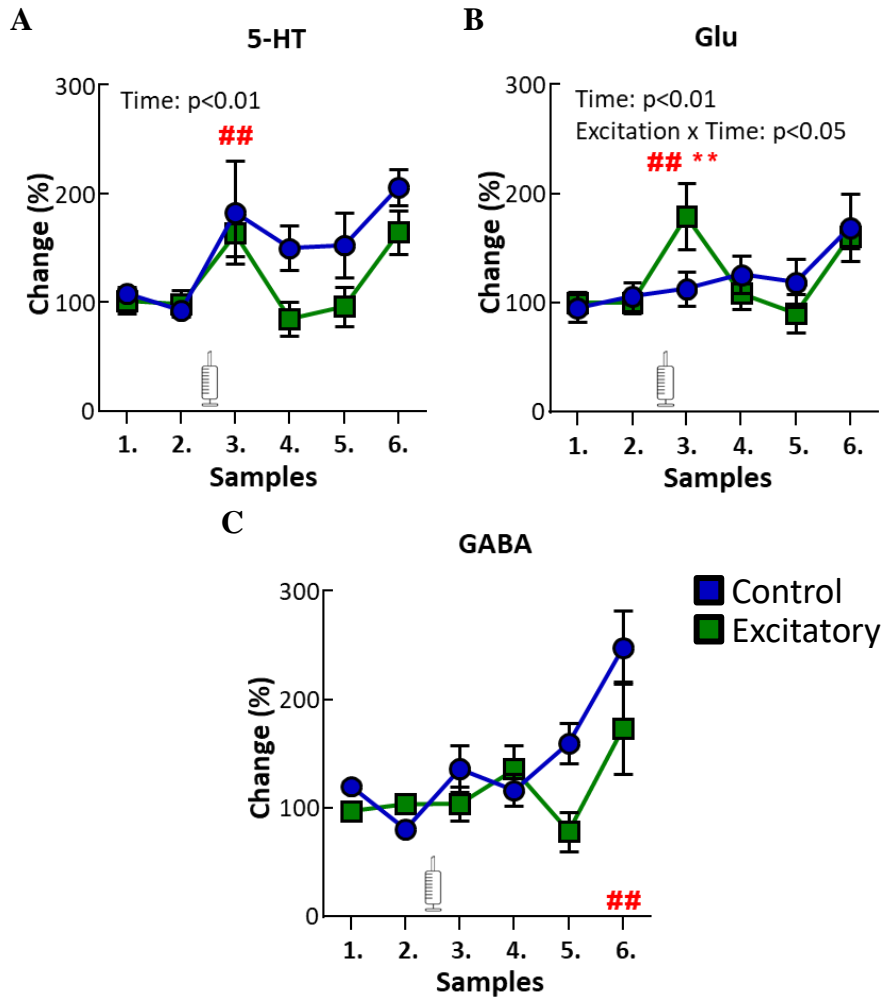


Figure 20. Neurotransmitter concentrations in HC after chemogenetic excitation of the MRR

(A) 5-HT levels increased after CNO injection (indicated by syringe) compared to previous samples in both groups, but the groups did not differ. (B) Glu levels increased only in the excitatory group after CNO injection. (C) There was no difference in GABA levels after CNO injection, or between the groups.

5-HT: serotonin; CNO: clozapine-N-oxide; HC: hippocampus; GABA: γ -aminobutyric acid; Glu: glutamate; MRR: median raphe region.

$p < 0.01$ vs previous samples; ** $p < 0.01$ vs control.

4.3.1.3. Validation 3: Validation of chemogenetic-induced neuronal activation by c-Fos immunohistochemistry

As expected, after CNO injection there was an increased cell activity in the stimulatory DREADD containing VGLUT3+ cells reflected by the higher number of c-Fos positive cells (41.333 ± 2.848) compared to the control group (2.389 ± 1.236) in the MRR ($t_{(7)} = -14.987$; $p < 0.01$) (**Figure 21**).

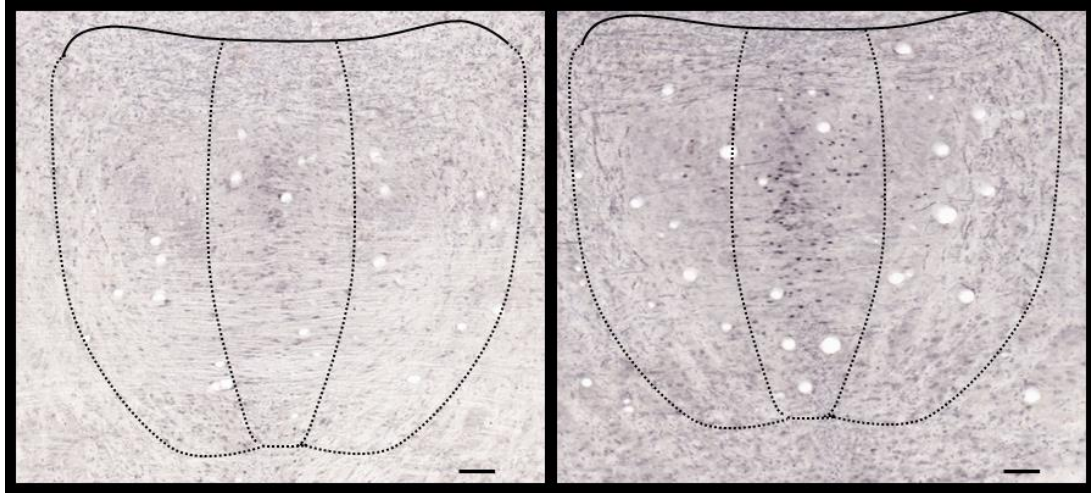


Figure 21. Representative picture of c-Fos immunopositivity in the MRR of a control (right) and excitatory (left) AAV injected VGLUT3-Cre mouse

Proper functioning of the Cre-dependently expressed excitatory (G_q) DREADD is shown by the increased c-Fos+ cell numbers after ip. CNO injection. Scale indicates 100 μm .

CNO: clozapine-N-oxide; DREADD: designer receptor activated by designer drugs; ip.: intraperitoneal; MRR: median raphe region; AAV: adenoassociated viral vector; VGLUT3: vesicular glutamate transporter type 3.

4.3.1.4. Summary of validations of chemogenetics

In order to make that Cre system works properly in the VGLUT3-Cre mice, we successfully validated newly introduced chemogenetic system in our laboratory: we showed that in the MRR, VGLUT3+ neurons expressed the Cre-dependent RFP; excitation of the MRR resulted in Glu release in the HC, which is a known projection area of the MRR; and finally, excitatory DREADD activation via CNO injection resulted in the elevated expression of c-Fos.

4.3.2. Project 3/b: Study of social behaviour

In order to see whether MRR-VGLUT3+ neurons could be responsible for the changes in VGLUT3 KO mice, we repeated the same experimental protocols VGLUT3-

Cre mice, who were injected with Cre-dependent DREADD (or control RFP) injected AAVs. Similarly to **Project 1**, first mobility and anxiety-like behaviour of the mice were assessed, as these are not only confounding factors for social behaviour, but it has been shown that MRR potentially plays a role in their regulation.

4.3.2.1. Mobility during exploration based tests

After chemogenetic manipulation of MRR-VGLUT3 cells, there was a tendency of the effect of manipulation for distance moved ($F_{(2,32)}=3.04$, $p=0.06$). Post hoc analysis showed that the inhibitory group moved less compared to both control ($p=0.08$) and excitatory groups ($p<0.05$). However, in the EPM and in the Y-maze, the locomotion did not differ between the groups (**Table 10**).

Table 10. Locomotion in different behavioural experiments after the manipulation of MRR-VGLUT3 neurons

Inhibition of the MRR-VGLUT3 neurons decreased the distance moved during OF, otherwise there was no effect on locomotion parameters in the different experiments. Data are expressed as mean \pm SEM.

EPM: elevated plus maze test; KO: knockout; OF: open field; VGLUT3: vesicular glutamate transporter type 3; WT: wild-type.

+ $p<0.05$ vs excitatory

Group		Control	Excitatory	Inhibitory
OF	Distance moved (cm)	2847.871 \pm 21 9.809	2892.461 \pm 160.103	2422.187 \pm 115.725+
Y-maze	Locomotion (frequency of arm entries)	24.750 \pm 2.226	21.846 \pm 1.671	22.800 \pm 1.607
EPM	Closed arm (frequency)	20.375 \pm 1.546	16.750 \pm 1.349	17.133 \pm 1.338

4.3.2.2. Anxiety-like behavioural tests

In the OF, neither the frequencies, nor the percentage of time spent in the centrum differed between the groups (**Figure 22A**). However, on the EPM, there was a significant effect of manipulation for the locomotion independent anxiety parameter (open/total %: $F_{(2,32)}=3.828$, $p<0.05$). Post hoc analysis showed that the excitatory group entered the open arms more often compared to the control group ($p<0.01$) (**Figure 22B**). The frequency of rearing showed a tendency ($F_{(2,31)}=2.769$, $p=0.08$), while that of head dipping showed a significant effect of manipulation ($F_{(2,31)}=3.572$, $p<0.05$). Post hoc test

of head dipping showed that the excitatory group exhibited more of this behaviour compared to control and inhibitory groups ($p < 0.05$ for both) (**Table 11**).

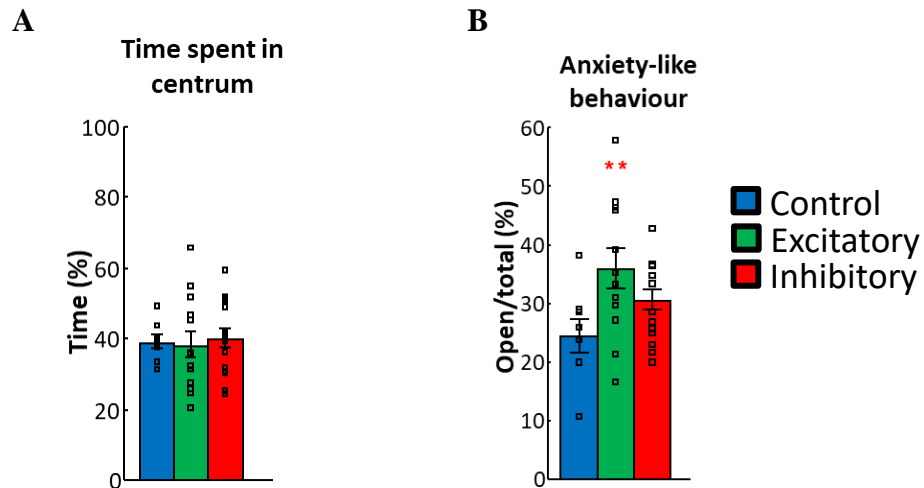


Figure 22. Anxiety-like behaviour after the manipulation of MRR-VGLUT3 neurons

(A) In the OF there was no difference between the percentage of time spent in the centrum between the groups. (B) On the other hand, on the EPM excitation resulted in an anxiolytic effect. Data are expressed as mean \pm SEM.

EPM: elevated plus maze; MRR: median raphe region; OF: open field; VGLUT3: vesicular glutamate transporter type 3.

** $p < 0.01$ vs control.

Table 11. Risk assessment behaviour after the manipulation of MRR-VGLUT3 neurons on the EPM apparatus

Excitation of the MRR-VGLUT3 neurons resulted in a significant increase of head dipping. Data are expressed as mean \pm SEM.

EPM: elevated plus maze test, SAP: stretched attend posture; VGLUT3: vesicular glutamate transporter type 3.

= $p < 0.05$ vs control; - $p < 0.05$ vs inhibitory.

Group	Control	Excitatory	Inhibitory
Head dipping	10.125 \pm 2.531	18.000 \pm 2.841 * -	10.867 \pm 1.588
SAP	24.875 \pm 4.340	35.545 \pm 4.509	38.600 \pm 6.375
Rearing	8.375 \pm 2.104	12.636 \pm 1.521	14.533 \pm 1.701
Grooming	2.000 \pm 0.267	1.273 \pm 0.333	1.267 \pm 0.228

Table 12. Results of sociability test after the manipulation of MRR-VGLUT3 neurons

Animals showed no side preferences during the object habituation phase. All groups preferred the social stimuli compared to the empty cage, but there was a decreased overall interest in the excitatory group. Data are expressed as mean±SEM.

MRR: median raphe region; SI: sociability index; VGLUT3: vesicular glutamate transporter type 3.

\$ p<0.05 vs random 0.

		Group	Control	Excitatory	Inhibitory
Object habituation phase	Frequency	Left cage	27.625± 1.580	25.364± 1.114	25.733± 1.318
		Right cage	28.625± 1.679	26.636± 0.856	28.667± 1.840
		Other	57.250± 2.889	52.818± 1.500	55.267± 2.907
	Time (%)	Left cage	11.750± 1.128	9.991± 0.754	12.307± 0.911
		Right cage	11.600± 1.262	10.318± 0.618	13.913± 1.584
		Other	74.963± 2.293	78.036± 1.030	72.047± 2.311
Sociability test	Frequency	Mouse	27.750± 1.346	23.833± 1.114	25.400± 2.522
		Cage	19.625± 1.164	17.667± 1.233	15.667± 1.508
		Other	47.875± 1.315	42.167± 1.957	40.400± 3.048
	Time (%)	Mouse	32.025± 2.030	24.467± 2.321	35.348± 3.283
		Cage	8.525± 1.078	8.067± 0.985	11.282± 2.235
		Other	58.000± 2.448	66.083± 2.309-	52.497± 3.447
		SI	78.991± 2.121\$	74.367± 3.327\$	76.518± 3.983\$

4.3.2.3. *Social interest*

During object habituation of the VGLUT3-Cre animals there were no differences between the time spent with sniffing each object, but there was a marginal effect of choice ($F_{(1,32)}=3.990$, $p=0.055$), without a significant post hoc test result (**Table 12**).

During sociability phase frequencies only showed a significant effect of choice ($F_{(1,32)}=33.030$, $p<0.01$), meaning that all animals preferred the stimulus animal over the empty cage (**Figure 23A** and **Table 12**). However, the percentage of time spent with the stimulus mouse had a significant effect of manipulation ($F_{(2,32)}=6.002$, $p<0.01$) and choice ($F_{(1,32)}=88.767$, $p<0.01$). Post hoc analysis of effect of choice revealed that all mice spent more time with the conspecific ($p<0.01$). Moreover, the excitatory group spent less time with the two cages together compared to the inhibitory group ($p<0.01$) (**Figure 23A**). Additionally, there was a significant effect of manipulation ($F_{(2,32)}=5.580$, $p<0.01$) for the percentage of time spent doing ‘other’ behaviours; post hoc analysis showed that the excitatory group spent more time with these behaviours compared to the inhibitory group ($p<0.01$). All three groups showed higher than 50% (random chance) SI (control: $t_{(7)}=13.670$, $p<0.01$; excitatory: $t_{(11)}=7.324$, $p<0.01$; inhibitory: $t_{(14)}=6.658$, $p<0.01$), with no differences between the groups (**Table 12**).

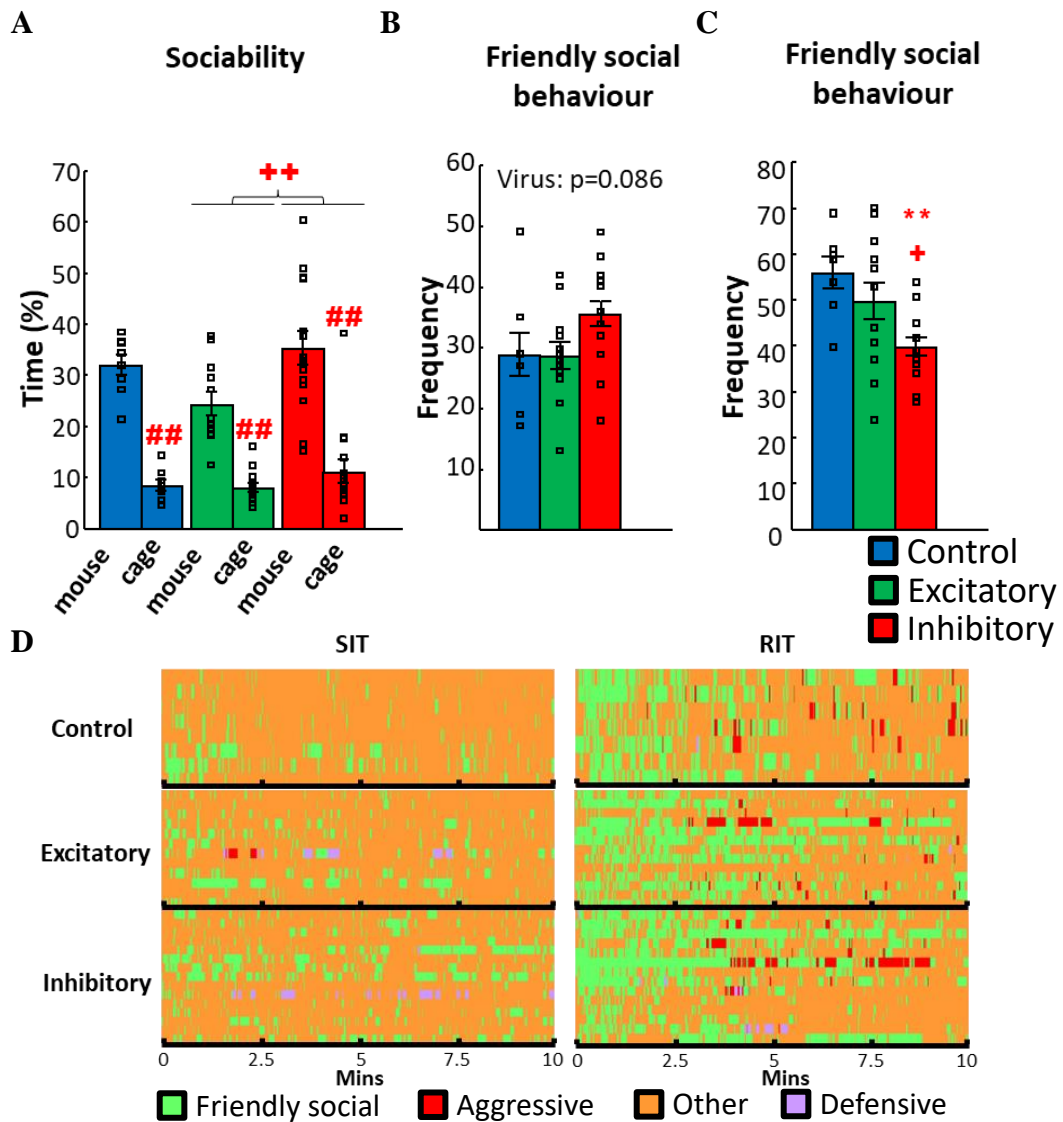


Figure 23. Social behaviour after the manipulation of MRR-VGLUT3 neurons (A) Neither excitation nor inhibition demolished social interest, but the excitatory group had a decreased interest compared to the inhibitory group. (B) Frequency of friendly social behaviour during SIT did not show significant differences between the groups, only a marginal increase in the inhibitory group was detectable. (C) During RIT, frequency of friendly social behaviour decreased in the inhibitory group. (D) Gantt-diagram illustrating the social behaviour of the VGLUT3-Cre animals during SIT (right) and RIT (left). Each row represents one animal in the Gantt-diagrams. Data are expressed as mean±SEM.

MRR: median raphe region; RIT: resident intruder test; SIT: social interaction test; VGLUT3: vesicular glutamate transporter type 3.

$p < 0.01$ vs mouse; ** $p < 0.01$ vs control; + $p < 0.05$, ++ $p < 0.01$ vs excitatory.

4.3.2.4. Social behaviour

During the SIT, there were no significant differences between the groups in the frequency of social behaviour, only a marginal effect of manipulation was found ($F_{(2,32)}=2.702$, $p=0.08$) (**Figure 23B,D** and **Table 13**) The frequency of ‘other’ behaviours had a significant effect of manipulation ($F_{(2,32)}=4.089$, $p<0.05$) and post hoc showed that the inhibitory group had higher frequency of this behaviour compared to control ($p<0.05$) and excitatory ($p<0.05$) groups. Additionally, the percentage of time spent doing ‘other’ behaviours showed a tendency for the effect of manipulation ($F_{(2,32)}=2.613$, $p=0.08$) (**Table 13**).

Table 13. Results of SIT and RIT experiments after manipulating MRR-VGLUT3 neurons

Detailed analysis of social behaviour. Inhibition marginally increased the frequency of friendly social behaviour during SIT, while during RIT it was decreased. Data are expressed as mean±SEM.

MRR: median raphe region; RIT: resident intruder test; SIT: social interaction test; VGLUT3: vesicular glutamate transporter type 3.

* $p<0.05$, ** $p<0.01$ vs control; + $p<0.05$ vs excitatory.

		Group	Control	Excitatory	Inhibitory
Social interaction test	Frequency	Social	29.000±3.505	28.833±2.246	35.600±2.099
		Aggressive	0.000±0.000	0.250±0.250	0.000±0.000
		Defensive	0.000±0.000	0.667±0.667	1.467±1.268
		Other	29.750±3.458	30.000±2.256	37.467±1.662 * +
	Time (%)	Social	9.364±2.704	11.758±1.897	17.459±3.170
		Aggressive	0.000±0.000	0.283±0.283	0.000±0.000
		Defensive	0.000±0.000	0.803±0.803	1.166±1.110
		Other	90.625±2.701	87.151±2.331	81.165±3.150
Resident intruder test	Frequency	Social	56.000±3.546	49.692±3.921	39.786±1.962 ** +
		Aggressive	5.000±1.543	3.154±0.926	3.857±1.600
		Defensive	0.143±0.143	0.308±0.175	0.857±0.404
		Other	54.571±2.877	49.000±3.718	38.714±2.879 ** +
	Time (%)	Social	29.479±2.909	35.205±4.572	35.068±4.854
		Aggressive	2.761±0.954	2.324±1.285	2.930±1.790
		Defensive	0.076±0.076	0.100±0.069	0.681±0.468
		Other	67.686±2.420	62.361±5.288	61.322±5.807

In the RIT analysis of the frequency of social behaviour showed a significant effect of manipulation ($F_{(2,31)}=5.938$, $p<0.01$). Post hoc analysis revealed that the inhibitory group initiated fewer social contacts compared to both control ($p<0.01$) and excitatory ($p<0.05$) groups. The frequency of ‘other’ behaviours also had a significant effect of manipulation ($F_{(2,31)}=5.308$, $p<0.05$) and post hoc analysis showed that the inhibitory group had lower frequency of this behaviour compared to control ($p<0.01$) and excitatory ($p<0.05$) groups (**Figure 23C,D** and **Table 12**).

4.3.2.5. Social discrimination test

None of the groups could differentiate between the ‘old’ and ‘new’ animals (**Table 14**). However, there was a significant effect of manipulation in both frequencies ($F_{(2,32)}=3.336$, $p<0.05$) and percentage of time ($F_{(2,32)}=7.070$, $p<0.01$) spent with conspecifics. Post hoc test showed that the inhibitory group initiated investigation more often than the control group ($p<0.05$), and marginally more than the excitatory group ($p=0.09$). Similarly, the inhibitory group also spent more time with conspecifics than the both control and excitatory groups ($p<0.01$ for all) (**Figure 24A**). Accordingly, the frequency ($F_{(2,32)}=2.586$, $p=0.09$) and percentage of time ($F_{(2,32)}=6.526$, $p<0.01$) spent

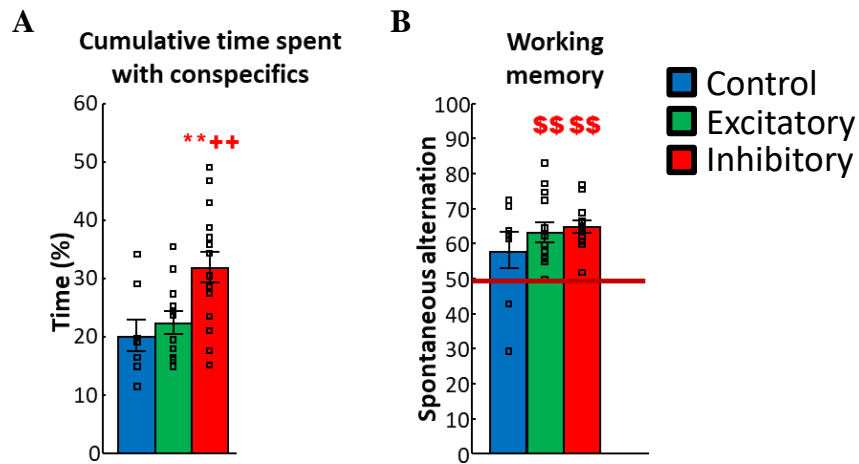


Figure 24. The effect of manipulation of MRR-VGLUT3 neurons on social discrimination and Y-maze behaviour

(A) During social discrimination phase, inhibition of the MRR-VGLUT3 neurons 24 hour before the test increased social interest. (B) Neither excitation, nor inhibition influenced the performance in Y-maze compared to controls. Red line indicates random chance level 50%. Data are expressed as mean±SEM.

MRR: median raphe region; VGLUT3: vesicular glutamate transporter type 3.

** $p<0.01$ vs control; ++ $p<0.01$ vs excitatory; \$\$\$ $p<0.01$ vs random 50%.

doing ‘other’ behaviours showed a marginal effect of manipulation. Post hoc analysis of the latter showed that the inhibitory group had a smaller frequency and spent less time with this behaviour compared to control ($p<0.01$) and excitatory groups ($p<0.01$) (**Table 14**).

Table 14. Results of social discrimination test 24-hour after the manipulation of MRR-VGLUT3 neurons

Although none of the animals had proper memory of the old mouse, the inhibitory group showed increased interest toward social stimuli. Data are expressed as mean \pm SEM.

MRR: median raphe region; SD: social discrimination index; VGLUT3: vesicular glutamate transporter type 3.

** $p<0.01$ vs control; ++ $p<0.01$ vs excitatory.

Group		Control	Excitatory	Inhibitory
Frequency	‘Old’ mouse	21.125 \pm 1.959	20.917 \pm 1.773	24.600 \pm 1.621
	‘New’ mouse	19.000 \pm 2.179	22.833 \pm 1.429	25.333 \pm 1.379
	Other	40.625 \pm 3.505	44.083 \pm 2.395	48.933 \pm 2.150
Time (%)	‘Old’ mouse	9.113 \pm 0.854	9.800 \pm 1.148	14.832 \pm 1.319
	‘New’ mouse	9.825 \pm 1.998	11.267 \pm 1.077	16.045 \pm 1.663
	Other	79.813 \pm 2.688	77.550 \pm 1.926	68.050 \pm 2.620 ** ++
SD		-1.394 \pm 7.819	7.801 \pm 6.172	1.420 \pm 5.198

4.3.2.6. Working memory

Spontaneous alternation on the Y-maze was intact for the manipulated groups (excitatory: $t_{(12)}=4.795$, $p<0.01$; inhibitory: $t_{(12)}=8.475$, $p<0.01$), but not for the control group (control: $t_{(7)}=1.605$, $p=0.153$), however, there were no significant differences between the groups (**Figure 24B**).

4.3.2.7. Summary of Project 3/b

By specifically manipulating MRR-VGLUT3 neurons, we showed that their activity may affect mobility, anxiety-like behaviour, and could have a role in the fine tuning of social behaviour. However, they do not affect long-term social or working memory.

4.3.3. Project 3/c: Role of MRR-VGLUT3 neurons in learning and memory formation

4.3.3.1. Chronic, chemogenetic excitation of MRR-VGLUT3 neurons

4.3.3.1.1. Mobility during exploration based tests

Excitation of MRR-VGLUT3 cells induced a marginal decrease in the distance moved in the OF ($F_{(1,21)}=3.387$, $p=0.08$) (**Figure 25A**). In the EPM we observed no effect of excitation or sex for distance moved and the frequency of closed arm entries (**Table 15**).

Table 15. Mobility and anxiety-like behaviour in the chemogenetics experiments in France

Excitation of the MRR-VGLUT3 had no effect on OF or EPM behaviour. Data are expressed as mean±SEM.

OF: open field; EPM: elevated plus maze.

Group			Control		Excitatory	
Sex			female	male	female	male
OF	Time (%)	Periphery	47.991± 2.723	60.942± 3.732	46.882± 4.572	51.647± 3.613
		Centrum	48.401± 2.419	34.1723± 3.762	48.350± 4.572	43.584± 3.613
EPM	Distance moved (cm)		2031.527± 203.351	2133.564± 215.358	1874.165± 242.029	2083.360± 206.010
	Closed arm (frequency)		26.500± 2.837	33.000± 4.152	26.667± 4.744	29.833± 3.478
	Time (%)	Closed arm	80.179± 1.6423	80.784± 3.041	81.885± 3.712	78.189± 3.0563
		Open arm	5.309± 1.341	6.699± 2.508	5.899± 2.100	9.123± 2.505

4.3.3.1.2. Anxiety-like behavioural tests

In the OF test, there was a significant effect of choice ($F_{(1,21)}=4.920$, $p<0.05$) and a choice×sex interaction ($F_{(1,21)}=6.106$, $p<0.05$) for the time spent in the different compartments. The post hoc test of the interaction showed significant difference between the compartments for males ($p<0.01$), but not for females ($p>0.5$). Interestingly, female mice did not show the natural preference for the periphery of the OF. Additionally, the time spent in the periphery (less anxiogenic compartment) was higher in the males compared to females ($p<0.05$) (**Table 15**). However, in the EPM test the locomotion-

independent anxiety parameter open/total% ratio showed no differences between the groups (**Figure 25B**).

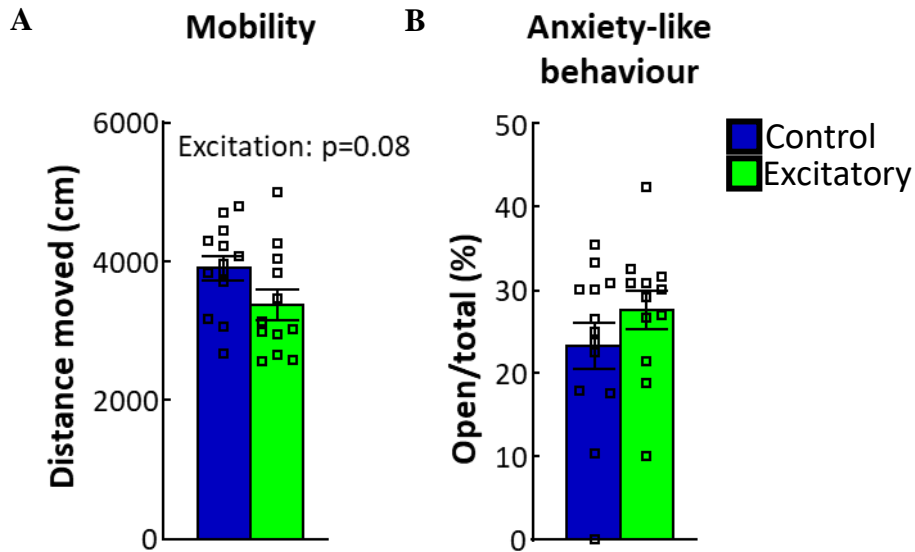


Figure 25. Results of OF and EPM after the chemogenetic excitation of MRR-VGLUT3 neurons in France

(A) Distance moved in the OF only showed a marginal difference between the groups. (B) On EPM, open/total% parameter did not differ between the groups. Data are expressed as mean±SEM.

EPM: elevated plus maze; MRR: median raphe region; OF: open field; VGLUT3: vesicular glutamate transporter type 3.

4.3.3.1.3. Learning- and memory formation

Without any manipulation, all animals were able to learn the spatial-independent task within 3 days (cue task phase; effect of time: $F_{(1,335,28.04)}=79.300$, $p<0.01$), and as expected, there were no differences between the groups or sexes (effect of sex: $F_{(1,21)}=2.263$, $p>0.5$) (**Figure 26A**).

Daily excitation of the MRR-VGLUT3 neurons did not have an effect on the learning curve during SRM task (effect of time: $F_{(3,594,75.48)}=8.681$, $p<0.01$; effect of group: $F_{(1,21)}=0.096$, $p>0.5$, effect of sex: $F_{(1,21)}=0.346$, $p>0.5$) (**Figure 26B**). However, during the memory tests (probes) there was a significant effect of excitation ($F_{(1,21)}=7.546$, $p<0.05$), a time×excitation interaction ($F_{(1,21)}=10.630$, $p<0.01$) and an excitation×sex interaction ($F_{(1,21)}=8.908$, $p<0.01$). Post hoc tests of the latter interaction showed that female control mice had the highest latencies reaching the supposed platform location

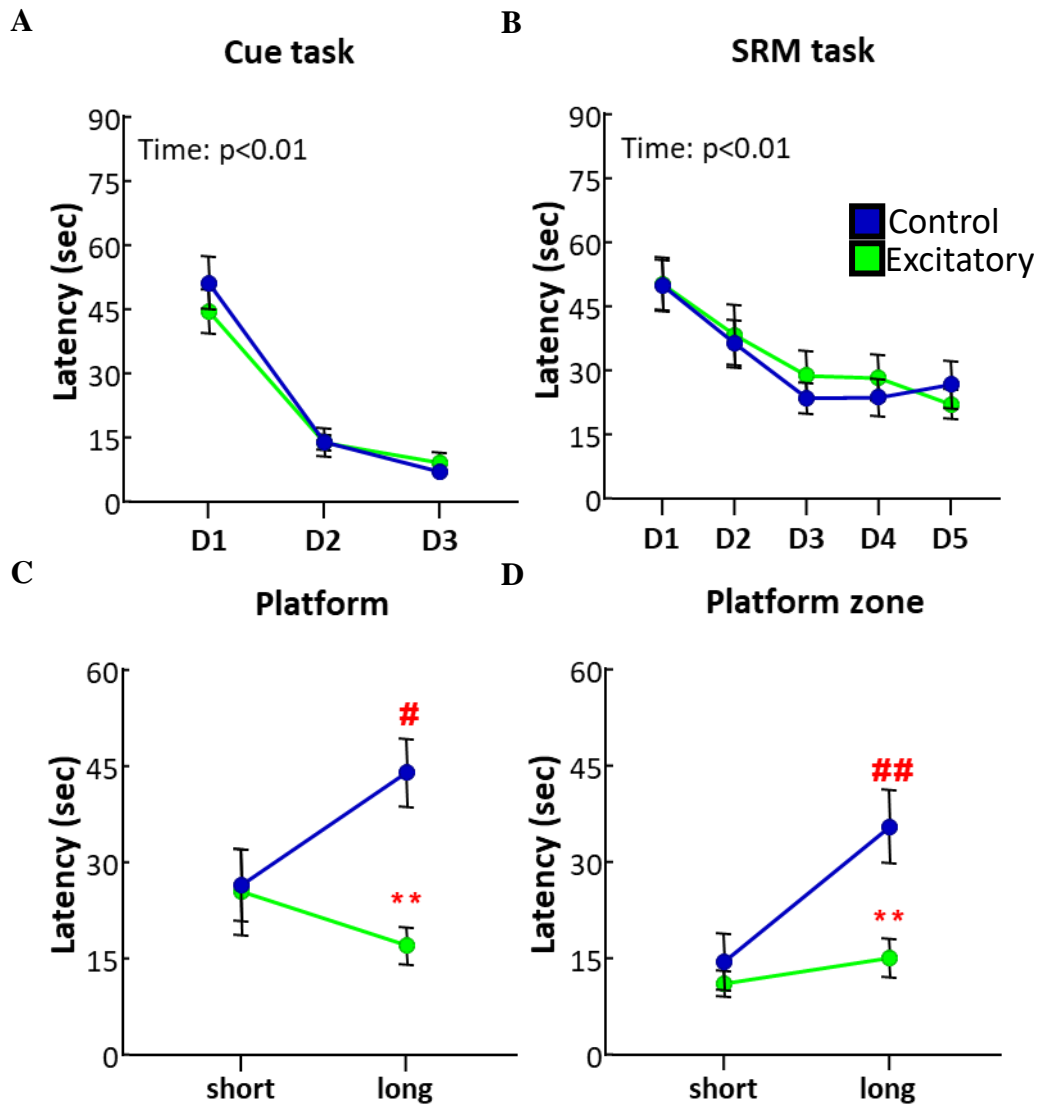


Figure 26. Latencies to find the platform during the different phases of MWM after chemogenetic excitation of MRR-VGLUT3 neurons in France

(A) Without CNO injections all animals could learn the Cue task within 3 days, without differences between the groups. (B) Despite the daily excitation, there were no differences between the groups during SRM task and both groups improved throughout the days. (C) Latencies to reach the platform zone during short-term memory probe did not differ between the groups, but 72 hours later (long-term memory probe) the excitatory group performed significantly better than the control group. (D) The result of latencies to platform was confirmed by the latencies to extended (x2) platform zone. Data are expressed as mean \pm SEM.

CNO: clozapine-N-oxide; MRR: median raphe region; MWM: Morris water maze; SRM: spatial reference memory; VGLUT3: vesicular glutamate transporter type 3.

$p < 0.05$, ## $p < 0.01$ vs short; ** $p < 0.01$ vs control.

($0.05 < p < 0.01$ vs. all other groups, data not shown). On the other hand, post hoc test of the time \times excitation interaction showed that during the short-term memory probe, there was no difference between the groups. The control group had a significant increase in the latency to reach the platform location two days later ($p < 0.05$), whereas the excitatory group showed comparable performances in both short- and long-term memory probes ($p > 0.1$). Additionally, the difference between the groups during the long-term memory probe was also significant ($p < 0.01$) (**Figure 26C**). This is supported by the finding latency of the extended (x2) platform zone: RM ANOVA showed a significant effect of time ($F_{(1,21)}=17.620$, $p < 0.01$), an effect of excitation ($F_{(1,21)}=8.042$, $p < 0.01$), a time \times excitation ($F_{(1,21)}=8.416$, $p < 0.01$), an excitation \times sex ($F_{(1,21)}=4.653$, $p < 0.05$) and a time \times excitation \times sex interaction ($F_{(1,21)}=4.375$, $p < 0.05$) also in this case. Post hoc test of time \times excitation \times sex interaction showed once again that control females were the slowest ($p < 0.05$ for all, data not shown). Time \times excitation interaction showed that the latencies to extended (x2) platform zone differed only during the long-term memory probe ($p < 0.01$), and while the control group showed natural forgetting between the probes ($p < 0.01$), the excitatory group did not ($p > 0.5$) (**Figure 26D**). At the same time, during the short-term probe test previously baited quadrant preference (percentage of time) was significantly higher than random chance 25% and was significantly higher compared to other quadrants for both control and excitatory groups (effect of choice: $F_{(2,213,46,47)}=16.07$, $p < 0.01$, post hoc $p < 0.05$ for all quadrants vs baited quadrant) (**Figure 27A**). Thus, we confirmed that the MRR-VGLUT3 excitation did not influence short-term memory (in the first 30s of the probe, control: $t_{(12)}=6.718$, $p < 0.01$; excitatory: $t_{(11)}=3.202$, $p < 0.01$), while long term memory was anyhow diminished (the time in previously baited quadrant was only marginally higher than the chance level 25%; control: $t_{(12)}=1.809$, $p=0.09$, excitatory: $t_{(11)}=2.042$, $p=0.06$). Although there were differences between the time spent in different quadrant during probe 2 ($F_{(2,425,50,92)}=3.336$, $p < 0.05$), post hoc test did not result in significant differences between the quadrants (**Figure 27B**). There were also no differences between the groups regarding the distance moved during the probes (**Table 16**).

Table 16. Distance moved on the probe days in Morris water maze experiments in France after repeated MRR-VGLUT3 excitations during learning

There was no significant difference between the groups.

Group	Control		Excitatory	
	female	male	female	male
Short-term	1572.483± 95.787	1751.200± 48.873	1698.267± 68.661	1640.333± 58.607
Long-term	1680.883± 71.089	1836.743± 53.066	1803.233± 76.106	1720.117± 67.630

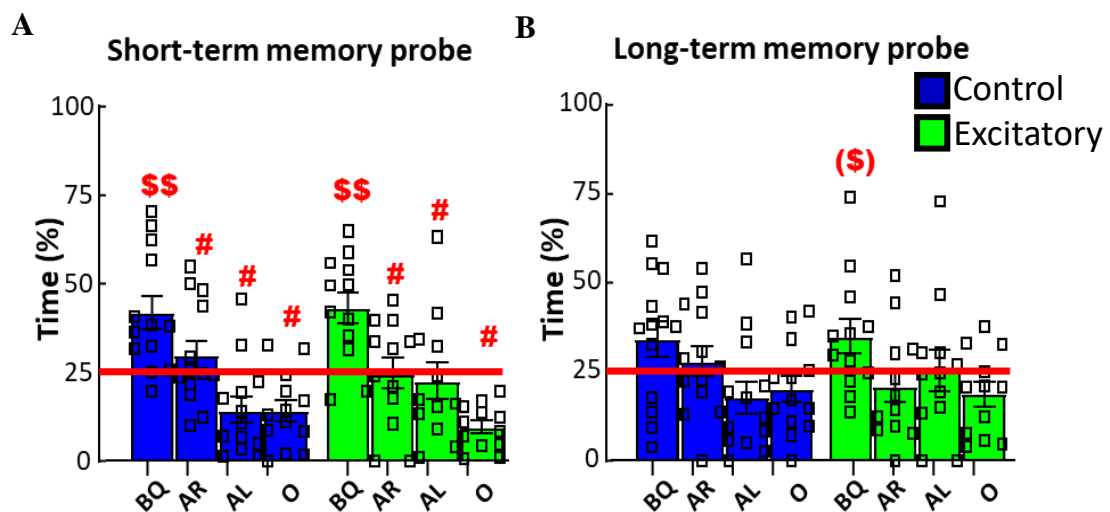


Figure 27. Time spent in different quadrants during memory probes of MWM in France after repeated chemogenetic MRR-VGLUT3 stimulation during learning (A) During short-term (10 mins) memory probe both groups preferred the BQ over the others and spent more time there than random 25% (red line), without any difference between the groups. (B) During long-term memory probe, only the excitatory group had a marginally higher preference for the BQ than random 25%. Data are expressed as mean±SEM.

BQ: baited quadrant; AR: adjacent right; AL: adjacent left; O: opposite.

(\$) p=0.06, \$\$ p<0.01 vs random 25%; # p<0.05 vs BQ.

To see whether these results are reproducible between the two different laboratories, we repeated these experiments in Hungary as well, with chemogenetics on the commercialised VGLUT3-Cre mouse strain. Shortly, all animals learnt the cue task in 3 days (effect of time: $F_{(2,46)}=153.800$, $p<0.01$) without differences between groups

($F_{(1,23)}=0.001$, $p>0.5$) or sex ($F_{(1,23)}=0.530$, $p>0.1$) (**Figure 28A**). Similarly, during the SRM task, there were no differences between the groups (effect of excitation: $F_{(1,23)}=0.601$, $p>0.1$) or sexes ($F_{(1,23)}=0.464$, $p>0.5$), only a significant effect of time ($F_{(2.837, 65.25)}=19.370$, $p<0.01$), indicating that all animals could learn the new task (**Figure 28B**). However, during probe tests, there was a significant time \times excitation interaction for latency to platform ($F_{(1,25)}=11.180$, $p<0.01$), without an effect of sex ($F_{(1,23)}=0.028$, $p>0.5$), where post hoc comparison showed that the control group had an increase in latency between short and long term-memory probes ($p<0.05$), while the excitatory group only had a marginal decrease ($p=0.09$), and the difference between the groups during long-term memory probe was significant ($p<0.01$) (**Figure 28C**). However, latency to the extended (x2) platform zone only had a marginal time \times excitation interaction ($F_{(1,25)}=3.935$, $p=0.058$), showing a similar trend than in the experiment conducted in France (**Figure 28D**). None of the groups had proper quadrant preferences during either short-term (in the first 30s of the probe, control: $t_{(13)}=1.262$, $p>0.1$; excitatory: $t_{(12)}=0.843$, $p>0.1$, baited quadrant vs other quadrants effect of choice: $F_{(3,69)}=4.355$, $p<0.01$, but post hoc test was not significant) (**Figure 28E**), or long-term memory tests (control: $t_{(13)}=0.544$, $p>0.5$; excitatory: $t_{(12)}=1.478$, $p>0.1$, baited quadrant vs other quadrants effect of choice: $F_{(3,69)}=1.253$, $p>0.1$) (**Figure 28F**). The distance moved during the probes also did not differ between the groups (short: $F_{(1,23)}=0.090$, $p>0.5$; long: $F_{(1,23)}=0.817$, $p>0.1$) and sexes (short: $F_{(1,23)}=0.006$, $p>0.5$; long: $F_{(1,23)}=0.843$, $p>0.1$) (**Table 17**).

In summary, while MRR-VGLUT3 neurons does not affect spatial learning in the SRM task, they affect long-term spatial memory. Additionally, by repeating the experiment in two countries, we strengthened the reproducibility of our result. However, we must note that despite the appropriate acquisition of cue and SRM tasks - with almost comparable levels of performances -, it seems that SRM cannot be solved in Hungary using exclusively spatial cues.

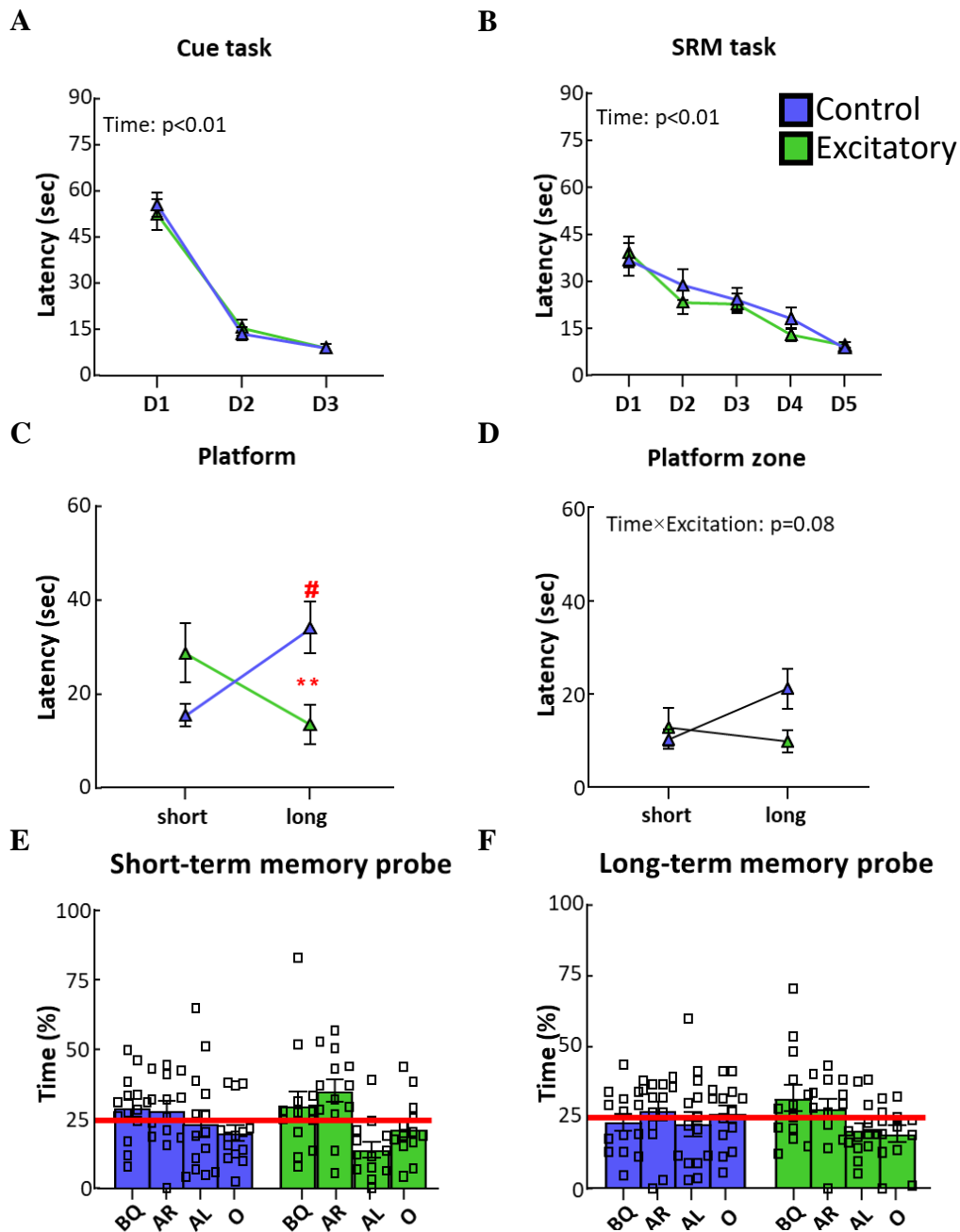


Figure 28. Reproducibility of the MWM chemogenetic results in Hungary

(A) Adequate adaptation of the protocol is reflected by the successful Cue task learning. (B) Similarly, SRM task was completed without difference between the groups. (C) Latency to platform statistically did not differ during short-term (10 mins) probe but replicated the same difference during long-term (72 hours) probe as was seen in France. (D) Latency to extended (x2) platform zone showed the same difference, but it was only marginally significant. (E and F) None of the groups showed proper quadrant preference during memory probes. Data are expressed as mean \pm SEM.

AL: adjacent left; AR: adjacent right; BQ: baited quadrant; MWM: Morris water maze; O: opposite; SRM: spatial reference memory.

$p < 0.05$ vs short; ** $p < 0.01$ vs control.

Table 17. Distance moved on the probe days in Morris water maze experiments in Hungary after repeated MRR-VGLUT3 excitations during learning

There was no significant difference between the groups.

Group		Control		Excitatory	
Sex		female	male	female	male
Distance moved (cm)	Short-term	1885.236± 50.343	1848.428± 68.824	1873.196± 62.156	1899.716± 77.421
	Long-term	1871.921± 57.359	1912.023± 80.425	1910.937± 65.013	2008.934± 101.237

4.3.3.2. Acute, optogenetic excitation of MRR-VGLUT3 neurons

4.3.3.2.1. Mobility during exploration based tests

The analysis of the distance moved during OF test showed a marginal effect of sex ($F_{(1,18)}=4.087$, $p=0.058$) and excitation ($F_{(1,18)}=3.528$, $p=0.07$), without interaction between them ($F_{(1,18)}=0.286$, $p>0.5$) (**Figure 29A**). When corrected with laser activity, the effect of sex became significant (ANCOVA: $F_{(1,19)}=14.560$, $p<0.01$), showing that females moved more.

In the EPM, excitation significantly increased the distance moved ($F_{(1,21)}=4.869$, $p<0.05$) and the frequencies of closed arm entries ($F_{(1,21)}=8.948$, $p<0.01$) (**Table 18**). However, in the ANCOVA, the covariate laser activity became significant, along with the effect of excitation in the case frequency of closed arm entries (covariate: $F_{(1,20)}=21.351$, $p<0.01$; effect of manipulation: $F_{(1,20)}=8.898$, $p<0.01$) and the distance moved (covariate: $F_{(1,20)}=9.527$, $p<0.01$; effect of manipulation: $F_{(1,20)}=3.277$, $p=0.08$).

4.3.3.2.2. Anxiety-like behavioural tests

The time spent in compartments showed a significant effect of choice ($F_{(1,20)}=89.870$, $p<0.01$), a choice×excitation interaction ($F_{(1,20)}=13.210$, $p<0.01$) and a marginal excitation×sex interaction ($F_{(1,20)}=3.366$, $p=0.08$). Post hoc test of the choice×excitation interaction showed that both groups preferred the periphery over the centrum ($p<0.01$ for all), but the ChR2 group spent more time in the periphery compared to the control group ($p<0.01$) (**Table 18**). Correction with laser activity resulted in

Table 18. Mobility and anxiety-like behaviour in the optogenetics experiments in Hungary

Both treatment groups preferred the periphery over the centrum, with Chr2 group preferred the periphery more than the control animals, but after correction for laser activity, this difference disappeared. On the contrary, on EPM after correction, the effect of manipulation became significant in most parameters (distance moved, closed arm frequency, percentage of time spent in closed and open arms), indicating an anxiolytic effect.

OF: open field; EPM: elevated plus maze.

Group			Control		Excitatory	
Sex			female	male	female	male
OF	Time (%)	Periphery	53.542± 3.342	62.054± 3.281	73.546± 5.198	70.511± 2.721
		Centrum	40.163± 3.511	32.720± 3.622	24.385± 5.167	23.846± 2.884
EPM	Distance moved (cm)		2388.182± 335.136	2296.032± 220.525	3166.213± 310.243	2792.891± 291.501
	Closed arm (frequency)		19.400± 1.691	26.286± 3.828	42.667± 6.711	35.714± 6.585
	Time (%)	Closed arm	85.096± 3.417	79.883± 4.116	61.716± 6.379	71.989± 4.281
		Centrum	9.343± 1.704	12.495± 2.010	25.928± 4.707	17.801± 2.379
		Open arm	3.394± 1.405	5.062± 2.289	10.648± 2.017	7.634± 1.581

significant differences regarding sex, excitation or interaction in the case of time spent in centrum, with a significant covariate of laser activity ($F_{(1,19)}=11.438$, $p<0.01$).

The open/total% parameter representing locomotion-independent anxiety-like behaviour showed only a marginal effect of sex ($F_{(1,21)}=3.251$, $p=0.08$) (**Figure 29B**), while time spent in different compartments had a significant effect of choice ($F_{(2,63)}=458.900$, $p<0.01$), a choice×excitation interaction ($F_{(2,63)}=16.480$, $p<0.01$) and choice×excitation×sex interaction ($F_{(2,63)}=4.124$, $p<0.05$). The post hoc test of the triple interaction showed that all groups preferred the closed arm compared to the other two compartments ($p<0.01$ for all), but Chr2 females spent less time in the closed arm compared to both control males ($p<0.05$) and control females ($p<0.01$) (**Table 18**). In the ANCOVA, the covariate laser activity became significant, along with the effect of excitation in the case the percentage of time spent in the open arms (covariate: $F_{(1,20)}=10.387$, $p<0.01$; effect of manipulation: $F_{(1,20)}=4.796$, $p<0.05$), percentage of time

spent in the closed arms (covariate: $F_{(1,20)}=26.425$, $p<0.01$; effect of manipulation: $F_{(1,20)}=12.334$, $p<0.01$). On the other hand, for the open/total parameter only the effect of sex became marginally significant (covariate: $F_{(1,20)}=2.824$, $p=0.1$; effect of sex: $F_{(1,20)}=3.421$, $p=0.08$).

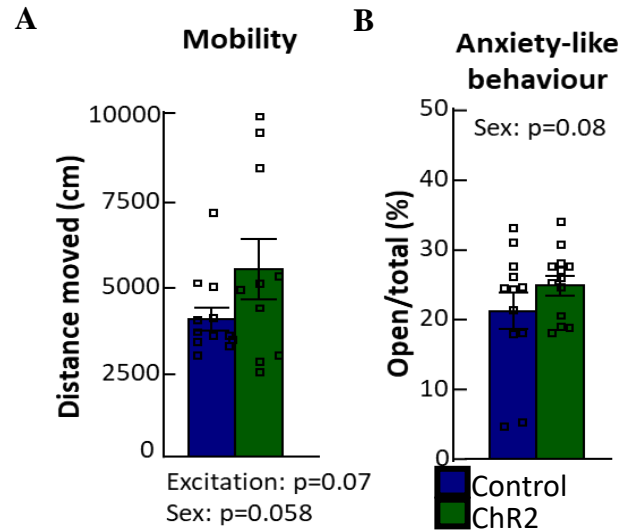


Figure 29. Mobility and anxiety-like behaviour during optogenetic excitation of MRR-VGLUT3 neurons in Hungary

(A) Excitation in the periphery resulted in marginal differences between the groups, which was not significant after correcting for laser activity. However, females generally moved more. (B) Optogenetic excitation while making decision in the centrum did not affect anxiety-like behaviour, but there was a tendency for females to be more anxious. Data are expressed as mean \pm SEM.

MRR: median raphe region; VGLUT3: vesicular glutamate transporter type 3.

4.3.3.2.3. Learning and memory formation

Similarly to chemogenetics, all animals completed the cue task (no manipulation) within 3 days (effect of time: $F_{(1.508,30.160)}=108.500$, $p<0.01$), and there were no differences between the groups (effect of excitation: $F_{(1,20)}=1.103$, $p>0.1$) (**Figure 30A**), but a general effect of sex was detectable ($F_{(1,20)}=5.638$, $p<0.05$), where females had slightly higher latencies to reach the platform (data not shown).

Daily excitation of the MRR-VGLUT3 neurons while the animals were sitting on the platform (20 Hz, 10 sec) induced a statistically significant effect of time ($F_{(3.126,62.52)}=10.810$, $p<0.01$); excitation ($F_{(1,20)}=0.018$, $p<0.01$), sex ($F_{(1,20)}=10.860$,

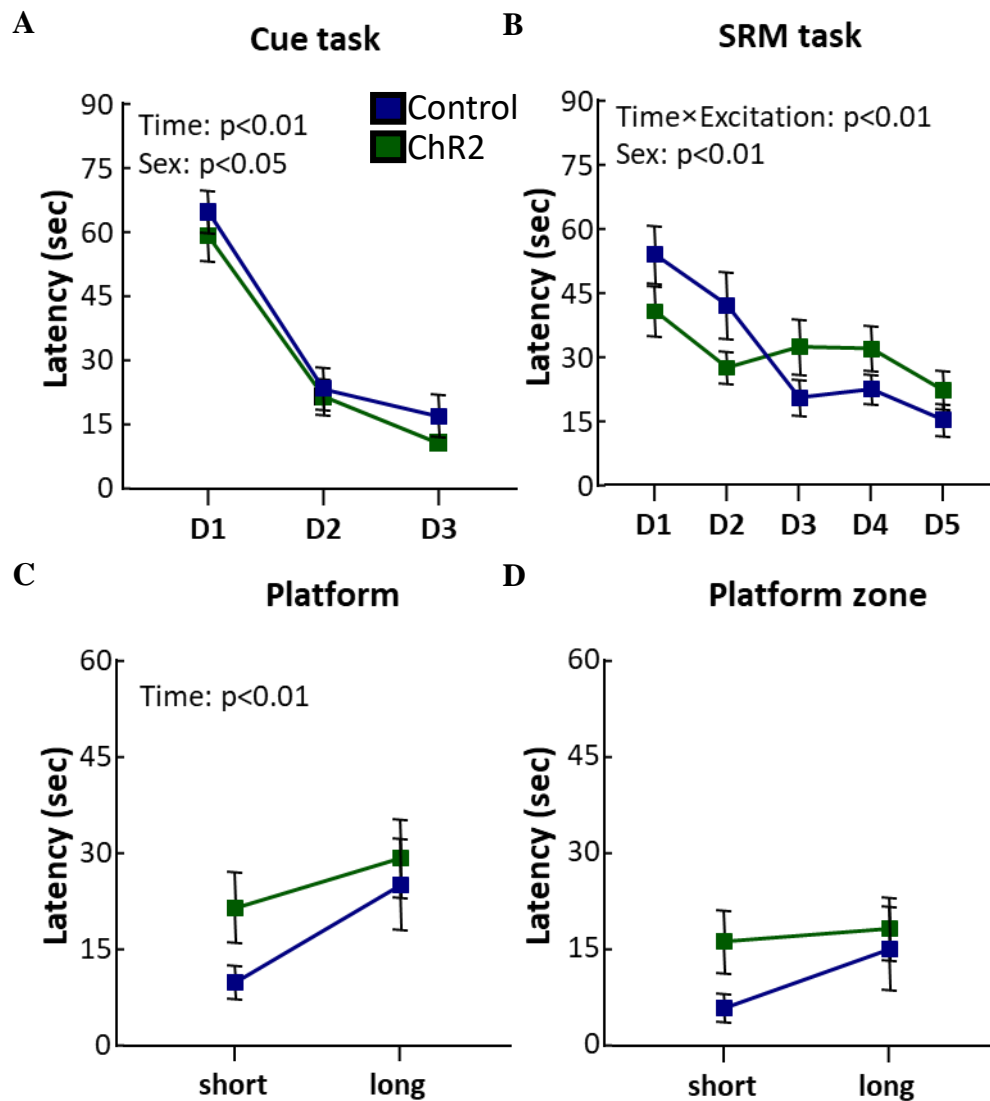


Figure 30. Latencies to finding the platform during the different phases of MWM after repeated optogenetic excitation of MRR-VGLUT3 cells in Hungary

(A) All animals could learn the Cue task within 3 days, without differences between the groups. (B) During SRM, although there was a significant time×excitation interaction, post hoc tests showed no differences between the days and groups. Effect of sex showed that all females had higher latencies, regardless of their groups. (C) Latencies to the missing platform during both memory probes did not differ between the groups. (D) Similarly, latencies to the extended (x2) platform zone did not show differences. Data are expressed as mean±SEM.

MWM: Morris water maze; SRM: spatial reference memory.

$p < 0.01$) and a time \times excitation interaction ($F_{(4,80)} = 3.794$, $p < 0.01$), without any significant differences in post hoc tests ($p > 0.5$ all). Although once again females had higher latencies (regardless of groups; data not shown), by the end of D5, all animals found the platform within 30 sec (**Figure 30B**).

During the probe tests there was a significant effect of time ($F_{(1,20)} = 5.723$, $p < 0.05$), showing an increase in the latencies by long-term memory probe, but no differences between the groups ($F_{(1,20)} = 1.382$, $p > 0.1$) or sexes ($F_{(1,20)} = 0.072$, $p > 0.5$) (**Figure 30C**). Latency of reaching the extended ($\times 2$) platform zone was not influenced by any studied factor (**Figure 30D**). The time spent in the previously baited quadrant was significantly higher than the random chance 25% for both control and excitatory groups in the short-term memory probe (in the first 30 sec of the probe, control: $t_{(9)} = 3.086$, $p < 0.05$; excitatory: $t_{(12)} = 3.748$, $p < 0.01$), and it was also significantly higher compared to other quadrants (effect of choice: $F_{(2,206,46,32)} = 9.762$, $p < 0.01$, post hoc $p < 0.05$ for all quadrants vs baited quadrant) (**Figure 31A**). However, during the long-term memory probe only the

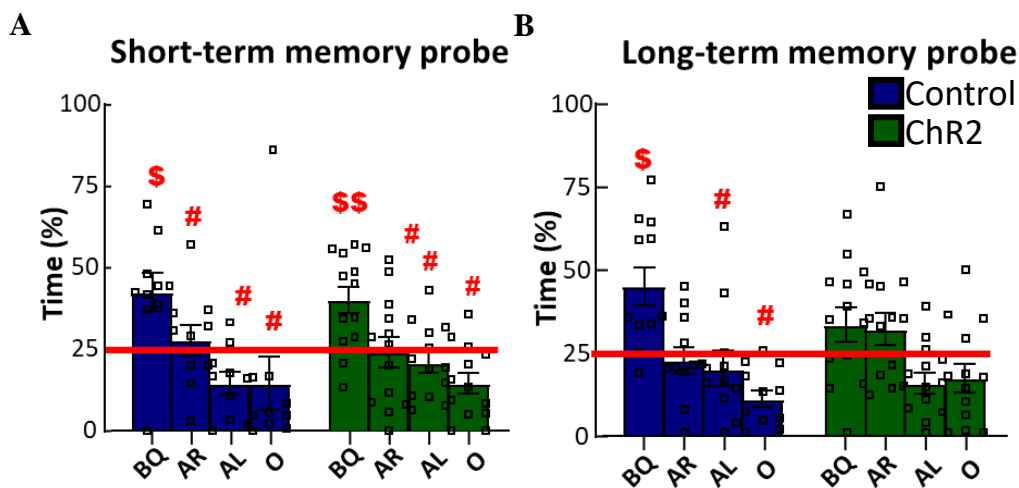


Figure 31. Time spent in different quadrants during memory probes of MWM after optogenetic excitation of MRR-VGLUT3 cells in Hungary

(A) During short-term (10 mins) memory probe, both groups preferred the BQ over the others and spent more time there than random 25% (red line), without any difference between the groups. (B) During long-term memory probe, only the control group had a marginally higher preference for the BQ than random 25%. Data are expressed as mean \pm SEM.

AL: adjacent left; AR: adjacent right; BQ: baited quadrant; MWM: Morris water maze; O: opposite.

\$ $p < 0.05$, \$\$ $p < 0.01$ vs random 25%; # $p < 0.05$ vs BQ.

control group had preference for the baited quadrant that was significantly higher than 25% (control: $t_{(10)}=3.101$, $p<0.05$, excitatory: $t_{(12)}=1.023$, $p>0.1$), and a significant effect of choice ($F_{(2.441,53.71)}=9.149$, $p<0.01$) for the control group, but not for the excitatory group (**Figure 31B**).

There were also no differences between the groups regarding the distance moved during the probes, only an effect of sex (short: $F_{(1,20)}=9.437$, $p<0.01$; long: $F_{(1,20)}=9.437$, $p<0.01$), with lower values in females was detected (**Table 19**).

Table 19. Distance moved on the probe days in MWM after optogenetic activation of MRR-VGLUT3 cells in Hungary

There was no significant difference between the groups, only an effect of sex was detected showing that females swam less than males. Data are expressed as mean \pm SEM.

MWM: Morris water maze.

Group	Control		Excitatory	
	female	male	female	male
Short-term	1386.7424 \pm 148.723	1685.708 \pm 68.791	1427.630 \pm 118.664	1784.081 \pm 89.918
Long-term	1472.682 \pm 129.560	1737.478 \pm 69.822	1468.192 \pm 101.818	1801.431 \pm 77.014

4.3.3.3. Summary of Project 3/c

Although the results reflecting mobility is not significant, but the excitation of MRR-VGLUT3 neurons might be anxiolytic. On the other hand, in learning and memory formation, we showed that the excitation has no effect on the learning curve. However, previous chronic excitation was needed to have an effect on long-term spatial memory.

5. Discussion

Table 20 contains the summary of results presented in this thesis.

Table 20. Summary of results

CNO: clozapine-N-oxide; Glu: glutamate; HC: hippocampus; KO: knockout; LPB: lateral parabrachial nucleus; MRR: median raphe region; OF: open field; PRF: pontine reticular formation; PRN: pontine raphe nucleus; RFP: red fluorescent protein; RN: midbrain raphe nuclei; RT-qPCR: reverse transcription quantitative polymerase chain reaction; sdFISH: double-probe fluorescent in situ hybridization; Tph2: Tryptophan hydroxylase 2; VGLUT3: vesicular glutamate transporter type 3.

Project	Parameter	Result(s)	
Project 1 Behaviour of VGLUT3 KO mice	Mobility	• no difference during active period	
	Anxiety-like behaviour	• increased anxiety • decreased risk assessment	
	Social behaviour	• increased social interest • increased aggression in anxiogenic context	
	Learning and memory	• impaired social memory (24h) • impaired memory revealed in the cognitive flexibility probe test	
Project 2 VGLUT3 mRNA in the brainstem	Mouse (sd-FISH)	• 20% of all VGLUT3+ neurons are Tph2+ as well in the MRR	
	Human (RT-qPCR)	• VGLUT3 mRNA in LPB, PRF, PRN and RN	
Project 3	Validation	Neurotransmitter release	• Glu release in the HC after MRR excitation
		AAV expression	• proper co-expression of RFP in VGLUT3+ cells
		c-Fos activity	• CNO-induced neuronal activity
	MRR-VGLUT3 in behaviour	Mobility	• MRR-VGLUT3 excitation was inconclusive (chemogenetics and optogenetics) • MRR-VGLUT3 inhibition decreases mobility (OF, chemogenetics)
		Anxiety-like behaviour	• MRR-VGLUT3 excitation is anxiolytic (chemogenetics, optogenetics)
		Social behaviour	• MRR-VGLUT3 inhibition has context dependent effect on social behaviour (chemogenetics) • MRR-VGLUT3 inhibition increases long-term social interest (chemogenetics)
		Learning and memory	• Chronic MRR-VGLUT3 excitation facilitates long-term memory formation (chemogenetics) • Acute MRR-VGLUT3 excitation has no effect (optogenetics)

5.1. The behaviour of VGLUT3 KO mice

To study the role of VGLUT3 in physiology and behaviour first VGLUT3 KO mice have been bred and studied. Majority of the literature agreed on two significant changes in them: they show altered locomotor activity (Divito et al., 2015, Gangarossa et al., 2016) and highly anxious behavioural phenotype (Amilhon et al., 2010, Balazsfi D. et al., 2016, Balazsfi D., Fodor, et al., 2018, Sakae et al., 2019).

Depending on the duration of the behavioural tests and the anxiogenic level of the environment, VGLUT3 KO mice proved to be hyperactive (Gras et al., 2008, Sakae et al., 2019) or hypoactive (Balazsfi D., Fodor, et al., 2018, Divito et al., 2015, Fazekas et al., 2019, Gangarossa et al., 2016, Gras et al., 2008, Horvath et al., 2018, Mansouri-Guilani et al., 2019, Sakae et al., 2019), respectively. In our hands the KO mice did not show any locomotor alterations during short observations in a new environment neither in **Project 1/a**, nor in **Project 1/b**. However, in **Project 1/a**, the animals were kept in a ‘reverse’ day-night cycle, meaning that the experiments were done during their active period. **Project 1/b** was done during the light period, but the context of the MWM task (that is, swimming in water) proved to be enough motivation. Thus, these results further strengthen the circadian activity dependent role of VGLUT3 in locomotion. Divito et al (Divito et al., 2015) have shown that regardless of environment (home cage vs. open field), VGLUT3 KO mice move more only during their active periods, but not during their subjective night. Coincidentally, exploratory rearing behaviour, which can be an anxiety-like indicator in OF (Sturman et al., 2018), was still lower in the KO mice, indicating that this hyperlocomotion is independent of anxiety. It was also shown that during subjective night VGLUT3 KO mice have increased DA synthesis in the striatum, which is a known regulator of locomotion (Barbera et al., 2016, Burns et al., 1994, Grillner et al., 2008) and found to be regulated, at least partly, by VGLUT3 (Divito et al., 2015).

Increased anxiety-like behaviour of VGLUT3 KO mice was confirmed in our local colony in **Project 1/a**: even in a less anxiogenic OF conducted in dark (under red light) KO animals preferred the periphery more than their WT littermates. Moreover, in the EPM they not only spent less time in the open arm, but also exhibited less risk assessment behaviours, such as rearing. It has been proposed that this behavioural phenotype is at least partially due to the higher HPA axis activity of KO mice (Balazsfi

D., Fodor, et al., 2018), which is already present during early postnatal life (Balazsfi D. et al., 2016) contributing to the development of anxiety. However, VGLUT3+ neurons can also be found in the CNS in key brain areas regulating anxiety-like behaviour in rodents. Interestingly, even amygdala contains a little amount of VGLUT3+ neurons (Fremeau et al., 2002, Gras et al., 2002, Harkany et al., 2003, Herzog et al., 2004, Hioki et al., 2003, Schafer et al., 2002, Stornetta et al., 2005), but their functional role has not been investigated. Anatomically, numerous VGLUT3+ projections end within the amygdala: for example, DR 5-HT+ and VGLUT3+ neurons project to the BLA parvalbumin+ neurons and regulate anxiety-like behaviour (Yu et al., 2022). Moreover, DR and MRR, nuclei both rich in VGLUT3+ neurons, are also interconnected and deeply implicated in anxiety-like behaviour (Teissier et al., 2015, Turcotte-Cardin et al., 2019). Although the literature mainly concentrates on the serotonergic component, we cannot rule out the role of neurons co-expressing 5-HT and VGLUT3 markers. Interestingly, HC also contributes to anxiety (Engin and Treit 2007), where numerous interneurons are VGLUT3+ (Fasano et al., 2017, Herzog et al., 2004, Sakae et al., 2019, Somogyi et al., 2004, Stensrud et al., 2015). Studies show that NMDA antagonists have an anxiolytic effect on EPM post-stress (Padovan et al., 2000), however, it has been suggested that ventral HC rather than the VGLUT3-containing dorsal part is responsible for this (Nascimento Hackl and Carobrez 2007).

In the sociability test, KO animals proved to be more social compared to their WT littermates, which we failed to observe in our previous study (Fazekas et al., 2019). This could be explained by the previously mentioned circadian difference (i.e. here the animals were tested during their active phase, while previously during the light phase), as well as by slight difference in the protocol (i.e. here a one-chamber device was used, while previously we used a three chamber arrangement). Interestingly, the KO animals showed aggressive behaviour only during SIT, which might be explained by the protocol. Although the habituation to the context of SIT is aimed to reduce aggression, the test was conducted in an anxiogenic (lighted) environment, which could have facilitated aggression in the sensitive KO mice. In accordance with the literature (Amilhon et al., 2010), in RIT there was no significant change in their behaviour, further supporting the anxiety-induced nature of aggression during SIT. Social behaviour requires complex cognitive capacities, and it is strongly tied to mPFC (Felix-Ortiz et al., 2016, Franklin et

al., 2017, Ko 2017, Lee et al., 2016, Sun et al., 2020), among many others. It has been suggested that alterations in social behaviour in psychological disorders, such as schizophrenia, is due to the disturbed balance between excitation and inhibition, for example caused by NMDA hypofunction (Kehrer et al., 2008). Although the cortex is more abundant in VGLUT1+ neurons or VGLUT2+ axon terminals (Kaneko and Fujiyama 2002), it is worth noting that scarce VGLUT3+ neurons with so far unknown roles in behaviour are also present here (Herzog et al., 2004). However, we must also add that social skills are heavily dependent on smelling, and it has been demonstrated that certain neuron populations of the olfactory bulb express VGLUT3 (Commons 2009, Fu et al., 2010), controlling the output of sensory information to the cortex (Fu et al., 2010).

Decreased VGLUT3 protein expression was linked to impaired memory (Cheng et al., 2011), and VGLUT3 is also expressed in the hippocampus (Gras et al., 2002, Herzog et al., 2004, Schafer et al., 2002, Somogyi et al., 2004). Indeed, VGLUT3 and CCK double positive basket cells seem to be necessary for optimal theta oscillation, offering the basis for normal spatial memory formation (Del Pino et al., 2017). Moreover, the deletion of VGLUT3 was shown to induce metaplastic shift to lower the frequency of theta rhythm, indicating an impairment in excitatory-inhibitory balance (Fasano et al., 2017). Despite this, complete knockout of VGLUT3 resulted only in minor impairments in learning and learning flexibility (Fazekas et al., 2019), and in **Project 1/a** we only found impairment in long-term (24-hour) social memory. Similarly, in our previous study VGLUT3 KO mice had intact social preference and short-term (4-hour), but no long-term (24-hour) social memory in the three-chamber sociability test. In the Y-maze, which measures working memory, we observed intact working memory, similarly to (De Almeida et al., 2023), as opposed to the previous impairment in our study (Fazekas et al., 2019).

Moreover, a known hippocampus dependent learning and memory formation paradigm (Lissner et al., 2021, Morris R. G. et al., 1982, Richter-Levin et al., 1995, Vorhees and Williams 2014), the MWM also failed to show any major impairments, similarly to (De Almeida et al., 2023) study. Additionally, there was also no effect on reward-based learning (operant conditioning or holeboard discrimination) paradigms (Fazekas et al., 2019). Reward is commonly associated with dopamine and its effects in the NAcc (Hikida et al., 2016). It has been demonstrated that VGLUT3 positive neurons

project to the dopaminergic neurons of the VTA (Qi et al., 2014), the latter sending afferents to the NAcc. The perikarya and dendrites of the NAcc neurons are also VGLUT3+ (Zou et al., 2020). Moreover, chronic consumption of sucrose, a reward, increased VGLUT3 expression in the NAcc (Tukey et al., 2013). Cocaine self-administration was increased in VGLUT3 KO mice in connection with enhanced glutamatergic transmission in their NAcc (Sakae et al., 2015). A new study on them confirmed their proper learning and recognition memory ability, but impaired pattern separation after aversive stimuli (De Almeida et al., 2023). Since the lack of difference was observed during the active phase without hypolocomotion in the present study, and in de Almeida's study during their inactive phase with visible hypolocomotion (De Almeida et al., 2023), this indicates a major sensitivity of these tests to environmental factors, as well as suggest that the KO-induced changes are subtle and can be easily compensated.

However, constitutive gene knockout animal models cannot rule out possible compensatory molecular, physiological and behavioural adaptations for survival. For example, VGLUT3 KO mice maintain normal DA release (Divito et al., 2015), but not synthesis (Barbera et al., 2016, Burns et al., 1994, Grillner et al., 2008) in the striatum, but have altered glutamatergic, dopaminergic and cholinergic receptor levels (Ibrahim et al., 2022) and serotonergic transmission (Amilhon et al., 2010, Voisin et al., 2016). Moreover, the fact that WT mice from different strains already show varied VGLUT3 levels throughout the brain show the necessity of both temporal and site-specific manipulations in order to reveal the exact role of VGLUT3 in behaviour (Sakae et al., 2019).

5.2. Presence of MRR-VGLUT3 neurons in the brainstem

Similarly to DR, there is a remarkable amount of VGLUT3+ neuronal population in the mouse's MRR (Sos et al., 2017). They are either purely glutamatergic, or co-express mainly serotonergic markers (Sos et al., 2017). Based on our sdFISH experiment (**Project 2/a**), we counted that up to ~20% of VGLUT3+ neurons also co-express Tph2 mRNA, a serotonergic marker in the MRR. This is slightly lower than the ratios that was found by Sós et al (Sos et al., 2017). The discrepancies could be explained by the different protocols used in the experiments. Sós et al sampled more slices: every second one, each

60 μm thick, while we took one slice every 150 μm , each 15 μm thick. This resulted in an approximately 10-fold decrease in the number of counted cells (5054 VGLUT3+ neurons on average in Sós et al, vs. 496 on average for us). Moreover, they counted on protein level, while we quantified the mRNA, and they used a more punctual technic with stereology. Nevertheless, both results indicate that the belief of raphe nuclei being mainly serotonergic is not true, and that the different subpopulations (purely VGLUT3, co-expressing 5-HT and VGLUT3, etc.) might be responsible for different aspects of behaviour.

We also showed detectable VGLUT3 mRNA levels in the human brainstem (**Project 2/b**), in both the midbrain and pontine raphe nuclei. Interestingly, previous *in situ* hybridization study in humans showed only strong mRNA labelling in the DR for VGLUT3 but not on other parts of the brainstem. On the other hand, on protein level they showed a similar distribution to that in mice (Vigneault et al., 2015). This discrepancy could be due to the different technic used, as RT-qPCR proved to be highly sensitive (Haupt et al., 2006, Medhurst et al., 2000, Naidoo et al., 2001).

5.3. Specific manipulation of MRR-VGLUT3 neurons

5.3.1. Validation of chemogenetics

Although Cre mouse lines and chemogenetics/optogenetics are excellent tools to investigate the roles of specific neuron populations, it is still challenging to separate complex systems. For instance, VGLUT3+/5-HT+ double phenotyped neurons from purely VGLUT3+ neurons still cannot be distinguished.

Even though Cre recombinase transgenic mice are widely used in modern science, researchers still face some drawbacks regarding this model. For instance, it is imperative to examine the expression of loxP-flanked target sequences in a specific cell population of different tissues, even on different brain areas, due to enormous variations in the sensitivity of loxP-flanked target genes to Cre-mediated recombination (Vooijs et al., 2001). Reports regarding detrimental effects of homozygous Cre transgenic mice are not uncommon (Forni et al., 2006, He L. et al., 2014), such as Cre toxicity during development (Lam et al., 2019, Schmidt et al., 2000). Therefore, using heterozygous Cre mice for research purposes is recommended, preferably originating from “normal” mother \times homozygous father mating. Another important issue is the “ectopic”

expression, when Cre appears in non-target cells (Papathanou et al., 2019). A possible explanation of this is that at some point during development, these cells expressed the target genes, which remained Cre-positive even in adulthood.

In order to exclude the above-mentioned hardships, we confirmed the functional validity of our VGLUT3-Cre and the chemogenetic system. We checked reporter protein expression in VGLUT3+ cells, neurotransmitter release and neuronal activity after CNO injection. Indeed, the AAV coded reporter protein, RFP, was restricted to VGLUT3+ neurons in the MRR, indicating proper Cre recombinase activity (**Validation 1**). This was a necessary measurement, since in the bed nucleus of stria terminalis in the same, commercially available VGLUT3-Cre mouse line ectopic Cre expression was detected (Fazekas et al., 2022). Moreover, MRR excitation resulted in an increased Glu release in the HC (**Validation 2**), where VGLUT3+ neurons form functional NMDA+ synapses on local inhibitory neurons (Szonyi et al., 2016), similarly to its projections in the mPFC (Balazsfi D., Zelena, et al., 2018). Finally, functionality of expressed excitatory (G_q) DREADD receptors were proved by appearance of c-Fos protein (**Validation 3**), a known marker for neuronal activity (Kovacs 2008), after CNO injection in VGLUT3-Cre animals with previously stimulatory DREADD-injection into their MRR.

5.3.2. MRR-VGLUT3 neurons in behaviour

Midbrain MRR is highly implicated in numerous emotional behaviours, learning and memory formation due to its extensive projections to key brain areas in the forebrain.

The activity of MRR has been linked to locomotion on numerous occasions. Previously, our laboratory found that the optogenetic stimulation of the MRR resulted in a decreased locomotion and a long-term fear memory formation without experiencing any aversive stimulus (Balazsfi D. G. et al., 2017). Electrical stimulation of the nucleus led to similar results (Bland et al., 2016). By using different agonists and antagonists (Shim et al., 2014), it was shown that the effect of MRR on locomotion was partly dependent on dopamine receptors (D2), but also partly independent. According to our results, the later pathway potentially includes VGLUT3+ neuronal (in)activity as inhibition of the VGLUT3+ MRR neurons resulted in a decrease of locomotion. However, stimulation was ineffective, and the locomotor effect was not detected in all tests. Interestingly, when all VGLUT3+ neurons of the body were excited with chemogenetics, then hypolocomotion was detected in the light phase of mice (Kljakic et al., 2022). We conducted an OF

experiment to measure locomotion in both **Project 3/b** and **Project 3/c**. However, the results were not conclusive: in **Project 3/b** inhibition resulted in a slight, but statistically not significant decrease in distance moved, but did not affect locomotor parameters in the EPM or the Y-maze. On the other hand, in **Project 3/c**, although the results were not yet significant, there was a tendency in the excitatory group; although in the case of optogenetics, this was also improved once statistical correction for real excitation time was conducted. Based on these, the role of VGLUT3 positive neurons in locomotion is complex and MRR is just one brain area which might participate in this role.

Anxiety-like behaviour is strongly tied to 5-HT, which is also present in the MRR. By using mRNA interference specific to the SERT in the MRR, anxiety-like behaviour was increased on EPM (Verheij et al., 2018). In contrast, in **Project 1/a**, excitation of VGLUT3+ cell of MRR decreased anxiety in EPM. This is in line with the increased anxiety of KO mice and can be explained by the vesicle loading role of VGLUT3 (Amilhon et al., 2010). Thus, we might assume that excitation of MRR-VGLUT neurons increased 5-HT loading, thereby, reducing anxiety. Interestingly, **Project 1/b** could only replicate these results partially: only after correction for laser activity could we detect a slight anxiolytic effect of MRR-VGLUT3 excitation on EPM. As described in **1.2.3. chapter**, mainly the serotonergic neurons of the MRR has been investigated in anxiety-like behaviour (Abela et al., 2020, Andrade et al., 2013, Verheij et al., 2018). There is a possibility that it is tied differently to the different neurotransmitter subpopulations within the nucleus, however, more intricate technics are needed in order to target the purely 5-HT+, purely VGLUT3+ and co-expressing neurons. Our results only let us speculate that either the VGLUT3+, or the co-expressing neurons might contribute to MRR-connected anxiety.

As of its role in social behaviour (**Project 3/b**), our laboratory demonstrated that optogenetic stimulation of the whole MRR decreased aggression in the SIT paradigm, which was accompanied by not only increased levels of 5-HT, but also glutamate in the mPFC (Balazsfi D., Zelena, et al., 2018). The decreased time spent with the conspecific, and the increased time spent with other behaviour during the sociability test in the MRR-VGLUT3 excitatory group indicated a decreased social interest. However, inhibition only increased social interest one day after manipulation, during SDT. Additionally, inhibition affected friendly social behaviour in a context specific manner: in the anxiogenic SIT, it

tended to increase, while in RIT, it decreased. However, despite our expectations, we were unable to find any other major regulatory role of MRR-VGLUT3 cells in social behaviour. Szónyi et al. showed that VGLUT3+ neurons not only project to the mPFC, MS and HC separately, but through collaterals a simultaneous effect on mPFC-MS and mPFC-HC can be also assumed (Szonyi et al., 2016). Moreover, these neurons can be both exclusively VGLUT3+ or co-expressing 5-HT.

MRR has been implicated in memory numerous times, and literature is more abundant about it. Theta oscillations are observable in both human and rodent HC during spatial navigations (Soltani Zangbar et al., 2020). As previously mentioned, our laboratory has already examined the effect of MRR on long term memory, during which excitation elicited a fear memory without actual aversive stimulus, while inhibition of the nucleus prevented the memory formation (Balazsfi D. G. et al., 2017). Anatomically it is well characterised that the MRR densely innervates the HC via direct projections (Aznar et al., 2004, Freund 1992, Kohler and Steinbusch 1982, Mckenna and Vertes 2001, Papp et al., 1999, Szonyi et al., 2016), coming especially from VGLUT3+ neurons (Jackson et al., 2009, Senft et al., 2021, Szonyi et al., 2016). However, their collaterals reach both HC and MS (Acsady et al., 1996, Kohler et al., 1982, Mckenna and Vertes 2001, Senft et al., 2021) and known to be VGLUT3+ (Jackson et al., 2009) and/or GABAergic. This raises the question whether MRR synchronise the activity of these brain areas, deeply influencing learning and memory. In support, Wang et al. stimulated the whole MRR of WT mice during dormant periods after fear conditioning, which resulted in a failure of memory consolidation (Wang D. V. et al., 2015). He et al specifically inhibited the MRR-VGLUT3-HC PV+ interneuron connection by chemogenetics, which, without affecting locomotion or anxiety-like behaviour, impaired HC-dependent spatial memory acquisition in a two-choice spatial discrimination, low separation task (He A. et al., 2022). Interestingly, when the recipient parvalbumin positive interneurons were excited via optogenetic theta burst, this impairment was corrected. Despite these observations, in our two memory related experiments (SDT and Y-maze) we failed to identify any effect (**Project 3/b**). Additionally, there was also no effect on learning in the HC-dependent MWM task, but during long-term (72 hour) memory probe previous excitation via chemogenetics resulted in a better performance (**Project 3/c**). Interestingly, we did not get the same results with optogenetics, during which excitation was only present while

the animals were sitting on the platform. It has been shown that DREADD activation can be detectable for hours after CNO administration (Alexander et al., 2009, Thompson et al., 2018). Interestingly, during REM sleep, when theta oscillations are dominant in the HC, MRR-VGLUT3 neurons are silent, and vice versa (Huang et al., 2022). Thus, a possible explanation is that the effect of long lasting chemogenetic activation of the MRR-VGLUT3 neurons on behaviour took place during the dormant period of the animals, and optogenetic excitation was untimely, thus, yielded no result. Nevertheless, an important fact must be noted regarding the chemogenetic experiments: because the short-term memory probe was conducted so close (10 mins later) to the last learning trial on day 5, it is impossible to exclude the possible effects of excitation on immediate memory retrieval. More experiments need to be conducted to confirm this current result in the short-term memory probe. Moreover, a different pattern of optogenetic excitation (e.g.: during immobility or sleeping) could be utilised to try replicating the chemogenetic results.

However, it has to be mentioned that around 20% of MR neurons are VGLUT2+ (Szonyi et al., 2019). These cells also project to HC parvalbumin+ interneurons, which are also known to regulate theta-rhythm and negative memory acquisition. Whether they regulate the same contexts as VGLUT3+ neurons or are responsible for different aspects still needs to be investigated.

6. Conclusions

These projects successfully expanded the literature on the role of VGLUT3+ neurons in behaviour. Moreover, human relevance of these studies was confirmed by the RT-qPCR detection of VGLUT3 mRNA in human raphe nuclei. Although direct parallels were not found between the VGLUT3 KO mice and MRR-VGLUT3 manipulated animals, it is possible that at least partially the inactivity of MRR-VGLUT3 neurons are responsible for the appearance of hypolocomotion and increased social interest in VGLUT3 KO mice. Moreover, the highly anxious behavioural phenotype of KO mice could be due also linked to MRR-VGLUT3, as their excitation was anxiolytic. Although in our case it was not possible to differentiate between the VGLUT3+ only and VGLUT3+/5-HT+ neurons, we might assume that either one or both subpopulations contribute to the anxiolytic effect of MRR activity but has subtle effect on complex social behaviour. However, the role of VGLUT3 in learning and memory formation is much more complex: while VGLUT3 KO mice showed only long-term social memory deficits, the excitation of MRR-VGLUT3+ neurons had a long-term affirmative effect in spatial memory formation. With the reproduction of the same results in two countries (**Project 3/c**, chemogenetics), the robustness of the results of MWM is promising. However, the ineffectiveness of optogenetic manipulations could indicate that this effect probably takes place during the dormant period(s) of the animals.

7. Summary

7.1. English

In the central nervous system, glutamatergic neurons are characterised by the expression of vesicular glutamate transporters (VGLUTs). The newest member of this protein family is VGLUT3, which role in behaviour and physiology is still being characterised. Moreover, in the median raphe region (MRR), there is a surprising amount of VGLUT3+ neurons, either purely glutamatergic, or within serotonergic neurons. Although VGLUT3 is found in key areas like the prefrontal cortex, hippocampus and other raphe nuclei, not much is known about its effects on behaviours, such as social behaviour, learning or memory processes. Additionally, MRR (and its VGLUT3+ neurons) also project to these areas, and potentially affect all these behaviours.

Thus, the goal of this PhD was to complement current literature on the role of VGLUT3 in behaviour with the help of VGLUT3 knockout (KO) mice. Specific subpopulation in the MRR was targeted by transgenic VGLUT3-Cre mouse line, chemogenetics and optogenetics. Behaviour paradigms were conducted in both VGLUT3 KO and VGLUT3-Cre strains to analyse social behaviour in great details and to control for possible confounding factors of locomotion and anxiety-like behaviour. Then, as the hippocampus is rich in both VGLUT3+ neurons and MRR-VGLUT3 afferents, a classical hippocampus-based spatial learning and memory test, the Morris water maze was also investigated. Additionally, molecular technics were also utilised to validate and confirm VGLUT3 mRNA expression in the MRR in mice and humans, MRR neurotransmitter release in the hippocampus, and the propriety of the newly introduced chemogenetics.

Results show that the total ablation of the VGLUT3 gene shifted the behaviour to be socially more active but seems to result in an inadequate appearance of aggression in anxiogenic contexts. We further confirmed the highly anxious phenotype and the long-term social memory impairment of the VGLUT3 KO animals. On the other hand, it seems like this lifelong, complete deficiency does not significantly impair spatial learning and memory. In the case of MRR-VGLUT3 neurons, we found that they could potentially play a role in locomotion and long-term social interest, while affecting friendly social behaviour in a context specific manner. Chronic, chemogenetic excitation of the MRR-VGLUT3 neurons facilitated memory formation in mice in a hippocampus dependent

spatial memory task. Additionally, we confirmed that in the MRR only a minority (~20%) of VGLUT3+ neurons co-express a serotonergic phenotype. Similarly to rodents, human raphe nuclei (among other brainstem areas) also express VGLUT3, thus, our results can potentially have clinical relevance in the future.

7.2. Hungarian

A központi idegrendszerben található glutamáterg idegsejteket az általuk kifejezett vezikuláris glutamáterg transzporterek (VGLUT) alapján csoportosíthatjuk. Közülük a legújabb felfedezett fehérje a VGLUT3, melynek a viselkedésben és fiziológiában betöltött szerepét még mindig kutatják. Érdekes módon a medián ráfe régióban (MRR) jelentős VGLUT3+ neuron populáció található, melyben mind tisztán glutamáterg, mind pedig szerotonerg markert kifejező sejteket is kimutattak. Több, a viselkedést meghatározó agyterületen is megtalálhatók VGLUT3+ neuronok, mint például a hippokampuszban, a prefrontális kéregben vagy más ráfe magvakban, de még keveset tudunk az általuk irányított viselkedésekben (pl.: szociális viselkedés, tanulás, memória) játszott szerepükről. Sőt, a MRR, és a benne megtalálható VGLUT3+ sejtek szintén beidegzik ezeket az agyterületeket, így befolyásolhatják is ezen viselkedésformákat.

Jelenlegi doktori értekezés célja, hogy bemutassa és kiegészítse a VGLUT3 szerepéről szóló irodalmat. Ennek érdekében VGLUT3 teljes génkiütött (KO), illetve a MRR-ban található alpopuláció befolyásolásához VGLUT3-Cre egértörzseket használtunk. Utóbbi állatok esetén a sejtek aktivitását két módszerrel, kemogenetikával és optogenetikával is befolyásoltuk. Viselkedési tesztek segítségével részletesen megvizsgáltuk a szociális viselkedésben és az ezt erőteljesen befolyásolható lokomócióban és szorongásszerű viselkedésben bekövetkezett változásokat. Mivel a hippokampusz gazdag mind VGLUT3+ neuronokban, illetve MRR-VGLUT3+ afferensekben, így az ismertén hippokampusz-függő térbeli tanulás és memóriával is foglalkoztunk a Morris-féle vízilabirintus teszt segítségével. Ezen felül molekuláris technikákkal megerősítettük a szakirodalomban is megtalálható adatokat a MRR-ban található VGLUT3 expresszióról egérben és emberben, kimutattuk a MRR eredetű neurotranszmitter felszabadulást a hippokampuszban, illetve validáltuk a laborunkban újonnan bevezetett kemogenetikát.

Eredményeink azt mutatják, hogy a VGLUT3 teljes hiánya fokozott szociális érdeklődést eredményezett, azonban helytelen kontextusban megjelenő agresszióval is járt. Sikerült megerősítenünk a KO egerek fokozottan szorongó viselkedési fenotípusát, illetve hosszútávú memória deficitet is találtunk szociális memória esetén, míg a térbeli tanulást és memóriát a VGLUT3 hiánya nem befolyásolta. Ehhez képest a MRR-VGLUT3+ neuronok legalább részben felelősek lehetnek a KO állatokban tapasztalt lokomóciós és hosszútávú szociális érdeklődést mutató viselkedésért, míg a barátságos szociális viselkedésre környezetfüggő hatásuk van. Hosszútávú, kemogenetikai serkentésük elősegítette a hippocampusz-függő térbeli memória kialakulását. Továbbá szintén megerősítettük, hogy a MRR-ban a sejtek csupán kisebb hányada (~20%) fejez ki mind VGLUT3-at, mind pedig szerotonerg jellemzőket. Rágcsálókhoz hasonlóan az emberi ráfe magokban (illetve más agytörzsi területeken is) kimutattuk a VGLUT3 mRNS-t, így eredményeinknek a jövőben klinikai felhasználása is lehet.

7.3. French

Dans le système nerveux central, les neurones glutamatergiques sont caractérisés par les transporteurs vésiculaires de glutamate (VGLUT). VGLUT3 est le transporteur le plus récemment identifié, et pour lequel l'implication dans les processus physiologiques et comportementaux est encore peu caractérisée. Dans la région du raphé médian (MRR), une quantité surprenante de neurones VGLUT3+ est observée, à la fois dans des cellules apparemment purement glutamatergiques mais également dans des cellules sérotoninergiques. Bien que VGLUT3 soit présent dans des régions clés telles que le cortex préfrontal, l'hippocampe et d'autres noyaux du raphé, peu d'études ont été menées sur son implication sur les comportements sociaux, ou les processus d'apprentissage et de mémoire. En outre, le MRR (et ses neurones VGLUT3+) se projette également dans ces zones et peut potentiellement affecter tous ces comportements.

L'objectif de cette thèse était donc de compléter la littérature actuelle sur le rôle du VGLUT3 dans les processus d'apprentissage et de mémoire à l'aide de souris invalidées en VGLUT3 (knock-out; VGLUT3 KO). Une sous-population spécifique du MRR a été ciblée grâce à l'utilisation d'une lignée de souris transgéniques VGLUT3-Cre couplée à de la chémozogénétique ou de l'optogénétique. Des paradigmes comportementaux ont été menés sur ces deux modèles VGLUT3 KO et VGLUT3-Cre afin d'analyser en

détail le comportement social, la locomotion et le comportement de type anxieux. L'hippocampe étant riche en neurones VGLUT3+ et en afférences MRR-VGLUT3+, l'apprentissage et la mémoire spatiale ont également été étudiés. En outre, des techniques moléculaires ont été utilisées pour valider et confirmer l'expression de l'ARNm VGLUT3 dans le MRR chez la souris et l'humain, la libération de divers neurotransmetteurs du MRR dans l'hippocampe et la chémogénétique nouvellement introduite.

Les résultats montrent que l'ablation totale du gène VGLUT3 non seulement augmente le comportement social, mais semble également entraîner une augmentation des comportements agressifs dans des contextes anxiogènes. Nous avons par ailleurs confirmé le phénotype anxieux des souris VGLUT3 KO et une altération de leur mémoire sociale à long terme. En revanche, il semble que l'absence de VGLUT3 n'altère pas de manière significative l'apprentissage et la mémoire spatiale. Dans le cas des neurones MRR-VGLUT3, nous avons découvert qu'ils pouvaient potentiellement jouer un rôle dans la locomotion et l'intérêt social à long terme, tout en affectant le comportement social amical d'une manière spécifique au contexte. L'excitation chronique des neurones MRR-VGLUT3 a facilité la formation de la mémoire chez les souris dans une tâche de mémoire spatiale dépendante de l'hippocampe. En outre, nous avons confirmé que dans le MRR, seule une minorité (~20%) de neurones VGLUT3+ co-expriment un phénotype sérotoninergique. Comme chez les rongeurs, les noyaux du raphé chez les humains (parmi d'autres régions du tronc cérébral) expriment également VGLUT3, nos résultats peuvent donc potentiellement avoir une pertinence clinique à l'avenir.

8. References

- Abela AR, Browne CJ, Sargin D, Prevot TD, Ji XD, Li Z, Lambe EK, Fletcher PJ. (2020) Median raphe serotonin neurons promote anxiety-like behavior via inputs to the dorsal hippocampus. *Neuropharmacology*, 168: 107985.
- Abellan MT, Adell A, Honrubia MA, Mengod G, Artigas F. (2000) GABAB-RI receptors in serotonergic neurons: effects of baclofen on 5-HT output in rat brain. *Neuroreport*, 11: 941-945.
- Acsady L, Arabadzisz D, Katona I, Freund TF. (1996) Topographic distribution of dorsal and median raphe neurons with hippocampal, septal and dual projection. *Acta Biol Hung*, 47: 9-19.
- Adolphs R. (2010) What does the amygdala contribute to social cognition? *Ann N Y Acad Sci*, 1191: 42-61.
- Akil O, Seal RP, Burke K, Wang C, Alemi A, During M, Edwards RH, Lustig LR. (2012) Restoration of hearing in the VGLUT3 knockout mouse using virally mediated gene therapy. *Neuron*, 75: 283-293.
- Aleman-Zapata A, Morris RGM, Genzel L. (2022) Sleep deprivation and hippocampal ripple disruption after one-session learning eliminate memory expression the next day. *Proc Natl Acad Sci U S A*, 119: e2123424119.
- Alexander GM, Rogan SC, Abbas AI, Armbruster BN, Pei Y, Allen JA, Nonneman RJ, Hartmann J, Moy SS, Nicolelis MA, McNamara JO, Roth BL. (2009) Remote control of neuronal activity in transgenic mice expressing evolved G protein-coupled receptors. *Neuron*, 63: 27-39.
- Almeida PV, Trovo MC, Tokumoto AM, Pereira AC, Padovan CM. (2013) Role of serotonin 1A receptors in the median raphe nucleus on the behavioral consequences of forced swim stress. *J Psychopharmacol*, 27: 1134-1140.
- Alreja M. (1996) Excitatory actions of serotonin on GABAergic neurons of the medial septum and diagonal band of Broca. *Synapse*, 22: 15-27.
- Amilhon B, Lepicard E, Renoir T, Mongeau R, Popa D, Poirel O, Miot S, Gras C, Gardier AM, Gallego J, Hamon M, Lanfumey L, Gasnier B, Giros B, El Mestikawy S. (2010) VGLUT3 (vesicular glutamate transporter type 3) contribution to the regulation of serotonergic transmission and anxiety. *J Neurosci*, 30: 2198-2210.

- Andrade TG, Zangrossi H, Jr., Graeff FG. (2013) The median raphe nucleus in anxiety revisited. *J Psychopharmacol*, 27: 1107-1115.
- Andrews N, Hogg S, Gonzalez LE, File SE. (1994) 5-HT_{1A} receptors in the median raphe nucleus and dorsal hippocampus may mediate anxiolytic and anxiogenic behaviours respectively. *Eur J Pharmacol*, 264: 259-264.
- Armbruster BN, Li X, Pausch MH, Herlitze S, Roth BL. (2007) Evolving the lock to fit the key to create a family of G protein-coupled receptors potently activated by an inert ligand. *Proc Natl Acad Sci U S A*, 104: 5163-5168.
- Aznar S, Qian ZX, Knudsen GM. (2004) Non-serotonergic dorsal and median raphe projection onto parvalbumin- and calbindin-containing neurons in hippocampus and septum. *Neuroscience*, 124: 573-581.
- Bai L, Xu H, Collins JF, Ghishan FK. (2001) Molecular and functional analysis of a novel neuronal vesicular glutamate transporter. *J Biol Chem*, 276: 36764-36769.
- Balazsfi D, Farkas L, Csikota P, Fodor A, Zsebok S, Haller J, Zelena D. (2016) Sex-dependent role of vesicular glutamate transporter 3 in stress-regulation and related anxiety phenotype during the early postnatal period. *Stress*, 19: 434-438.
- Balazsfi D, Fodor A, Torok B, Ferenczi S, Kovacs KJ, Haller J, Zelena D. (2018) Enhanced innate fear and altered stress axis regulation in VGLUT3 knockout mice. *Stress*, 21: 151-161.
- Balazsfi D, Zelena D, Demeter K, Miskolczi C, Varga ZK, Nagyvaradi A, Nyiri G, Cserep C, Baranyi M, Sperlagh B, Haller J. (2018) Differential Roles of the Two Raphe Nuclei in Amiable Social Behavior and Aggression - An Optogenetic Study. *Front Behav Neurosci*, 12: 163.
- Balazsfi DG, Zelena D, Farkas L, Demeter K, Barna I, Cserep C, Takacs VT, Nyiri G, Goloncser F, Sperlagh B, Freund TF, Haller J. (2017) Median raphe region stimulation alone generates remote, but not recent fear memory traces. *PLoS One*, 12: e0181264.
- Bang SJ, Jensen P, Dymecki SM, Commons KG. (2012) Projections and interconnections of genetically defined serotonin neurons in mice. *Eur J Neurosci*, 35: 85-96.
- Banker SM, Gu X, Schiller D, Foss-Feig JH. (2021) Hippocampal contributions to social and cognitive deficits in autism spectrum disorder. *Trends Neurosci*, 44: 793-807.

- Bankhead P, Loughrey MB, Fernandez JA, Dombrowski Y, McArt DG, Dunne PD, McQuaid S, Gray RT, Murray LJ, Coleman HG, James JA, Salto-Tellez M, Hamilton PW. (2017) QuPath: Open source software for digital pathology image analysis. *Sci Rep*, 7: 16878.
- Barbera G, Liang B, Zhang L, Gerfen CR, Culurciello E, Chen R, Li Y, Lin DT. (2016) Spatially Compact Neural Clusters in the Dorsal Striatum Encode Locomotion Relevant Information. *Neuron*, 92: 202-213.
- Belmer A, Beecher K, Jacques A, Patkar OL, Slicherre F, Bartlett SE. (2019) Axonal Non-segregation of the Vesicular Glutamate Transporter VGLUT3 Within Serotonergic Projections in the Mouse Forebrain. *Front Cell Neurosci*, 13: 193.
- Bicks LK, Koike H, Akbarian S, Morishita H. (2015) Prefrontal Cortex and Social Cognition in Mouse and Man. *Front Psychol*, 6: 1805.
- Biro L, Toth M, Sipos E, Bruzsik B, Tulogdi A, Bendahan S, Sandi C, Haller J. (2017) Structural and functional alterations in the prefrontal cortex after post-weaning social isolation: relationship with species-typical and deviant aggression. *Brain Struct Funct*, 222: 1861-1875.
- Bland BH, Bland CE, MacIver MB. (2016) Median raphe stimulation-induced motor inhibition concurrent with suppression of type 1 and type 2 hippocampal theta. *Hippocampus*, 26: 289-300.
- Bruschetta G, Jin S, Liu ZW, Kim JD, Diano S. (2020) MC(4)R Signaling in Dorsal Raphe Nucleus Controls Feeding, Anxiety, and Depression. *Cell Rep*, 33: 108267.
- Burgess N, Maguire EA, O'Keefe J. (2002) The human hippocampus and spatial and episodic memory. *Neuron*, 35: 625-641.
- Burns LH, Everitt BJ, Kelley AE, Robbins TW. (1994) Glutamate-dopamine interactions in the ventral striatum: role in locomotor activity and responding with conditioned reinforcement. *Psychopharmacology (Berl)*, 115: 516-528.
- Burnstock G. (1976) Do some nerve cells release more than one transmitter? *Neuroscience*, 1: 239-248.
- Buzsaki G. (1986) Hippocampal sharp waves: their origin and significance. *Brain Res*, 398: 242-252.
- Buzsaki G. (2015) Hippocampal sharp wave-ripple: A cognitive biomarker for episodic memory and planning. *Hippocampus*, 25: 1073-1188.

- Buzsaki G, Leung LW, Vanderwolf CH. (1983) Cellular bases of hippocampal EEG in the behaving rat. *Brain Res*, 287: 139-171.
- Calizo LH, Akanwa A, Ma X, Pan YZ, Lemos JC, Craige C, Heemstra LA, Beck SG. (2011) Raphe serotonin neurons are not homogenous: electrophysiological, morphological and neurochemical evidence. *Neuropharmacology*, 61: 524-543.
- Callaerts-Vegh Z, Moechars D, Van Acker N, Daneels G, Goris I, Leo S, Naert A, Meert T, Balschun D, D'Hooge R. (2013) Haploinsufficiency of VGluT1 but not VGluT2 impairs extinction of spatial preference and response suppression. *Behav Brain Res*, 245: 13-21.
- Campbell EJ, Marchant NJ. (2018) The use of chemogenetics in behavioural neuroscience: receptor variants, targeting approaches and caveats. *Br J Pharmacol*, 175: 994-1003.
- Case DT, Burton SD, Gedeon JY, Williams SG, Urban NN, Seal RP. (2017) Layer- and cell type-selective co-transmission by a basal forebrain cholinergic projection to the olfactory bulb. *Nat Commun*, 8: 652.
- Chaves T, Torok B, Fazekas CL, Correia P, Sipos E, Varkonyi D, Hellinger A, Erk D, Zelena D. (2022) Median raphe region GABAergic neurons contribute to social interest in mouse. *Life Sci*, 289: 120223.
- Chen X, Choo H, Huang XP, Yang X, Stone O, Roth BL, Jin J. (2015) The first structure-activity relationship studies for designer receptors exclusively activated by designer drugs. *ACS Chem Neurosci*, 6: 476-484.
- Cheng XR, Yang Y, Zhou WX, Zhang YX. (2011) Expression of VGLUTs contributes to degeneration and acquisition of learning and memory. *Neurobiol Learn Mem*, 95: 361-375.
- Colgin LL. (2016) Rhythms of the hippocampal network. *Nat Rev Neurosci*, 17: 239-249.
- Commons KG. (2009) Locally collateralizing glutamate neurons in the dorsal raphe nucleus responsive to substance P contain vesicular glutamate transporter 3 (VGLUT3). *J Chem Neuroanat*, 38: 273-281.
- Crepel F, Galante M, Habbas S, McLean H, Daniel H. (2011) Role of the vesicular transporter VGLUT3 in retrograde release of glutamate by cerebellar Purkinje cells. *J Neurophysiol*, 105: 1023-1032.

- Crooks R, Jackson J, Bland BH. (2012) Dissociable pathways facilitate theta and non-theta states in the median raphe--septohippocampal circuit. *Hippocampus*, 22: 1567-1576.
- Cropper EC, Jing J, Vilim FS, Weiss KR. (2018) Peptide Cotransmitters as Dynamic, Intrinsic Modulators of Network Activity. *Front Neural Circuits*, 12: 78.
- Crunelli V, Segal M. (1985) An electrophysiological study of neurones in the rat median raphe and their projections to septum and hippocampus. *Neuroscience*, 15: 47-60.
- Csicsvari J, Dupret D. (2014) Sharp wave/ripple network oscillations and learning-associated hippocampal maps. *Philos Trans R Soc Lond B Biol Sci*, 369: 20120528.
- Daumas S, Hunter CJ, Mistry RB, More L, Privitera L, Cooper DD, Reyskens KM, Flynn HT, Morris RG, Arthur JS, Frenguelli BG. (2017) The Kinase Function of MSK1 Regulates BDNF Signaling to CREB and Basal Synaptic Transmission, But Is Not Required for Hippocampal Long-Term Potentiation or Spatial Memory. *eNeuro*, 4.
- de Almeida C, Chabbah N, Eyraud C, Fasano C, Bernard V, Pietrancosta N, Fabre V, El Mestikawy S, Daumas S. (2023) Absence of VGLUT3 Expression Leads to Impaired Fear Memory in Mice. *eNeuro*, 10.
- Del Pino I, Brotons-Mas JR, Marques-Smith A, Marighetto A, Frick A, Marin O, Rico B. (2017) Abnormal wiring of CCK(+) basket cells disrupts spatial information coding. *Nat Neurosci*, 20: 784-792.
- Divito CB, Steece-Collier K, Case DT, Williams SP, Stancati JA, Zhi L, Rubio ME, Sortwell CE, Collier TJ, Sulzer D, Edwards RH, Zhang H, Seal RP. (2015) Loss of VGLUT3 Produces Circadian-Dependent Hyperdopaminergia and Ameliorates Motor Dysfunction and l-Dopa-Mediated Dyskinesias in a Model of Parkinson's Disease. *J Neurosci*, 35: 14983-14999.
- Dobrzanski G, Kossut M. (2017) Application of the DREADD technique in biomedical brain research. *Pharmacol Rep*, 69: 213-221.
- Domonkos A, Nikitidou L, Laszlovszky T, Cserep C, Borhegyi Z, Papp E, Nyiri G, Freund TF, Varga V. (2016) Divergent in vivo activity of non-serotonergic and serotonergic VGLUT3-neurons in the median raphe region. *J Physiol*, 594: 3775-3790.

- dos Santos L, de Andrade TG, Graeff FG. (2010) Social separation and diazepam withdrawal increase anxiety in the elevated plus-maze and serotonin turnover in the median raphe and hippocampus. *J Psychopharmacol*, 24: 725-731.
- Dragoi G, Carpi D, Recce M, Csicsvari J, Buzsaki G. (1999) Interactions between hippocampus and medial septum during sharp waves and theta oscillation in the behaving rat. *J Neurosci*, 19: 6191-6199.
- Dumas S, Wallen-Mackenzie A. (2019) Developmental Co-expression of Vglut2 and Nurr1 in a Mes-Di-Encephalic Continuum Precedes Dopamine and Glutamate Neuron Specification. *Front Cell Dev Biol*, 7: 307.
- Ego-Stengel V, Wilson MA. (2010) Disruption of ripple-associated hippocampal activity during rest impairs spatial learning in the rat. *Hippocampus*, 20: 1-10.
- El Mestikawy S, Wallen-Mackenzie A, Fortin GM, Descarries L, Trudeau LE. (2011) From glutamate co-release to vesicular synergy: vesicular glutamate transporters. *Nat Rev Neurosci*, 12: 204-216.
- Engin E, Treit D. (2007) The role of hippocampus in anxiety: intracerebral infusion studies. *Behav Pharmacol*, 18: 365-374.
- Fasano C, Rocchetti J, Pietrajtis K, Zander JF, Manseau F, Sakae DY, Marcus-Sells M, Ramet L, Morel LJ, Carrel D, Dumas S, Bolte S, Bernard V, Vigneault E, Goutagny R, Ahnert-Hilger G, Giros B, Daumas S, Williams S, El Mestikawy S. (2017) Regulation of the Hippocampal Network by VGLUT3-Positive CCK-GABAergic Basket Cells. *Front Cell Neurosci*, 11: 140.
- Fazekas CL, Balazsfi D, Horvath HR, Balogh Z, Aliczki M, Puhova A, Balagova L, Chmelova M, Jezova D, Haller J, Zelena D. (2019) Consequences of VGLUT3 deficiency on learning and memory in mice. *Physiol Behav*, 212: 112688.
- Fazekas CL, Bellardie M, Torok B, Sipos E, Toth B, Baranyi M, Sperlagh B, Dobos-Kovacs M, Chaillou E, Zelena D. (2021) Pharmacogenetic excitation of the median raphe region affects social and depressive-like behavior and core body temperature in male mice. *Life Sci*, 286: 120037.
- Fazekas CL, Szabo A, Torok B, Banrevi K, Correia P, Chaves T, Daumas S, Zelena D. (2022) A New Player in the Hippocampus: A Review on VGLUT3+ Neurons and Their Role in the Regulation of Hippocampal Activity and Behaviour. *Int J Mol Sci*, 23.

- Felix-Ortiz AC, Burgos-Robles A, Bhagat ND, Leppla CA, Tye KM. (2016) Bidirectional modulation of anxiety-related and social behaviors by amygdala projections to the medial prefrontal cortex. *Neuroscience*, 321: 197-209.
- File SE, Deakin JF. (1980) Chemical lesions of both dorsal and median raphe nuclei and changes in social and aggressive behaviour in rats. *Pharmacol Biochem Behav*, 12: 855-859.
- Finlay JM, Dunham GA, Isherwood AM, Newton CJ, Nguyen TV, Reppar PC, Snitkovski I, Paschall SA, Greene RW. (2015) Effects of prefrontal cortex and hippocampal NMDA NR1-subunit deletion on complex cognitive and social behaviors. *Brain Res*, 1600: 70-83.
- Fletcher PJ, Ming ZH, Higgins GA. (1993) Conditioned place preference induced by microinjection of 8-OH-DPAT into the dorsal or median raphe nucleus. *Psychopharmacology (Berl)*, 113: 31-36.
- Fontaine HM, Silva PR, Neiswanger C, Tran R, Abraham AD, Land BB, Neumaier JF, Chavkin C. (2022) Stress decreases serotonin tone in the nucleus accumbens in male mice to promote aversion and potentiate cocaine preference via decreased stimulation of 5-HT(1B) receptors. *Neuropsychopharmacology*, 47: 891-901.
- Forni PE, Scuoppo C, Imayoshi I, Taulli R, Dastru W, Sala V, Betz UA, Muzzi P, Martinuzzi D, Vercelli AE, Kageyama R, Ponzetto C. (2006) High levels of Cre expression in neuronal progenitors cause defects in brain development leading to microencephaly and hydrocephaly. *J Neurosci*, 26: 9593-9602.
- Fortin-Houde J, Henderson F, Dumas S, Ducharme G, Amilhon B. (2023) Parallel streams of raphe VGLUT3-positive inputs target the dorsal and ventral hippocampus in each hemisphere. *J Comp Neurol*, 531: 702-719.
- Franklin TB, Silva BA, Perova Z, Marrone L, Masferrer ME, Zhan Y, Kaplan A, Greetham L, Verrechia V, Halman A, Pagella S, Vyssotski AL, Illarionova A, Grinevich V, Branco T, Gross CT. (2017) Prefrontal cortical control of a brainstem social behavior circuit. *Nat Neurosci*, 20: 260-270.
- Freneau RT, Jr., Burman J, Qureshi T, Tran CH, Proctor J, Johnson J, Zhang H, Sulzer D, Copenhagen DR, Storm-Mathisen J, Reimer RJ, Chaudhry FA, Edwards RH. (2002) The identification of vesicular glutamate transporter 3 suggests novel modes of signaling by glutamate. *Proc Natl Acad Sci U S A*, 99: 14488-14493.

- Freneau RT, Jr., Kam K, Qureshi T, Johnson J, Copenhagen DR, Storm-Mathisen J, Chaudhry FA, Nicoll RA, Edwards RH. (2004) Vesicular glutamate transporters 1 and 2 target to functionally distinct synaptic release sites. *Science*, 304: 1815-1819.
- Freneau RT, Jr., Troyer MD, Pahner I, Nygaard GO, Tran CH, Reimer RJ, Bellocchio EE, Fortin D, Storm-Mathisen J, Edwards RH. (2001) The expression of vesicular glutamate transporters defines two classes of excitatory synapse. *Neuron*, 31: 247-260.
- Freund TF. (1992) GABAergic septal and serotonergic median raphe afferents preferentially innervate inhibitory interneurons in the hippocampus and dentate gyrus. *Epilepsy Res Suppl*, 7: 79-91.
- Freund TF, Gulyas AI, Acsady L, Gorcs T, Toth K. (1990) Serotonergic control of the hippocampus via local inhibitory interneurons. *Proc Natl Acad Sci U S A*, 87: 8501-8505.
- Fu W, Le Maitre E, Fabre V, Bernard JF, David Xu ZQ, Hokfelt T. (2010) Chemical neuroanatomy of the dorsal raphe nucleus and adjacent structures of the mouse brain. *J Comp Neurol*, 518: 3464-3494.
- Gagnon D, Parent M. (2014) Distribution of VGLUT3 in highly collateralized axons from the rat dorsal raphe nucleus as revealed by single-neuron reconstructions. *PLoS One*, 9: e87709.
- Gammelsaeter R, Coppola T, Marcaggi P, Storm-Mathisen J, Chaudhry FA, Attwell D, Regazzi R, Gundersen V. (2011) A role for glutamate transporters in the regulation of insulin secretion. *PLoS One*, 6: e22960.
- Gangarossa G, Guzman M, Prado VF, Prado MA, Daumas S, El Mestikawy S, Valjent E. (2016) Role of the atypical vesicular glutamate transporter VGLUT3 in l-DOPA-induced dyskinesia. *Neurobiol Dis*, 87: 69-79.
- Gaspar P, Lillesaar C. (2012) Probing the diversity of serotonin neurons. *Philos Trans R Soc Lond B Biol Sci*, 367: 2382-2394.
- Geyer MA, Puerto A, Menkes DB, Segal DS, Mandell AJ. (1976) Behavioral studies following lesions of the mesolimbic and mesostriatal serotonergic pathways. *Brain Res*, 106: 257-269.

- Gezelius H, Wallen-Mackenzie A, Enjin A, Lagerstrom M, Kullander K. (2006) Role of glutamate in locomotor rhythm generating neuronal circuitry. *J Physiol Paris*, 100: 297-303.
- Girardeau G, Zugaro M. (2011) Hippocampal ripples and memory consolidation. *Curr Opin Neurobiol*, 21: 452-459.
- Goloncser F, Baranyi M, Balazsfi D, Demeter K, Haller J, Freund TFF, Zelena D, Sperlagh B. (2017) Regulation of Hippocampal 5-HT Release by P2X7 Receptors in Response to Optogenetic Stimulation of Median Raphe Terminals of Mice. *Front Mol Neurosci*, 10: 325.
- Gonzalez MC, Radiske A, Rossato JI, Conde-Ocazonez S, Bevilaqua LRM, Cammarota M. (2022) Optogenetic inactivation of the medial septum impairs long-term object recognition memory formation. *Mol Brain*, 15: 50.
- Gras C, Amilhon B, Lepicard EM, Poirel O, Vinatier J, Herbin M, Dumas S, Tzavara ET, Wade MR, Nomikos GG, Hanoun N, Saurini F, Kemel ML, Gasnier B, Giros B, El Mestikawy S. (2008) The vesicular glutamate transporter VGLUT3 synergizes striatal acetylcholine tone. *Nat Neurosci*, 11: 292-300.
- Gras C, Herzog E, Bellenchi GC, Bernard V, Ravassard P, Pohl M, Gasnier B, Giros B, El Mestikawy S. (2002) A third vesicular glutamate transporter expressed by cholinergic and serotonergic neurons. *J Neurosci*, 22: 5442-5451.
- Griguoli M, Pimpinella D. (2022) Medial septum: relevance for social memory. *Front Neural Circuits*, 16: 965172.
- Grillner S, Wallen P, Saitoh K, Kozlov A, Robertson B. (2008) Neural bases of goal-directed locomotion in vertebrates--an overview. *Brain Res Rev*, 57: 2-12.
- Grimes WN, Seal RP, Oesch N, Edwards RH, Diamond JS. (2011) Genetic targeting and physiological features of VGLUT3+ amacrine cells. *Vis Neurosci*, 28: 381-392.
- Guo ZL, Moazzami AR, Longhurst JC. (2005) Stimulation of cardiac sympathetic afferents activates glutamatergic neurons in the parabrachial nucleus: relation to neurons containing nNOS. *Brain Res*, 1053: 97-107.
- Hangya B, Li Y, Muller RU, Czurko A. (2010) Complementary spatial firing in place cell-interneuron pairs. *J Physiol*, 588: 4165-4175.
- Harkany T, Hartig W, Berghuis P, Dobszay MB, Zilberter Y, Edwards RH, Mackie K, Ernfors P. (2003) Complementary distribution of type 1 cannabinoid receptors

- and vesicular glutamate transporter 3 in basal forebrain suggests input-specific retrograde signalling by cholinergic neurons. *Eur J Neurosci*, 18: 1979-1992.
- Harkany T, Holmgren C, Hartig W, Qureshi T, Chaudhry FA, Storm-Mathisen J, Dobszay MB, Berghuis P, Schulte G, Sousa KM, Fremeau RT, Jr., Edwards RH, Mackie K, Ernfors P, Zilberter Y. (2004) Endocannabinoid-independent retrograde signaling at inhibitory synapses in layer 2/3 of neocortex: involvement of vesicular glutamate transporter 3. *J Neurosci*, 24: 4978-4988.
- Haupt C, Tolner EA, Heinemann U, Witte OW, Frahm C. (2006) The combined use of non-radioactive in situ hybridization and real-time RT-PCR to assess gene expression in cryosections. *Brain Res*, 1118: 232-238.
- He A, Zhang C, Ke X, Yi Y, Yu Q, Zhang T, Yu H, Du H, Li H, Tian Q, Zhu LQ, Lu Y. (2022) VGLUT3 neurons in median raphe control the efficacy of spatial memory retrieval via ETV4 regulation of VGLUT3 transcription. *Sci China Life Sci*, 65: 1590-1607.
- He L, Marioutina M, Dunaief JL, Marneros AG. (2014) Age- and gene-dosage-dependent cre-induced abnormalities in the retinal pigment epithelium. *Am J Pathol*, 184: 1660-1667.
- Herzog E, Bellenchi GC, Gras C, Bernard V, Ravassard P, Bedet C, Gasnier B, Giros B, El Mestikawy S. (2001) The existence of a second vesicular glutamate transporter specifies subpopulations of glutamatergic neurons. *J Neurosci*, 21: RC181.
- Herzog E, Gilchrist J, Gras C, Muzerelle A, Ravassard P, Giros B, Gaspar P, El Mestikawy S. (2004) Localization of VGLUT3, the vesicular glutamate transporter type 3, in the rat brain. *Neuroscience*, 123: 983-1002.
- Higley MJ, Gittis AH, Oldenburg IA, Balthasar N, Seal RP, Edwards RH, Lowell BB, Kreitzer AC, Sabatini BL. (2011) Cholinergic interneurons mediate fast VGluT3-dependent glutamatergic transmission in the striatum. *PLoS One*, 6: e19155.
- Hikida T, Morita M, Macpherson T. (2016) Neural mechanisms of the nucleus accumbens circuit in reward and aversive learning. *Neurosci Res*, 108: 1-5.
- Hioki H, Fujiyama F, Nakamura K, Wu SX, Matsuda W, Kaneko T. (2004) Chemically specific circuit composed of vesicular glutamate transporter 3- and preprotachykinin B-producing interneurons in the rat neocortex. *Cereb Cortex*, 14: 1266-1275.

- Hioki H, Fujiyama F, Taki K, Tomioka R, Furuta T, Tamamaki N, Kaneko T. (2003) Differential distribution of vesicular glutamate transporters in the rat cerebellar cortex. *Neuroscience*, 117: 1-6.
- Hioki H, Nakamura H, Ma YF, Konno M, Hayakawa T, Nakamura KC, Fujiyama F, Kaneko T. (2010) Vesicular glutamate transporter 3-expressing nonserotonergic projection neurons constitute a subregion in the rat midbrain raphe nuclei. *J Comp Neurol*, 518: 668-686.
- Hitti FL, Siegelbaum SA. (2014) The hippocampal CA2 region is essential for social memory. *Nature*, 508: 88-92.
- Honsek SD, Seal RP, Sandkuhler J. (2015) Presynaptic inhibition of optogenetically identified VGLUT3+ sensory fibres by opioids and baclofen. *Pain*, 156: 243-251.
- Hopman AH, Ramaekers FC, Speel EJ. (1998) Rapid synthesis of biotin-, digoxigenin-, trinitrophenyl-, and fluorochrome-labeled tyramides and their application for In situ hybridization using CARD amplification. *J Histochem Cytochem*, 46: 771-777.
- Horvath HR, Fazekas CL, Balazsfi D, Jain SK, Haller J, Zelena D. (2018) Contribution of Vesicular Glutamate Transporters to Stress Response and Related Psychopathologies: Studies in VGLUT3 Knockout Mice. *Cell Mol Neurobiol*, 38: 37-52.
- Hsiao YT, Yi PL, Cheng CH, Chang FC. (2013) Disruption of footshock-induced theta rhythms by stimulating median raphe nucleus reduces anxiety in rats. *Behav Brain Res*, 247: 193-200.
- Huang W, Ikemoto S, Wang DV. (2022) Median Raphe Nonserotonergic Neurons Modulate Hippocampal Theta Oscillations. *J Neurosci*, 42: 1987-1998.
- Ibrahim KS, El Mestikawy S, Abd-Elrahman KS, Ferguson SSG. (2022) VGLUT3 Ablation Differentially Modulates Glutamate Receptor Densities in Mouse Brain. *eNeuro*, 9.
- Jackson J, Bland BH, Antle MC. (2009) Nonserotonergic projection neurons in the midbrain raphe nuclei contain the vesicular glutamate transporter VGLUT3. *Synapse*, 63: 31-41.

- Jalabert M, Aston-Jones G, Herzog E, Manzoni O, Georges F. (2009) Role of the bed nucleus of the stria terminalis in the control of ventral tegmental area dopamine neurons. *Prog Neuropsychopharmacol Biol Psychiatry*, 33: 1336-1346.
- Jensen P, Farago AF, Awatramani RB, Scott MM, Deneris ES, Dymecki SM. (2008) Redefining the serotonergic system by genetic lineage. *Nat Neurosci*, 11: 417-419.
- Jeong N, Singer AC. (2022) Learning from inhibition: Functional roles of hippocampal CA1 inhibition in spatial learning and memory. *Curr Opin Neurobiol*, 76: 102604.
- Jiang J, Cui H, Rahmouni K. (2017) Optogenetics and pharmacogenetics: principles and applications. *Am J Physiol Regul Integr Comp Physiol*, 313: R633-R645.
- Jin T, Chen R, Shao M, Yang X, Ma L, Wang F. (2020) Dorsal hippocampus- and ACC-projecting medial septum neurons differentially contribute to the recollection of episodic-like memory. *FASEB J*, 34: 11741-11753.
- Joshi Y, Petit CP, Miot S, Guillet M, Sendin G, Bourien J, Wang J, Pujol R, El Mestikawy S, Puel JL, Nouvian R. (2021) VGLUT3-p.A211V variant fuses stereocilia bundles and elongates synaptic ribbons. *J Physiol*, 599: 5397-5416.
- Juneja A, Barenboim L, Jacobson L. (2020) Selective effects of dorsal raphe nucleus glucocorticoid receptor deletion on depression-like behavior in female C57BL/6J mice. *Neurosci Lett*, 717: 134697.
- Kaneko T, Fujiyama F. (2002) Complementary distribution of vesicular glutamate transporters in the central nervous system. *Neurosci Res*, 42: 243-250.
- Kaneko T, Fujiyama F, Hioki H. (2002) Immunohistochemical localization of candidates for vesicular glutamate transporters in the rat brain. *J Comp Neurol*, 444: 39-62.
- Karray S, Kress C, Cuvellier S, Hue-Beauvais C, Damotte D, Babinet C, Levi-Strauss M. (2004) Complete loss of Fas ligand gene causes massive lymphoproliferation and early death, indicating a residual activity of gld allele. *J Immunol*, 172: 2118-2125.
- Kawai H, Bouchekioua Y, Nishitani N, Niitani K, Izumi S, Morishita H, Andoh C, Nagai Y, Koda M, Hagiwara M, Toda K, Shirakawa H, Nagayasu K, Ohmura Y, Kondo M, Kaneda K, Yoshioka M, Kaneko S. (2022) Median raphe serotonergic neurons projecting to the interpeduncular nucleus control preference and aversion. *Nat Commun*, 13: 7708.

- Kehrer C, Maziashvili N, Dugladze T, Gloveli T. (2008) Altered Excitatory-Inhibitory Balance in the NMDA-Hypofunction Model of Schizophrenia. *Front Mol Neurosci*, 1: 6.
- Kim KX, Payne S, Yang-Hood A, Li SZ, Davis B, Carlquist J, B VG, Gantz JA, Kallogjeri D, Fitzpatrick JAJ, Ohlemiller KK, Hirose K, Rutherford MA. (2019) Vesicular Glutamatergic Transmission in Noise-Induced Loss and Repair of Cochlear Ribbon Synapses. *J Neurosci*, 39: 4434-4447.
- Kljakic O, Hogan-Cann AE, Yang H, Dover B, Al-Onaizi M, Prado MAM, Prado VF. (2022) Chemogenetic activation of VGLUT3-expressing neurons decreases movement. *Eur J Pharmacol*, 935: 175298.
- Ko J. (2017) Neuroanatomical Substrates of Rodent Social Behavior: The Medial Prefrontal Cortex and Its Projection Patterns. *Front Neural Circuits*, 11: 41.
- Kocsis B, Vertes RP. (1996) Midbrain raphe cell firing and hippocampal theta rhythm in urethane-anaesthetized rats. *Neuroreport*, 7: 2867-2872.
- Kohler C, Chan-Palay V, Steinbusch H. (1982) The distribution and origin of serotonin-containing fibers in the septal area: a combined immunohistochemical and fluorescent retrograde tracing study in the rat. *J Comp Neurol*, 209: 91-111.
- Kohler C, Steinbusch H. (1982) Identification of serotonin and non-serotonin-containing neurons of the mid-brain raphe projecting to the entorhinal area and the hippocampal formation. A combined immunohistochemical and fluorescent retrograde tracing study in the rat brain. *Neuroscience*, 7: 951-975.
- Korotkova T, Ponomarenko A, Monaghan CK, Poulter SL, Cacucci F, Wills T, Hasselmo ME, Lever C. (2018) Reconciling the different faces of hippocampal theta: The role of theta oscillations in cognitive, emotional and innate behaviors. *Neurosci Biobehav Rev*, 85: 65-80.
- Kovacs KJ. (2008) Measurement of immediate-early gene activation- c-fos and beyond. *J Neuroendocrinol*, 20: 665-672.
- Kudo T, Uchigashima M, Miyazaki T, Konno K, Yamasaki M, Yanagawa Y, Minami M, Watanabe M. (2012) Three types of neurochemical projection from the bed nucleus of the stria terminalis to the ventral tegmental area in adult mice. *J Neurosci*, 32: 18035-18046.

- Kudrimoti HS, Barnes CA, McNaughton BL. (1999) Reactivation of hippocampal cell assemblies: effects of behavioral state, experience, and EEG dynamics. *J Neurosci*, 19: 4090-4101.
- Kusljic S, Van Den Buuse M. (2012) Differential role of serotonin projections from the dorsal and median raphe nuclei in phencyclidine-induced hyperlocomotion and fos-like immunoreactivity in rats. *Synapse*, 66: 885-892.
- Lam PT, Padula SL, Hoang TV, Poth JE, Liu L, Liang C, LeFever AS, Wallace LM, Ashery-Padan R, Riggs PK, Shields JE, Shaham O, Rowan S, Brown NL, Glaser T, Robinson ML. (2019) Considerations for the use of Cre recombinase for conditional gene deletion in the mouse lens. *Hum Genomics*, 13: 10.
- Lanzenberger R, Kranz GS, Haeusler D, Akimova E, Savli M, Hahn A, Mitterhauser M, Spindelegger C, Philippe C, Fink M, Wadsak W, Karanikas G, Kasper S. (2012) Prediction of SSRI treatment response in major depression based on serotonin transporter interplay between median raphe nucleus and projection areas. *Neuroimage*, 63: 874-881.
- Larsson M, Broman J. (2019) Synaptic Organization of VGLUT3 Expressing Low-Threshold Mechanosensitive C Fiber Terminals in the Rodent Spinal Cord. *eNeuro*, 6.
- Lazarini-Lopes W, Corsi-Zuelli F, Padovan CM. (2020) Attenuation of stress-induced behavioral changes by activation of serotonin type 7 receptors in the median raphe nucleus of rats. *J Psychopharmacol*, 34: 901-913.
- Le AD, Funk D, Harding S, Juzysch W, Li Z, Fletcher PJ. (2008) Intra-median raphe nucleus (MRN) infusions of muscimol, a GABA-A receptor agonist, reinstate alcohol seeking in rats: role of impulsivity and reward. *Psychopharmacology (Berl)*, 195: 605-615.
- Lee E, Rhim I, Lee JW, Ghim JW, Lee S, Kim E, Jung MW. (2016) Enhanced Neuronal Activity in the Medial Prefrontal Cortex during Social Approach Behavior. *J Neurosci*, 36: 6926-6936.
- Leranth C, Vertes RP. (1999) Median raphe serotonergic innervation of medial septum/diagonal band of Broca (MSDB) parvalbumin-containing neurons: possible involvement of the MSDB in the desynchronization of the hippocampal EEG. *J Comp Neurol*, 410: 586-598.

- Li D, Herault K, Silm K, Evrard A, Wojcik S, Oheim M, Herzog E, Ropert N. (2013) Lack of evidence for vesicular glutamate transporter expression in mouse astrocytes. *J Neurosci*, 33: 4434-4455.
- Liguz-Leczna M, Skangiel-Kramska J. (2007) Vesicular glutamate transporters (VGLUTs): the three musketeers of glutamatergic system. *Acta Neurobiol Exp (Wars)*, 67: 207-218.
- Lissner LJ, Wartchow KM, Toniazzi AP, Goncalves CA, Rodrigues L. (2021) Object recognition and Morris water maze to detect cognitive impairment from mild hippocampal damage in rats: A reflection based on the literature and experience. *Pharmacol Biochem Behav*, 210: 173273.
- Liu W, Alreja M. (1997) Atypical antipsychotics block the excitatory effects of serotonin in septohippocampal neurons in the rat. *Neuroscience*, 79: 369-382.
- Liu Z, Zhou J, Li Y, Hu F, Lu Y, Ma M, Feng Q, Zhang JE, Wang D, Zeng J, Bao J, Kim JY, Chen ZF, El Mestikawy S, Luo M. (2014) Dorsal raphe neurons signal reward through 5-HT and glutamate. *Neuron*, 81: 1360-1374.
- Lopez-Rojas J, de Solis CA, Leroy F, Kandel ER, Siegelbaum SA. (2022) A direct lateral entorhinal cortex to hippocampal CA2 circuit conveys social information required for social memory. *Neuron*, 110: 1559-1572 e1554.
- Lopez Hill X, Pascovich C, Urbanavicius J, Torterolo P, Scorza MC. (2013) The median raphe nucleus participates in the depressive-like behavior induced by MCH: differences with the dorsal raphe nucleus. *Peptides*, 50: 96-99.
- Lou S, Duan B, Vong L, Lowell BB, Ma Q. (2013) Runx1 controls terminal morphology and mechanosensitivity of VGLUT3-expressing C-mechanoreceptors. *J Neurosci*, 33: 870-882.
- Louie K, Wilson MA. (2001) Temporally structured replay of awake hippocampal ensemble activity during rapid eye movement sleep. *Neuron*, 29: 145-156.
- Mansouri-Guilani N, Bernard V, Vigneault E, Vialou V, Daumas S, El Mestikawy S, Gangarossa G. (2019) VGLUT3 gates psychomotor effects induced by amphetamine. *J Neurochem*, 148: 779-795.
- Manvich DF, Webster KA, Foster SL, Farrell MS, Ritchie JC, Porter JH, Weinshenker D. (2018) The DREADD agonist clozapine N-oxide (CNO) is reverse-

- metabolized to clozapine and produces clozapine-like interoceptive stimulus effects in rats and mice. *Sci Rep*, 8: 3840.
- Martin-Ibanez R, Jenstad M, Berghuis P, Edwards RH, Hioki H, Kaneko T, Mulder J, Canals JM, Ernfors P, Chaudhry FA, Harkany T. (2006) Vesicular glutamate transporter 3 (VGLUT3) identifies spatially segregated excitatory terminals in the rat substantia nigra. *Eur J Neurosci*, 23: 1063-1070.
- Maru E, Takahashi LK, Iwahara S. (1979) Effects of median raphe nucleus lesions on hippocampal EEG in the freely moving rat. *Brain Res*, 163: 223-234.
- McKenna JT, Vertes RP. (2001) Collateral projections from the median raphe nucleus to the medial septum and hippocampus. *Brain Res Bull*, 54: 619-630.
- McLellan MA, Rosenthal NA, Pinto AR. (2017) Cre-loxP-Mediated Recombination: General Principles and Experimental Considerations. *Curr Protoc Mouse Biol*, 7: 1-12.
- Medhurst AD, Harrison DC, Read SJ, Campbell CA, Robbins MJ, Pangalos MN. (2000) The use of TaqMan RT-PCR assays for semiquantitative analysis of gene expression in CNS tissues and disease models. *J Neurosci Methods*, 98: 9-20.
- Melik E, Babar-Melik E, Ozgunen T, Binokay S. (2000) Median raphe nucleus mediates forming long-term but not short-term contextual fear conditioning in rats. *Behav Brain Res*, 112: 145-150.
- Michelsen KA, Schmitz C, Steinbusch HW. (2007) The dorsal raphe nucleus--from silver stainings to a role in depression. *Brain Res Rev*, 55: 329-342.
- Miot S, Voituron N, Sterlin A, Vigneault E, Morel L, Matrot B, Ramanantsoa N, Amilhon B, Poirel O, Lepicard E, Mestikawy SE, Hilaire G, Gallego J. (2012) The vesicular glutamate transporter VGLUT3 contributes to protection against neonatal hypoxic stress. *J Physiol*, 590: 5183-5198.
- Moechars D, Weston MC, Leo S, Callaerts-Vegh Z, Goris I, Daneels G, Buist A, Cik M, van der Spek P, Kass S, Meert T, D'Hooge R, Rosenmund C, Hampson RM. (2006) Vesicular glutamate transporter VGLUT2 expression levels control quantal size and neuropathic pain. *J Neurosci*, 26: 12055-12066.
- Montagrin A, Saiote C, Schiller D. (2018) The social hippocampus. *Hippocampus*, 28: 672-679.

- Morris R. (1984) Developments of a water-maze procedure for studying spatial learning in the rat. *J Neurosci Methods*, 11: 47-60.
- Morris RG, Garrud P, Rawlins JN, O'Keefe J. (1982) Place navigation impaired in rats with hippocampal lesions. *Nature*, 297: 681-683.
- Moser EI, Moser MB, McNaughton BL. (2017) Spatial representation in the hippocampal formation: a history. *Nat Neurosci*, 20: 1448-1464.
- Munguba GC, Camp AS, Risco M, Tapia ML, Bhattacharya SK, Lee RK. (2011) Vesicular glutamate transporter 3 in age-dependent optic neuropathy. *Mol Vis*, 17: 413-419.
- Muzerelle A, Scotto-Lomassese S, Bernard JF, Soiza-Reilly M, Gaspar P. (2016) Conditional anterograde tracing reveals distinct targeting of individual serotonin cell groups (B5-B9) to the forebrain and brainstem. *Brain Struct Funct*, 221: 535-561.
- Nagel G, Szellas T, Huhn W, Kateriya S, Adeishvili N, Berthold P, Ollig D, Hegemann P, Bamberg E. (2003) Channelrhodopsin-2, a directly light-gated cation-selective membrane channel. *Proc Natl Acad Sci U S A*, 100: 13940-13945.
- Naidoo V, Mahabeer R, Raidoo DM. (2001) Cellular distribution of endothelin-1 mRNA in human brain by in situ RT-PCR. *Metab Brain Dis*, 16: 207-218.
- Nakamura K, Matsumura K, Kobayashi S, Kaneko T. (2005) Sympathetic premotor neurons mediating thermoregulatory functions. *Neurosci Res*, 51: 1-8.
- Nascimento Hackl LP, Carobrez AP. (2007) Distinct ventral and dorsal hippocampus AP5 anxiolytic effects revealed in the elevated plus-maze task in rats. *Neurobiol Learn Mem*, 88: 177-185.
- Nelson AB, Bussert TG, Kreitzer AC, Seal RP. (2014) Striatal cholinergic neurotransmission requires VGLUT3. *J Neurosci*, 34: 8772-8777.
- Nickerson Poulin A, Guerci A, El Mestikawy S, Semba K. (2006) Vesicular glutamate transporter 3 immunoreactivity is present in cholinergic basal forebrain neurons projecting to the basolateral amygdala in rat. *J Comp Neurol*, 498: 690-711.
- Noh J, Seal RP, Garver JA, Edwards RH, Kandler K. (2010) Glutamate co-release at GABA/glycinergic synapses is crucial for the refinement of an inhibitory map. *Nat Neurosci*, 13: 232-238.

- Nusbaum MP, Blitz DM, Marder E. (2017) Functional consequences of neuropeptide and small-molecule co-transmission. *Nat Rev Neurosci*, 18: 389-403.
- Obholzer N, Wolfson S, Trapani JG, Mo W, Nechiporuk A, Busch-Nentwich E, Seiler C, Sidi S, Sollner C, Duncan RN, Boehland A, Nicolson T. (2008) Vesicular glutamate transporter 3 is required for synaptic transmission in zebrafish hair cells. *J Neurosci*, 28: 2110-2118.
- Ogawa SK, Cohen JY, Hwang D, Uchida N, Watabe-Uchida M. (2014) Organization of monosynaptic inputs to the serotonin and dopamine neuromodulatory systems. *Cell Rep*, 8: 1105-1118.
- Okaty BW, Commons KG, Dymecki SM. (2019) Embracing diversity in the 5-HT neuronal system. *Nat Rev Neurosci*, 20: 397-424.
- Okaty BW, Freret ME, Rood BD, Brust RD, Hennessy ML, deBairos D, Kim JC, Cook MN, Dymecki SM. (2015) Multi-Scale Molecular Deconstruction of the Serotonin Neuron System. *Neuron*, 88: 774-791.
- Oliva A, Fernandez-Ruiz A, Leroy F, Siegelbaum SA. (2020) Hippocampal CA2 sharp-wave ripples reactivate and promote social memory. *Nature*, 587: 264-269.
- Olivan AM, Perez-Rodriguez R, Roncero C, Arce C, Gonzalez MP, Oset-Gasque MJ. (2011) Plasma membrane and vesicular glutamate transporter expression in chromaffin cells of bovine adrenal medulla. *J Neurosci Res*, 89: 44-57.
- Oliveira AL, Hydling F, Olsson E, Shi T, Edwards RH, Fujiyama F, Kaneko T, Hokfelt T, Cullheim S, Meister B. (2003) Cellular localization of three vesicular glutamate transporter mRNAs and proteins in rat spinal cord and dorsal root ganglia. *Synapse*, 50: 117-129.
- Omiya Y, Uchigashima M, Konno K, Yamasaki M, Miyazaki T, Yoshida T, Kusumi I, Watanabe M. (2015) VGluT3-expressing CCK-positive basket cells construct invaginating synapses enriched with endocannabinoid signaling proteins in particular cortical and cortex-like amygdaloid regions of mouse brains. *J Neurosci*, 35: 4215-4228.
- Ormel L, Stensrud MJ, Chaudhry FA, Gundersen V. (2012) A distinct set of synaptic-like microvesicles in astroglial cells contain VGLUT3. *Glia*, 60: 1289-1300.

- Padovan CM, Del Bel EA, Guimaraes FS. (2000) Behavioral effects in the elevated plus maze of an NMDA antagonist injected into the dorsal hippocampus: influence of restraint stress. *Pharmacol Biochem Behav*, 67: 325-330.
- Papathanou M, Dumas S, Pettersson H, Olson L, Wallen-Mackenzie A. (2019) Off-Target Effects in Transgenic Mice: Characterization of Dopamine Transporter (DAT)-Cre Transgenic Mouse Lines Exposes Multiple Non-Dopaminergic Neuronal Clusters Available for Selective Targeting within Limbic Neurocircuitry. *eNeuro*, 6.
- Papp EC, Hajos N, Acsady L, Freund TF. (1999) Medial septal and median raphe innervation of vasoactive intestinal polypeptide-containing interneurons in the hippocampus. *Neuroscience*, 90: 369-382.
- Paxinos GF, Keith B. J. The mouse brain in stereotaxic coordinates. Academic San Diego, Calif., London, 2001.
- Peck BK, Vanderwolf CH. (1991) Effects of raphe stimulation on hippocampal and neocortical activity and behaviour. *Brain Res*, 568: 244-252.
- Pelkey KA, Calvigioni D, Fang C, Vargish G, Ekins T, Auville K, Wester JC, Lai M, Mackenzie-Gray Scott C, Yuan X, Hunt S, Abebe D, Xu Q, Dimidschstein J, Fishell G, Chittajallu R, McBain CJ. (2020) Paradoxical network excitation by glutamate release from VGluT3(+) GABAergic interneurons. *Elife*, 9.
- Peng Z, Wang GP, Zeng R, Guo JY, Chen CF, Gong SS. (2013) Temporospatial expression and cellular localization of VGLUT3 in the rat cochlea. *Brain Res*, 1537: 100-110.
- Perez-Caballero L, Torres-Sanchez S, Bravo L, Mico JA, Berrocoso E. (2014) Fluoxetine: a case history of its discovery and preclinical development. *Expert Opin Drug Discov*, 9: 567-578.
- Pollak Dorocic I, Furth D, Xuan Y, Johansson Y, Pozzi L, Silberberg G, Carlen M, Meletis K. (2014) A whole-brain atlas of inputs to serotonergic neurons of the dorsal and median raphe nuclei. *Neuron*, 83: 663-678.
- Prakash N, Stark CJ, Keisler MN, Luo L, Der-Avakian A, Dulcis D. (2020) Serotonergic Plasticity in the Dorsal Raphe Nucleus Characterizes Susceptibility and Resilience to Anhedonia. *J Neurosci*, 40: 569-584.

- Preobraschenski J, Zander JF, Suzuki T, Ahnert-Hilger G, Jahn R. (2014) Vesicular glutamate transporters use flexible anion and cation binding sites for efficient accumulation of neurotransmitter. *Neuron*, 84: 1287-1301.
- Qi J, Zhang S, Wang HL, Wang H, de Jesus Aceves Buendia J, Hoffman AF, Lupica CR, Seal RP, Morales M. (2014) A glutamatergic reward input from the dorsal raphe to ventral tegmental area dopamine neurons. *Nat Commun*, 5: 5390.
- Ramet L, Zimmermann J, Bersot T, Poirel O, De Gois S, Silm K, Sakae DY, Mansouri-Guilani N, Bourque MJ, Trudeau LE, Pietrancosta N, Daumas S, Bernard V, Rosenmund C, El Mestikawy S. (2017) Characterization of a Human Point Mutation of VGLUT3 (p.A211V) in the Rodent Brain Suggests a Nonuniform Distribution of the Transporter in Synaptic Vesicles. *J Neurosci*, 37: 4181-4199.
- Ren J, Friedmann D, Xiong J, Liu CD, Ferguson BR, Weerakkody T, DeLoach KE, Ran C, Pun A, Sun Y, Weissbourd B, Neve RL, Huguenard J, Horowitz MA, Luo L. (2018) Anatomically Defined and Functionally Distinct Dorsal Raphe Serotonin Sub-systems. *Cell*, 175: 472-487 e420.
- Ren J, Isakova A, Friedmann D, Zeng J, Grutzner SM, Pun A, Zhao GQ, Kolluru SS, Wang R, Lin R, Li P, Li A, Raymond JL, Luo Q, Luo M, Quake SR, Luo L. (2019) Single-cell transcriptomes and whole-brain projections of serotonin neurons in the mouse dorsal and median raphe nuclei. *Elife*, 8.
- Richter-Levin G, Canevari L, Bliss TV. (1995) Long-term potentiation and glutamate release in the dentate gyrus: links to spatial learning. *Behav Brain Res*, 66: 37-40.
- Robinson MB. (2006) Acute regulation of sodium-dependent glutamate transporters: a focus on constitutive and regulated trafficking. *Handb Exp Pharmacol*, doi:10.1007/3-540-29784-7_13: 251-275.
- Robinson NTM, Descamps LAL, Russell LE, Buchholz MO, Bicknell BA, Antonov GK, Lau JYN, Nutbrown R, Schmidt-Hieber C, Hausser M. (2020) Targeted Activation of Hippocampal Place Cells Drives Memory-Guided Spatial Behavior. *Cell*, 183: 2041-2042.
- Rosin DL, Chang DA, Guyenet PG. (2006) Afferent and efferent connections of the rat retrotrapezoid nucleus. *J Comp Neurol*, 499: 64-89.
- Roth BL. (2016) DREADDs for Neuroscientists. *Neuron*, 89: 683-694.

- Rovira-Esteban L, Peterfi Z, Vikor A, Mate Z, Szabo G, Hajos N. (2017) Morphological and physiological properties of CCK/CB1R-expressing interneurons in the basal amygdala. *Brain Struct Funct*, 222: 3543-3565.
- Ruel J, Emery S, Nouvian R, Bersot T, Amilhon B, Van Rybroek JM, Rebillard G, Lenoir M, Eybalin M, Delprat B, Sivakumaran TA, Giros B, El Mestikawy S, Moser T, Smith RJ, Lesperance MM, Puel JL. (2008) Impairment of SLC17A8 encoding vesicular glutamate transporter-3, VGLUT3, underlies nonsyndromic deafness DFNA25 and inner hair cell dysfunction in null mice. *Am J Hum Genet*, 83: 278-292.
- Russo AM, Lawther AJ, Prior BM, Isbel L, Somers WG, Lesku JA, Richdale AL, Dissanayake C, Kent S, Lowry CA, Hale MW. (2019) Social approach, anxiety, and altered tryptophan hydroxylase 2 activity in juvenile BALB/c and C57BL/6J mice. *Behav Brain Res*, 359: 918-926.
- Sakae DY, Marti F, Lecca S, Vorspan F, Martin-Garcia E, Morel LJ, Henrion A, Gutierrez-Cuesta J, Besnard A, Heck N, Herzog E, Bolte S, Prado VF, Prado MA, Bellivier F, Eap CB, Crettol S, Vanhoutte P, Caboche J, Gratton A, Moquin L, Giros B, Maldonado R, Daumas S, Mameli M, Jamain S, El Mestikawy S. (2015) The absence of VGLUT3 predisposes to cocaine abuse by increasing dopamine and glutamate signaling in the nucleus accumbens. *Mol Psychiatry*, 20: 1448-1459.
- Sakae DY, Ramet L, Henrion A, Poirel O, Jamain S, El Mestikawy S, Daumas S. (2019) Differential expression of VGLUT3 in laboratory mouse strains: Impact on drug-induced hyperlocomotion and anxiety-related behaviors. *Genes Brain Behav*, 18: e12528.
- Sarihi A, Motamedi F, Rashidy-Pour A, Naghdi N, Behzadi G. (1999) Reversible inactivation of the median raphe nucleus enhances consolidation and retrieval but not acquisition of passive avoidance learning in rats. *Brain Res*, 817: 59-66.
- Schafer MK, Varoqui H, Defamie N, Weihe E, Erickson JD. (2002) Molecular cloning and functional identification of mouse vesicular glutamate transporter 3 and its expression in subsets of novel excitatory neurons. *J Biol Chem*, 277: 50734-50748.

- Schmidt EE, Taylor DS, Prigge JR, Barnett S, Capecchi MR. (2000) Illegitimate Cre-dependent chromosome rearrangements in transgenic mouse spermatids. *Proc Natl Acad Sci U S A*, 97: 13702-13707.
- Seager MA, Johnson LD, Chabot ES, Asaka Y, Berry SD. (2002) Oscillatory brain states and learning: Impact of hippocampal theta-contingent training. *Proc Natl Acad Sci U S A*, 99: 1616-1620.
- Seal RP, Akil O, Yi E, Weber CM, Grant L, Yoo J, Clause A, Kandler K, Noebels JL, Glowatzki E, Lustig LR, Edwards RH. (2008) Sensorineural deafness and seizures in mice lacking vesicular glutamate transporter 3. *Neuron*, 57: 263-275.
- Senft RA, Freret ME, Sturrock N, Dymecki SM. (2021) Neurochemically and Hodologically Distinct Ascending VGLUT3 versus Serotonin Subsystems Comprise the r2-Pet1 Median Raphe. *J Neurosci*, 41: 2581-2600.
- Sengupta A, Bocchio M, Bannerman DM, Sharp T, Capogna M. (2017) Control of Amygdala Circuits by 5-HT Neurons via 5-HT and Glutamate Cotransmission. *J Neurosci*, 37: 1785-1796.
- Sengupta A, Holmes A. (2019) A Discrete Dorsal Raphe to Basal Amygdala 5-HT Circuit Calibrates Aversive Memory. *Neuron*, 103: 489-505 e487.
- Shim I, Stratford TR, Wirtshafter D. (2014) Dopamine is differentially involved in the locomotor hyperactivity produced by manipulations of opioid, GABA and glutamate receptors in the median raphe nucleus. *Behav Brain Res*, 261: 65-70.
- Shutoh F, Ina A, Yoshida S, Konno J, Hisano S. (2008) Two distinct subtypes of serotonergic fibers classified by co-expression with vesicular glutamate transporter 3 in rat forebrain. *Neurosci Lett*, 432: 132-136.
- Silva RC, Gargaro AC, Brandao ML. (2004) Differential regulation of the expression of contextual freezing and fear-potentiated startle by 5-HT mechanisms of the median raphe nucleus. *Behav Brain Res*, 151: 93-101.
- Soltani Zangbar H, Ghadiri T, Seyedi Vafae M, Ebrahimi Kalan A, Fallahi S, Ghorbani M, Shahabi P. (2020) Theta Oscillations Through Hippocampal/Prefrontal Pathway: Importance in Cognitive Performances. *Brain Connect*, 10: 157-169.
- Somogyi J, Baude A, Omori Y, Shimizu H, El Mestikawy S, Fukaya M, Shigemoto R, Watanabe M, Somogyi P. (2004) GABAergic basket cells expressing cholecystokinin contain vesicular glutamate transporter type 3 (VGLUT3) in their

- synaptic terminals in hippocampus and isocortex of the rat. *Eur J Neurosci*, 19: 552-569.
- Sos KE, Mayer MI, Cserep C, Takacs FS, Szonyi A, Freund TF, Nyiri G. (2017) Cellular architecture and transmitter phenotypes of neurons of the mouse median raphe region. *Brain Struct Funct*, 222: 287-299.
- Staib JM, Della Valle R, Knox DK. (2018) Disruption of medial septum and diagonal bands of Broca cholinergic projections to the ventral hippocampus disrupt auditory fear memory. *Neurobiol Learn Mem*, 152: 71-79.
- Stensrud MJ, Chaudhry FA, Leergaard TB, Bjaalie JG, Gundersen V. (2013) Vesicular glutamate transporter-3 in the rodent brain: vesicular colocalization with vesicular gamma-aminobutyric acid transporter. *J Comp Neurol*, 521: 3042-3056.
- Stensrud MJ, Sogn CJ, Gundersen V. (2015) Immunogold characteristics of VGLUT3-positive GABAergic nerve terminals suggest corelease of glutamate. *J Comp Neurol*, 523: 2698-2713.
- Sternberg N, Hamilton D. (1981) Bacteriophage P1 site-specific recombination. I. Recombination between loxP sites. *J Mol Biol*, 150: 467-486.
- Stornetta RL, Rosin DL, Simmons JR, McQuiston TJ, Vujovic N, Weston MC, Guyenet PG. (2005) Coexpression of vesicular glutamate transporter-3 and gamma-aminobutyric acidergic markers in rat rostral medullary raphe and intermediolateral cell column. *J Comp Neurol*, 492: 477-494.
- Sturman O, Germain PL, Bohacek J. (2018) Exploratory rearing: a context- and stress-sensitive behavior recorded in the open-field test. *Stress*, 21: 443-452.
- Sun Q, Li X, Li A, Zhang J, Ding Z, Gong H, Luo Q. (2020) Ventral Hippocampal-Prefrontal Interaction Affects Social Behavior via Parvalbumin Positive Neurons in the Medial Prefrontal Cortex. *iScience*, 23: 100894.
- Szonyi A, Mayer MI, Cserep C, Takacs VT, Watanabe M, Freund TF, Nyiri G. (2016) The ascending median raphe projections are mainly glutamatergic in the mouse forebrain. *Brain Struct Funct*, 221: 735-751.
- Szonyi A, Zicho K, Barth AM, Gonczi RT, Schlingloff D, Torok B, Sipos E, Major A, Bardoczi Z, Sos KE, Gulyas AI, Varga V, Zelena D, Freund TF, Nyiri G. (2019) Median raphe controls acquisition of negative experience in the mouse. *Science*, 366.

- Takamori S, Malherbe P, Broger C, Jahn R. (2002) Molecular cloning and functional characterization of human vesicular glutamate transporter 3. *EMBO Rep*, 3: 798-803.
- Takamori S, Rhee JS, Rosenmund C, Jahn R. (2000) Identification of a vesicular glutamate transporter that defines a glutamatergic phenotype in neurons. *Nature*, 407: 189-194.
- Tang W, Jadhav SP. (2019) Sharp-wave ripples as a signature of hippocampal-prefrontal reactivation for memory during sleep and waking states. *Neurobiol Learn Mem*, 160: 11-20.
- Tatti R, Bhaukaurally K, Gschwend O, Seal RP, Edwards RH, Rodriguez I, Carleton A. (2014) A population of glomerular glutamatergic neurons controls sensory information transfer in the mouse olfactory bulb. *Nat Commun*, 5: 3791.
- Tavares LCS, Tort ABL. (2022) Hippocampal-prefrontal interactions during spatial decision-making. *Hippocampus*, 32: 38-54.
- Teissier A, Chemiakine A, Inbar B, Bagchi S, Ray RS, Palmiter RD, Dymecki SM, Moore H, Ansorge MS. (2015) Activity of Raphe Serotonergic Neurons Controls Emotional Behaviors. *Cell Rep*, 13: 1965-1976.
- Thompson KJ, Khajehali E, Bradley SJ, Navarrete JS, Huang XP, Slocum S, Jin J, Liu J, Xiong Y, Olsen RHJ, Diberto JF, Boyt KM, Pina MM, Pati D, Molloy C, Bundgaard C, Sexton PM, Kash TL, Krashes MJ, Christopoulos A, Roth BL, Tobin AB. (2018) DREADD Agonist 21 Is an Effective Agonist for Muscarinic-Based DREADDs in Vitro and in Vivo. *ACS Pharmacol Transl Sci*, 1: 61-72.
- Tsanov M. (2018) Differential and complementary roles of medial and lateral septum in the orchestration of limbic oscillations and signal integration. *Eur J Neurosci*, 48: 2783-2794.
- Tukey DS, Lee M, Xu D, Eberle SE, Goffer Y, Manders TR, Ziff EB, Wang J. (2013) Differential effects of natural rewards and pain on vesicular glutamate transporter expression in the nucleus accumbens. *Mol Brain*, 6: 32.
- Turcotte-Cardin V, Vahid-Ansari F, Luckhart C, Daigle M, Geddes SD, Tanaka KF, Hen R, James J, Merali Z, Beique JC, Albert PR. (2019) Loss of Adult 5-HT1A Autoreceptors Results in a Paradoxical Anxiogenic Response to Antidepressant Treatment. *J Neurosci*, 39: 1334-1346.

- Varga V, Losonczy A, Zemelman BV, Borhegyi Z, Nyiri G, Domonkos A, Hangya B, Holderith N, Magee JC, Freund TF. (2009) Fast synaptic subcortical control of hippocampal circuits. *Science*, 326: 449-453.
- Varga V, Sik A, Freund TF, Kocsis B. (2002) GABA(B) receptors in the median raphe nucleus: distribution and role in the serotonergic control of hippocampal activity. *Neuroscience*, 109: 119-132.
- Verheij MMM, Contet C, Karel P, Latour J, van der Doelen RHA, Geenen B, van Hulten JA, Meyer F, Kozicz T, George O, Koob GF, Homberg JR. (2018) Median and Dorsal Raphe Serotonergic Neurons Control Moderate Versus Compulsive Cocaine Intake. *Biol Psychiatry*, 83: 1024-1035.
- Vertes RP, Fortin WJ, Crane AM. (1999) Projections of the median raphe nucleus in the rat. *J Comp Neurol*, 407: 555-582.
- Vertes RP, Hoover WB, Viana Di Prisco G. (2004) Theta rhythm of the hippocampus: subcortical control and functional significance. *Behav Cogn Neurosci Rev*, 3: 173-200.
- Viana Di Prisco G, Albo Z, Vertes RP, Kocsis B. (2002) Discharge properties of neurons of the median raphe nucleus during hippocampal theta rhythm in the rat. *Exp Brain Res*, 145: 383-394.
- Vigneault E, Poirel O, Riad M, Prud'homme J, Dumas S, Turecki G, Fasano C, Mechawar N, El Mestikawy S. (2015) Distribution of vesicular glutamate transporters in the human brain. *Front Neuroanat*, 9: 23.
- Vincent MY, Jacobson L. (2014) Glucocorticoid receptor deletion from the dorsal raphe nucleus of mice reduces dysphoria-like behavior and impairs hypothalamic-pituitary-adrenocortical axis feedback inhibition. *Eur J Neurosci*, 39: 1671-1681.
- Vinogradova OS, Kitchigina VF, Kudina TA, Zenchenko KI. (1999) Spontaneous activity and sensory responses of hippocampal neurons during persistent theta-rhythm evoked by median raphe nucleus blockade in rabbit. *Neuroscience*, 94: 745-753.
- Voisin AN, Mnie-Filali O, Giguere N, Fortin GM, Vigneault E, El Mestikawy S, Descarries L, Trudeau LE. (2016) Axonal Segregation and Role of the Vesicular Glutamate Transporter VGLUT3 in Serotonin Neurons. *Front Neuroanat*, 10: 39.

- Vooijs M, Jonkers J, Berns A. (2001) A highly efficient ligand-regulated Cre recombinase mouse line shows that LoxP recombination is position dependent. *EMBO Rep*, 2: 292-297.
- Vorhees CV, Williams MT. (2014) Value of water mazes for assessing spatial and egocentric learning and memory in rodent basic research and regulatory studies. *Neurotoxicol Teratol*, 45: 75-90.
- Wallen-Mackenzie A, Gezelius H, Thoby-Brisson M, Nygard A, Enjin A, Fujiyama F, Fortin G, Kullander K. (2006) Vesicular glutamate transporter 2 is required for central respiratory rhythm generation but not for locomotor central pattern generation. *J Neurosci*, 26: 12294-12307.
- Wallen-Mackenzie A, Wootz H, Englund H. (2010) Genetic inactivation of the vesicular glutamate transporter 2 (VGLUT2) in the mouse: what have we learnt about functional glutamatergic neurotransmission? *Ups J Med Sci*, 115: 11-20.
- Wang DV, Yau HJ, Broker CJ, Tsou JH, Bonci A, Ikemoto S. (2015) Mesopontine median raphe regulates hippocampal ripple oscillation and memory consolidation. *Nat Neurosci*, 18: 728-735.
- Wang HL, Zhang S, Qi J, Wang H, Cachope R, Mejias-Aponte CA, Gomez JA, Mateo-Semidey GE, Beaudoin GMJ, Paladini CA, Cheer JF, Morales M. (2019) Dorsal Raphe Dual Serotonin-Glutamate Neurons Drive Reward by Establishing Excitatory Synapses on VTA Mesoaccumbens Dopamine Neurons. *Cell Rep*, 26: 1128-1142 e1127.
- Wang J, Mei Y, Zhang X, Wei X, Zhang Y, Wang D, Huang J, Zhu K, Peng G, Sun B. (2023) Aberrant serotonergic signaling contributes to the hyperexcitability of CA1 pyramidal neurons in a mouse model of Alzheimer's disease. *Cell Rep*, 42: 112152.
- Weston MC, Nehring RB, Wojcik SM, Rosenmund C. (2011) Interplay between VGLUT isoforms and endophilin A1 regulates neurotransmitter release and short-term plasticity. *Neuron*, 69: 1147-1159.
- Wichmann C, Kuner T. (2022) Heterogeneity of glutamatergic synapses: cellular mechanisms and network consequences. *Physiol Rev*, 102: 269-318.
- Wilson MA, McNaughton BL. (1993) Dynamics of the hippocampal ensemble code for space. *Science*, 261: 1055-1058.

- Wirtshafter D, McWilliams C. (1987) Suppression of locomotor activity produced by acute injections of kainic acid into the median raphe nucleus. *Brain Res*, 408: 349-352.
- Wirtshafter D, Montana W, Asin KE. (1986) Behavioral and biochemical studies of the substrates of median raphe lesion induced hyperactivity. *Physiol Behav*, 38: 751-759.
- Wu D, Gao D, Yu H, Pi G, Xiong R, Lei H, Wang X, Liu E, Ye J, Yu H, Gao Y, He T, Jiang T, Sun F, Su J, Song G, Peng W, Yang Y, Wang JZ. (2021) Medial septum tau accumulation induces spatial memory deficit via disrupting medial septum-hippocampus cholinergic pathway. *Clin Transl Med*, 11: e428.
- Wu X, Morishita W, Beier KT, Heifets BD, Malenka RC. (2021) 5-HT modulation of a medial septal circuit tunes social memory stability. *Nature*, 599: 96-101.
- Wunderlich FT, Wildner H, Rajewsky K, Edenhofer F. (2001) New variants of inducible Cre recombinase: a novel mutant of Cre-PR fusion protein exhibits enhanced sensitivity and an expanded range of inducibility. *Nucleic Acids Res*, 29: E47.
- Yizhar O. (2012) Optogenetic insights into social behavior function. *Biol Psychiatry*, 71: 1075-1080.
- Yu XD, Zhu Y, Sun QX, Deng F, Wan J, Zheng D, Gong W, Xie SZ, Shen CJ, Fu JY, Huang H, Lai HY, Jin J, Li Y, Li XM. (2022) Distinct serotonergic pathways to the amygdala underlie separate behavioral features of anxiety. *Nat Neurosci*, 25: 1651-1663.
- Zelena D, Demeter K, Haller J, Balazsfi D. (2017) Considerations for the use of virally delivered genetic tools for in-vivo circuit analysis and behavior in mutant mice: a practical guide to optogenetics. *Behav Pharmacol*, 28: 598-609.
- Zerari-Mailly F, Braud A, Davido N, Toure B, Azerad J, Boucher Y. (2012) Glutamate control of pulpal blood flow in the incisor dental pulp of the rat. *Eur J Oral Sci*, 120: 402-407.
- Zimmermann J, Herman MA, Rosenmund C. (2015) Co-release of glutamate and GABA from single vesicles in GABAergic neurons exogenously expressing VGLUT3. *Front Synaptic Neurosci*, 7: 16.
- Zou WJ, Song YL, Wu MY, Chen XT, You QL, Yang Q, Luo ZY, Huang L, Kong Y, Feng J, Fang DX, Li XW, Yang JM, Mei L, Gao TM. (2020) A discrete

serotonergic circuit regulates vulnerability to social stress. *Nat Commun*, 11: 4218.

9. Bibliography

9.1. Publications related to the thesis

Fazekas CL, Balazsfi D, Horvath HR, Balogh Z, Aliczki M, Puhova A, Balagova L, Chmelova M, Jezova D, Haller J, Zelena D. (2019) Consequences of VGLUT3 deficiency on learning and memory in mice. *Physiol Behav*, 212: 112688.

Fazekas CL, Bellardie M, Torok B, Sipos E, Toth B, Baranyi M, Sperlagh B, Dobos-Kovacs M, Chaillou E, Zelena D. (2021) Pharmacogenetic excitation of the median raphe region affects social and depressive-like behavior and core body temperature in male mice. *Life Sci*, 286: 120037.

Fazekas CL, Szabo A, Torok B, Banrevi K, Correia P, Chaves T, Daumas S, Zelena D. (2022) A New Player in the Hippocampus: A Review on VGLUT3+ Neurons and Their Role in the Regulation of Hippocampal Activity and Behaviour. *Int J Mol Sci*, 23.

Horvath HR, Fazekas CL, Balazsfi D, Jain SK, Haller J, Zelena D. (2018) Contribution of Vesicular Glutamate Transporters to Stress Response and Related Psychopathologies: Studies in VGLUT3 Knockout Mice. *Cell Mol Neurobiol*, 38: 37-52.

9.2. Other publications

Chaves T, Fazekas CL, Horvath K, Correia P, Szabo A, Torok B, Banrevi K, Zelena D. (2021) Stress Adaptation and the Brainstem with Focus on Corticotropin-Releasing Hormone. *Int J Mol Sci*, 22.

Chaves T, Torok B, Fazekas CL, Correia P, Sipos E, Varkonyi D, Hellinger A, Erk D, Zelena D. (2022) Median raphe region GABAergic neurons contribute to social interest in mouse. *Life Sci*, 289: 120223.

Farkas S, Szabo A, Hegyi AE, Torok B, Fazekas CL, Ernszt D, Kovacs T, Zelena D. (2022) Estradiol and Estrogen-like Alternative Therapies in Use: The Importance of the Selective and Non-Classical Actions. *Biomedicines*, 10.

Farkas S, Szabo A, Torok B, Solyomvari C, Fazekas CL, Banrevi K, Correia P, Chaves T, Zelena D. (2022) Ovariectomy-induced hormone deprivation aggravates Abeta(1-42) deposition in the basolateral amygdala and cholinergic fiber loss in the cortex but not cognitive behavioral symptoms in a triple transgenic mouse model of Alzheimer's disease. *Front Endocrinol (Lausanne)*, 13: 985424.

Fazekas CL, Sipos E, Klaric T, Torok B, Bellardie M, Erjave GN, Perkovic MN, Lauc G, Pivac N, Zelena D. (2020) Searching for glycomic biomarkers for predicting resilience and vulnerability in a rat model of posttraumatic stress disorder. *Stress*, 23: 715-731.

Love SA, Haslin E, Bellardie M, Andersson F, Barantin L, Filipiak I, Adriaensen H, Fazekas CL, Leroy L, Zelena D, Morisse M, Elleboudt F, Moussu C, Levy F, Nowak R, Chaillou E. (2022) Maternal deprivation and milk replacement affect the integrity of gray and white matter in the developing lamb brain. *Dev Neurobiol*, 82: 214-232.

Torok B, Fazekas CL, Szabo A, Zelena D. (2021) Epigenetic Modulation of Vasopressin Expression in Health and Disease. *Int J Mol Sci*, 22.

Varkonyi D, Torok B, Sipos E, Fazekas CL, Banrevi K, Correia P, Chaves T, Farkas S, Szabo A, Martinez-Bellver S, Hangya B, Zelena D. (2022) Investigation of Anxiety- and Depressive-like Symptoms in 4- and 8-Month-Old Male Triple Transgenic Mouse Models of Alzheimer's Disease. *Int J Mol Sci*, 23.

10. Acknowledgements

I would like to thank first and foremost my supervisors who allowed me to work and realise the experiments included in this work: Dr. Dóra Zelena, who took me in as an undergraduate student and personally taught me how to be a researcher throughout the years; and Stéphanie Daumas, who agreed to the joint PhD program and showed me new perspectives and technics. Their patience and guidance were invaluable. Then, I would like to express my deepest gratitude to all the reviewers that allowed this work to pass and the committee members, who agreed to evaluate my work.

I am also grateful to my wonderful co-workers at the time, Krisztina G. Bánrévik, Alice Abbondanza, Adrienn Szabó, Pedro Correia, Tiago Chaves, Dorottya Várkonyi, Véronique Fabres and the other members of the Behavioural and Stress Studies Group first at the Institute of Experimental Medicine (IEM, Budapest, Hungary), then at the Institute of Physiology, University of Pécs (Pécs, Hungary), and Neuropharmacology of VGLUTs at Sorbonne Université, Institute de Biologie Paris Seine (IBPS, Paris, France) groups, who all helped me in the laboratory and accompanied me during all these years. I am especially thankful to Bibiána Török, who was not only a great senior PhD student since the beginnings, but also an amazing friend and mental support while we worked together, and during the writing of this thesis.

This work could not have been completed without the amazing facilities and services of the institutes where my laboratories were placed: the IEM, and Sorbonne Université. I would also like to highlight the Behavioural Studies Unit at IEM, led by Kornél Demeter, who established a wonderful facility that let us realise almost any kind of protocol, provided technical support, and kept us entertained during the long hours of work. Similarly, the Virus Technology Unit and its leader, Eszter Sipos, and the Light Microscopy Center at IEM with Pál Vági were also great contributors to this success. From the French side, I would like to acknowledge the guidance of Véronique Bernard, and Sylvie Dumas (Oramacell), who helped me conduct the FISH experiments.

I am also grateful for the financial support that was provided by the Semmelweis University, the New National Excellence Program of the Hungarian Ministry of Human Capacities (ÚNKP-18-2, ÚNKP-21-3), but especially the Campus France during the joint PhD-program. Lastly, I would like to thank my family and friends that allowed me to take this long road and encouraged me to take on all the challenges.